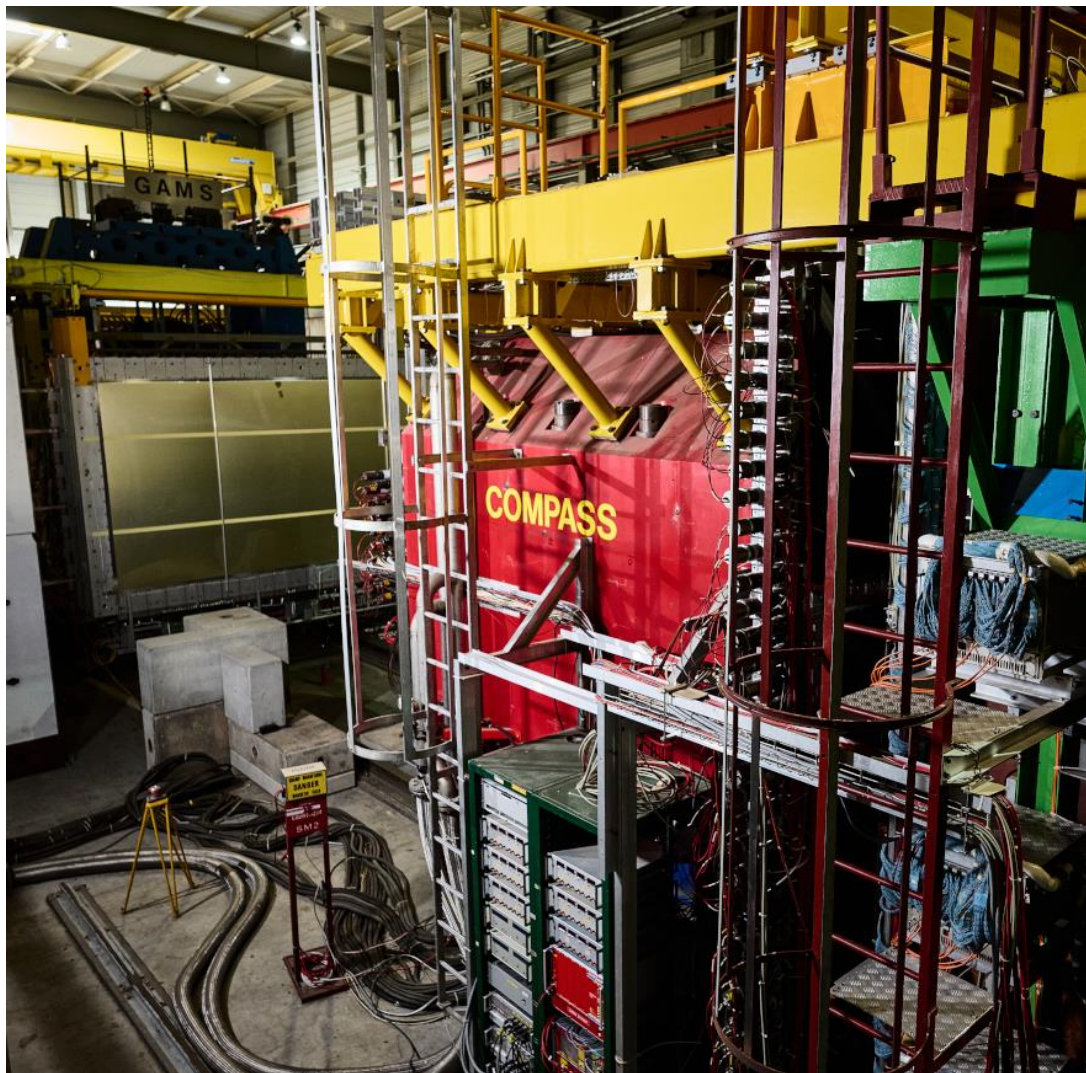
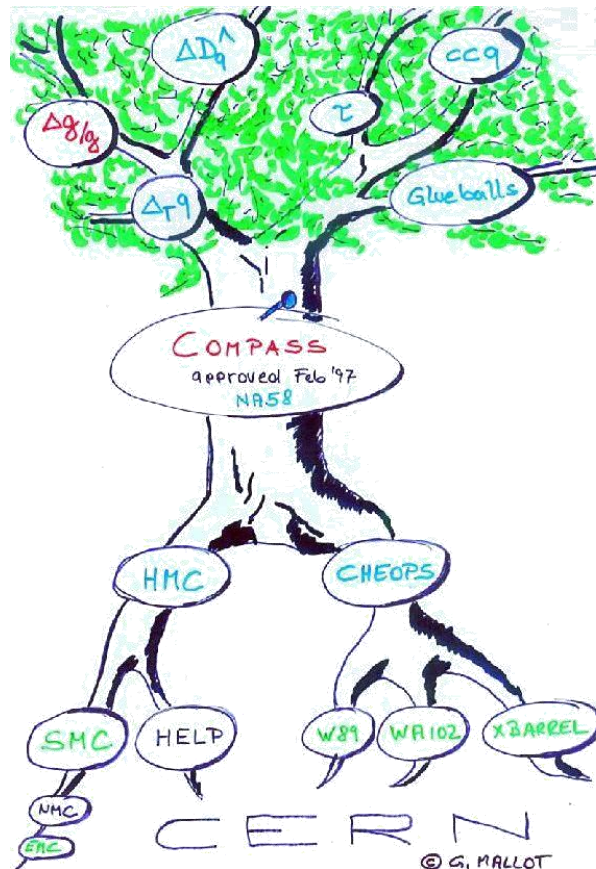


Status and plans of the COMPASS (NA58) Experiment



Bakur Parsamyan
for the COMPASS collaboration
(INFN-Torino, JINR, CERN)

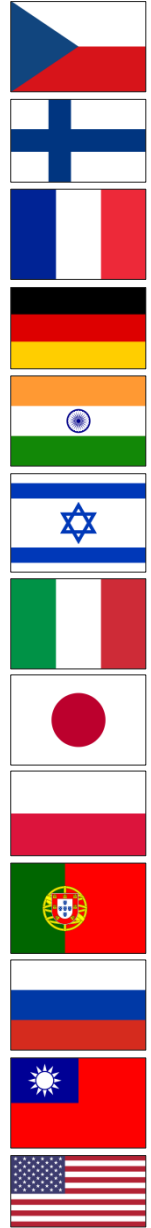


146th Meeting of the SPSC

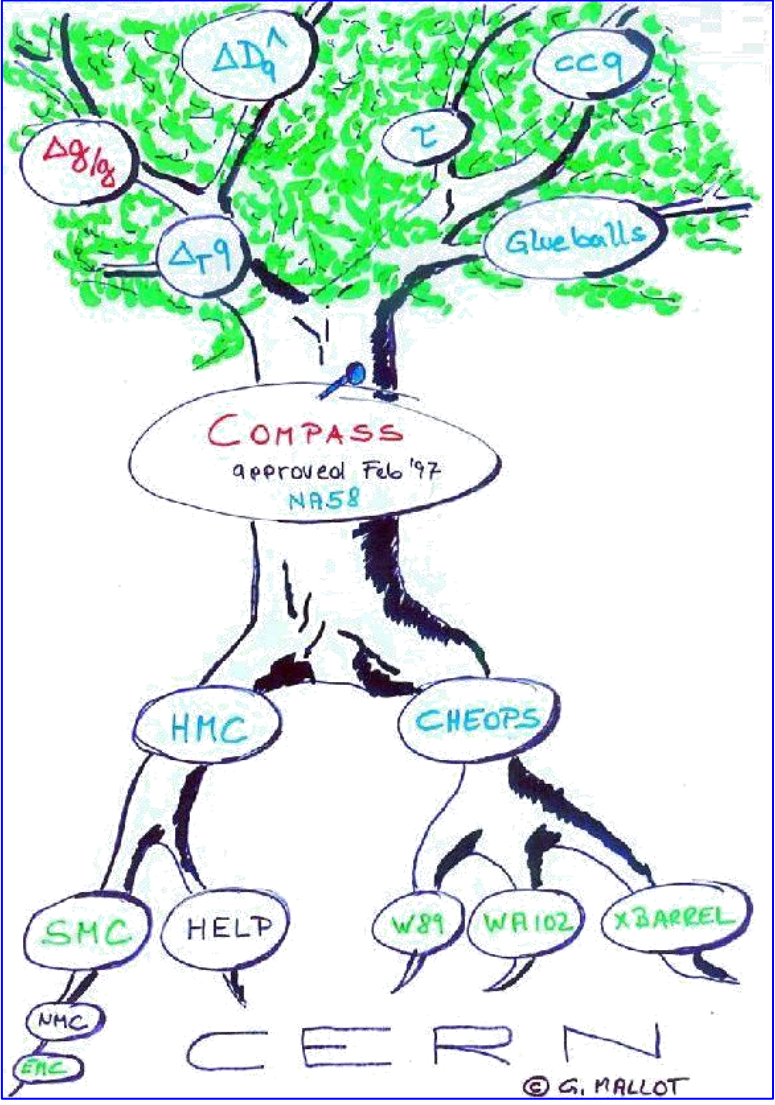
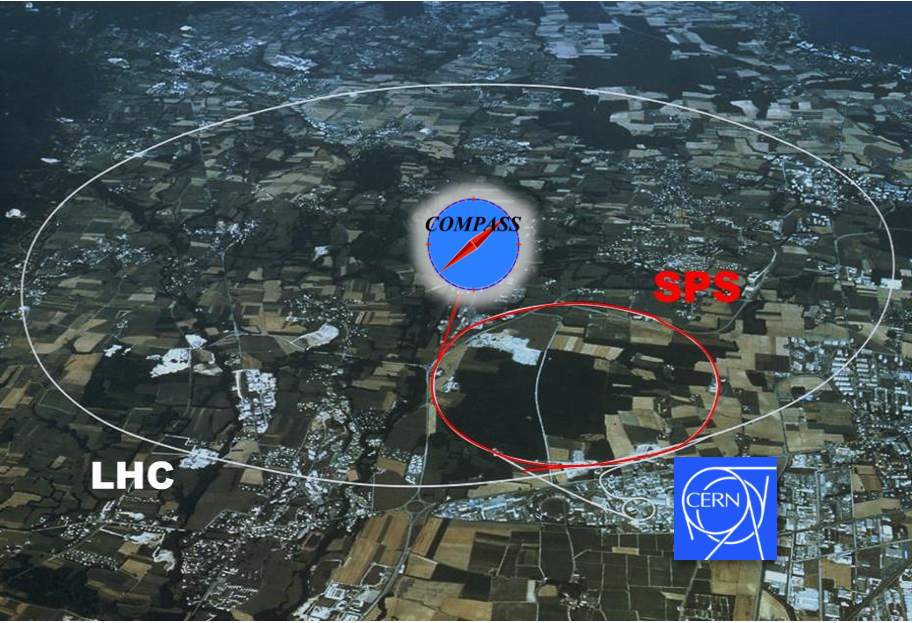
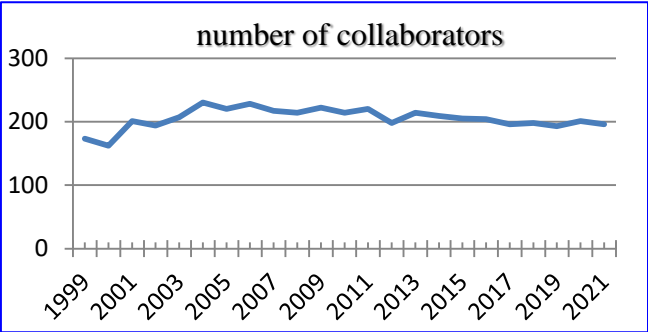
June 9th 2022, CERN

COMPASS collaboration

Common Muon and Proton Apparatus for Structure and Spectroscopy



25 institutions from 13 countries
 – nearly 200 physicists



COMPASS collaboration

Common Muon and Proton Apparatus for Structure and Spectroscopy

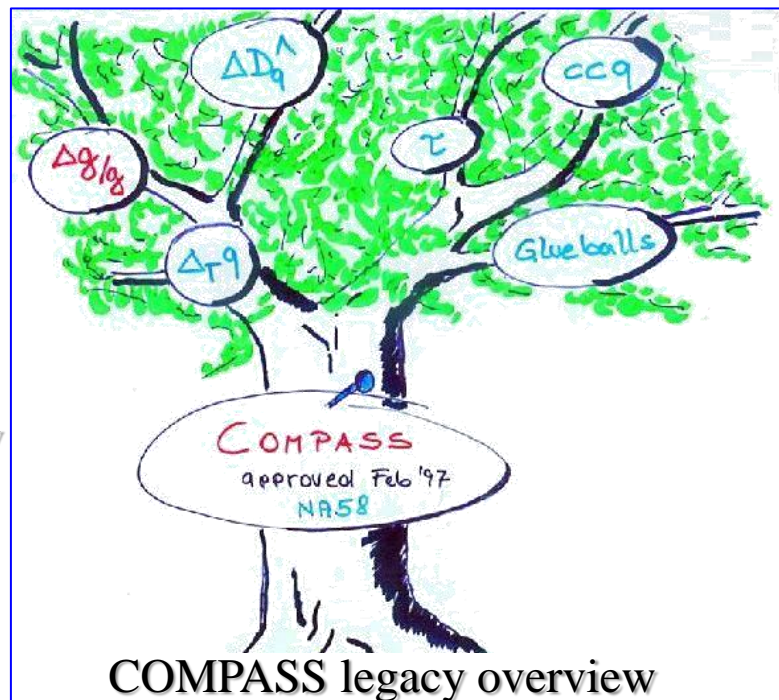


25 institutions from 13 countries
– nearly 200 physicists

- CERN SPS north area
- Fixed target experiment
- Approved in 1997 (**25 years**)
- Taking data since 2002 (**20 years**)

International Workshop on Hadron Structure and Spectroscopy
IWHSS-2022 workshop (**anniversary edition**)

CERN Globe, August 29-31, 2022



F. Bradamante S. Paul G. Mallot

<https://indico.cern.ch/e/IWHSS-2022>

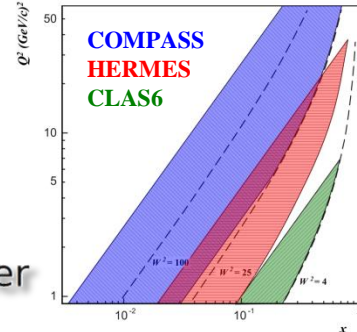
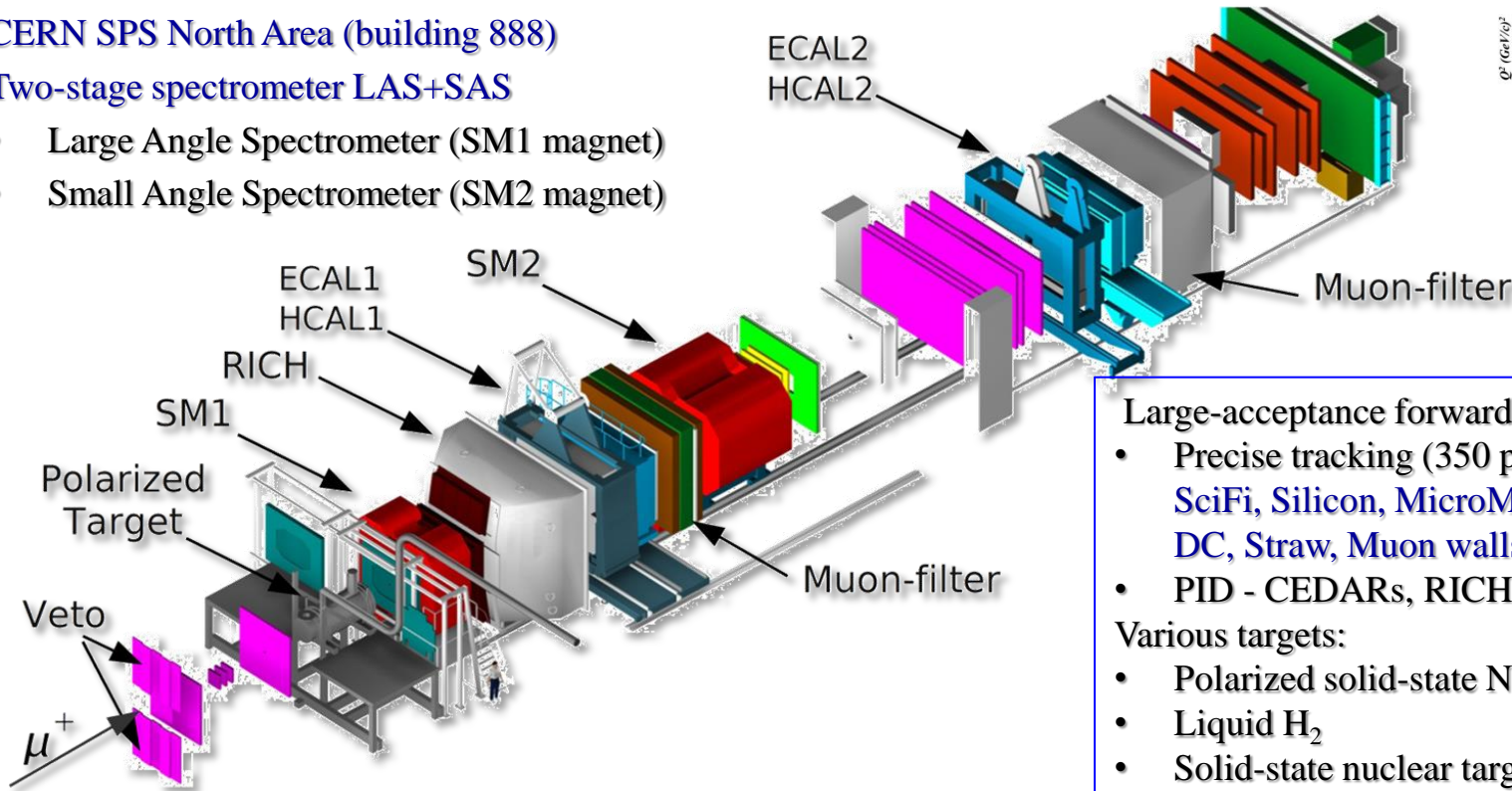


COMPASS experimental setup

COmmon MUon Proton Apparatus for Structure and Spectroscopy

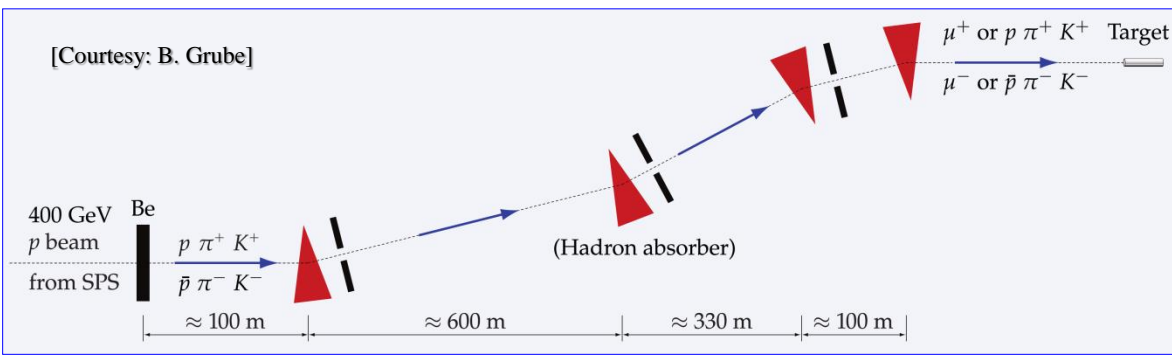
CERN SPS North Area (building 888)
Two-stage spectrometer LAS+SAS

- Large Angle Spectrometer (SM1 magnet)
- Small Angle Spectrometer (SM2 magnet)



- Large-acceptance forward spectrometer
- Precise tracking (350 planes)
SciFi, Silicon, MicroMegas, GEM, MWPC, DC, Straw, Muon walls
 - PID - CEDARs, RICH, calorimeters, MWs
- Various targets:
- Polarized solid-state NH₃ or ⁶LiD
 - Liquid H₂
 - Solid-state nuclear targets (e.g. Ni, W, Pb)

- Primary beam - 400 GeV *p* from SPS
 - impinging on Be production target (T6)
- 190 GeV secondary hadron beams
 - h⁻ beam: 97% π⁻, 2% K⁻, 1% *p*
 - h⁺ beam: 75% *p*, 24% π⁺, 1% K⁺
- 160 GeV tertiary muon beams
 - μ[±] longitudinally polarized



COMPASS experimental setup: Phase II (DVCS programme)

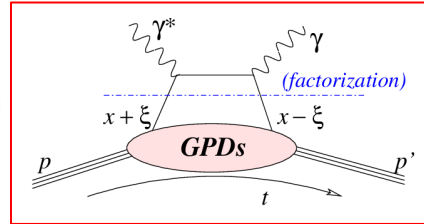
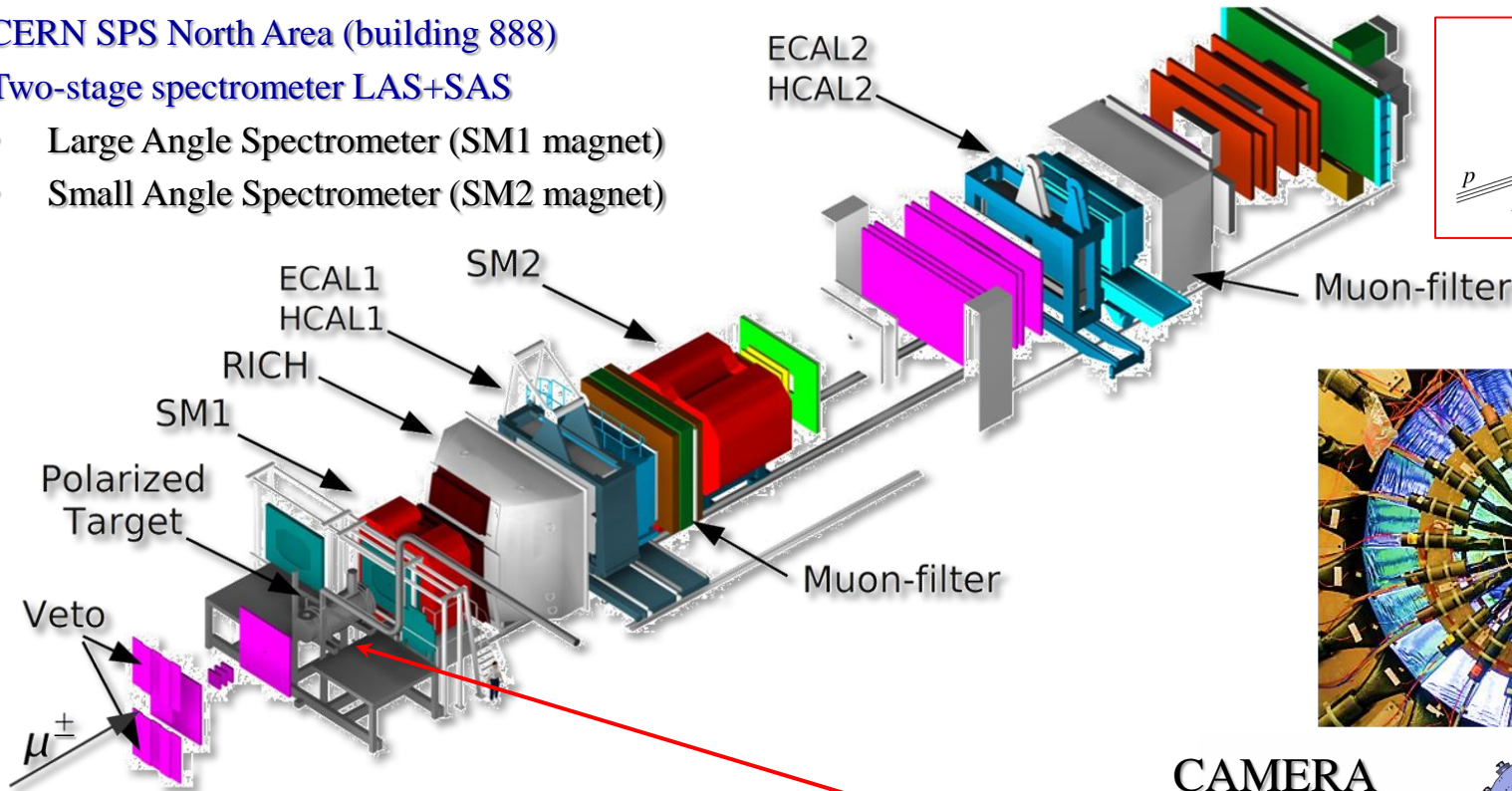


COmmon MUon Proton Apparatus for Structure and Spectroscopy

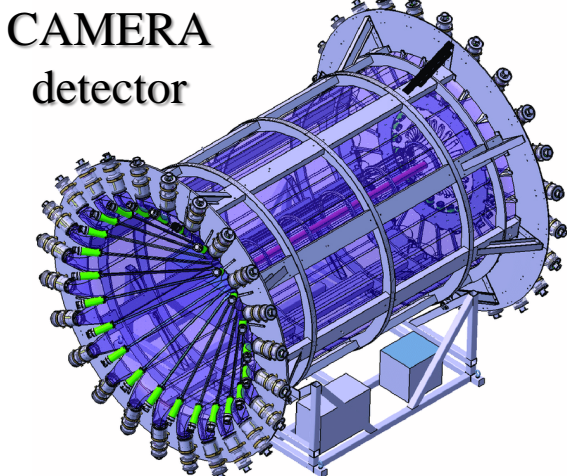
CERN SPS North Area (building 888)

Two-stage spectrometer LAS+SAS

- Large Angle Spectrometer (SM1 magnet)
- Small Angle Spectrometer (SM2 magnet)



- Primary beam - 400 GeV p from SPS
 - impinging on Be production target (T6)
- 190 GeV secondary hadron beams
 - h^- beam: 97% π^- , 2% K^- , 1% p
 - h^+ beam: 75% p , 24% π^+ , 1% K^+
- 160 GeV tertiary muon beams
 - μ^\pm longitudinally polarized



COMPASS experimental setup: Phase II (SIDIS programme)

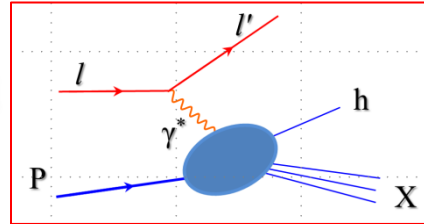
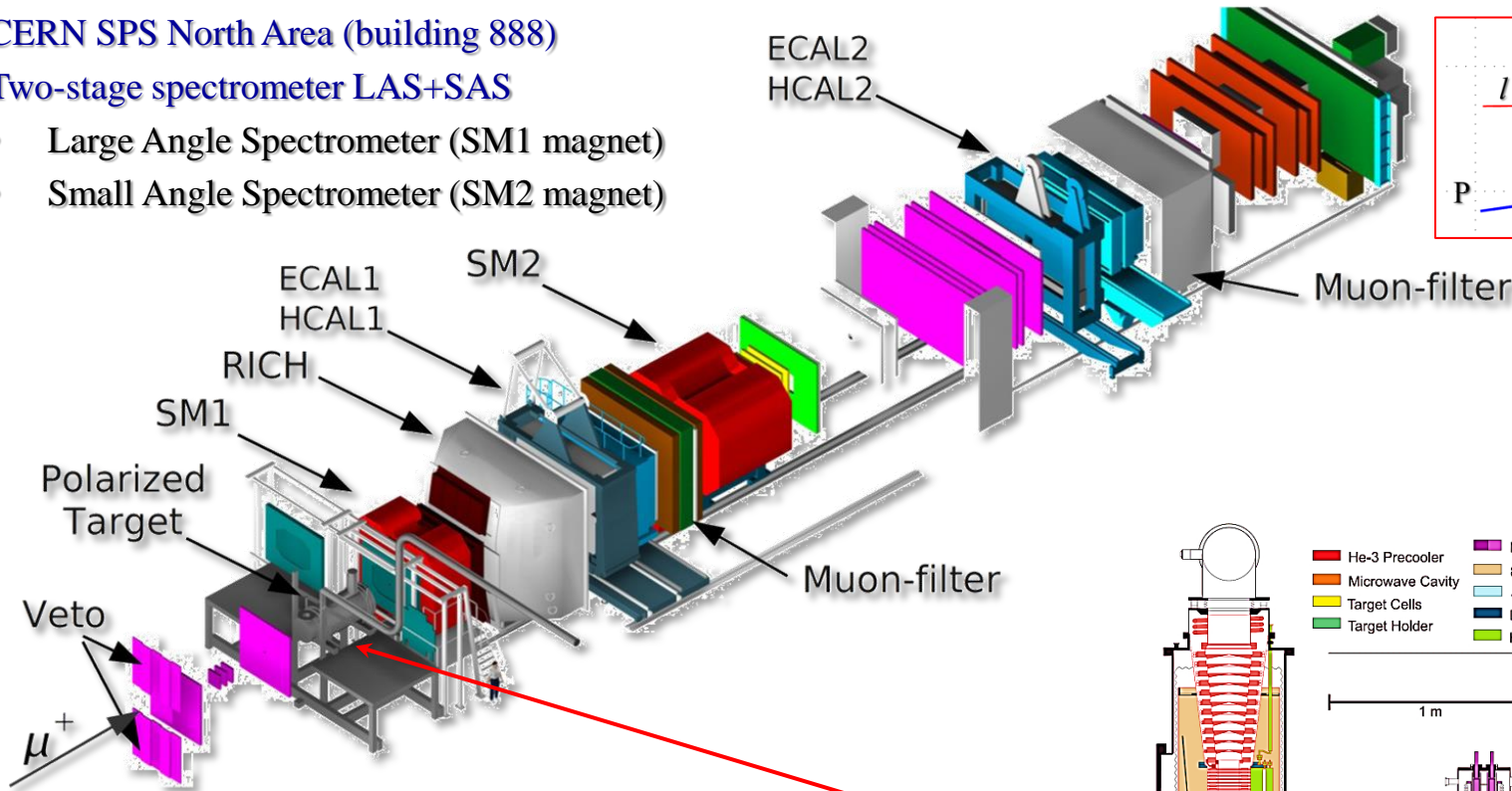


Common Muon Proton Apparatus for Structure and Spectroscopy

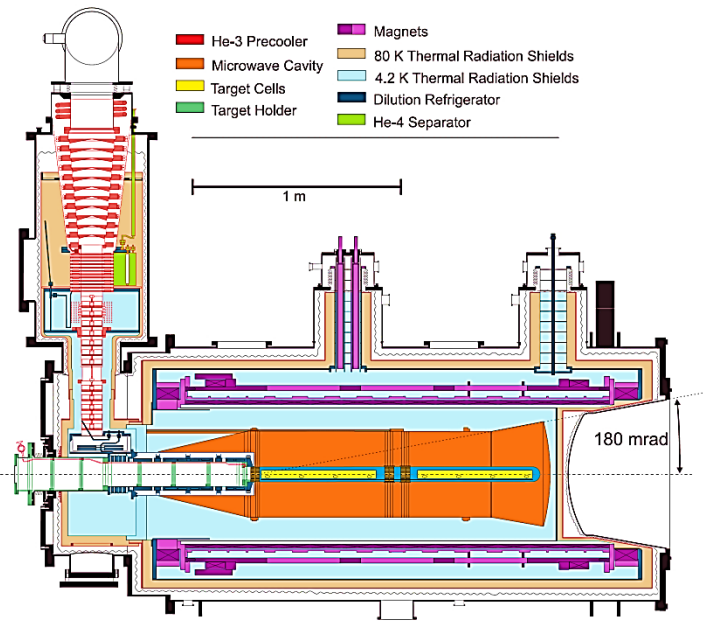
CERN SPS North Area (building 888)

Two-stage spectrometer LAS+SAS

- Large Angle Spectrometer (SM1 magnet)
- Small Angle Spectrometer (SM2 magnet)



- Primary beam - 400 GeV p from SPS
 - impinging on Be production target (T6)
- 190 GeV secondary hadron beams
 - h^- beam: 97% π^- , 2% K^- , 1% p
 - h^+ beam: 75% p , 24% π^+ , 1% K^+
- 160 GeV tertiary muon beams
 - μ^+ longitudinally polarized





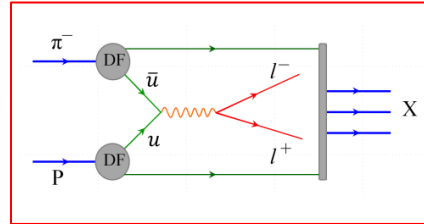
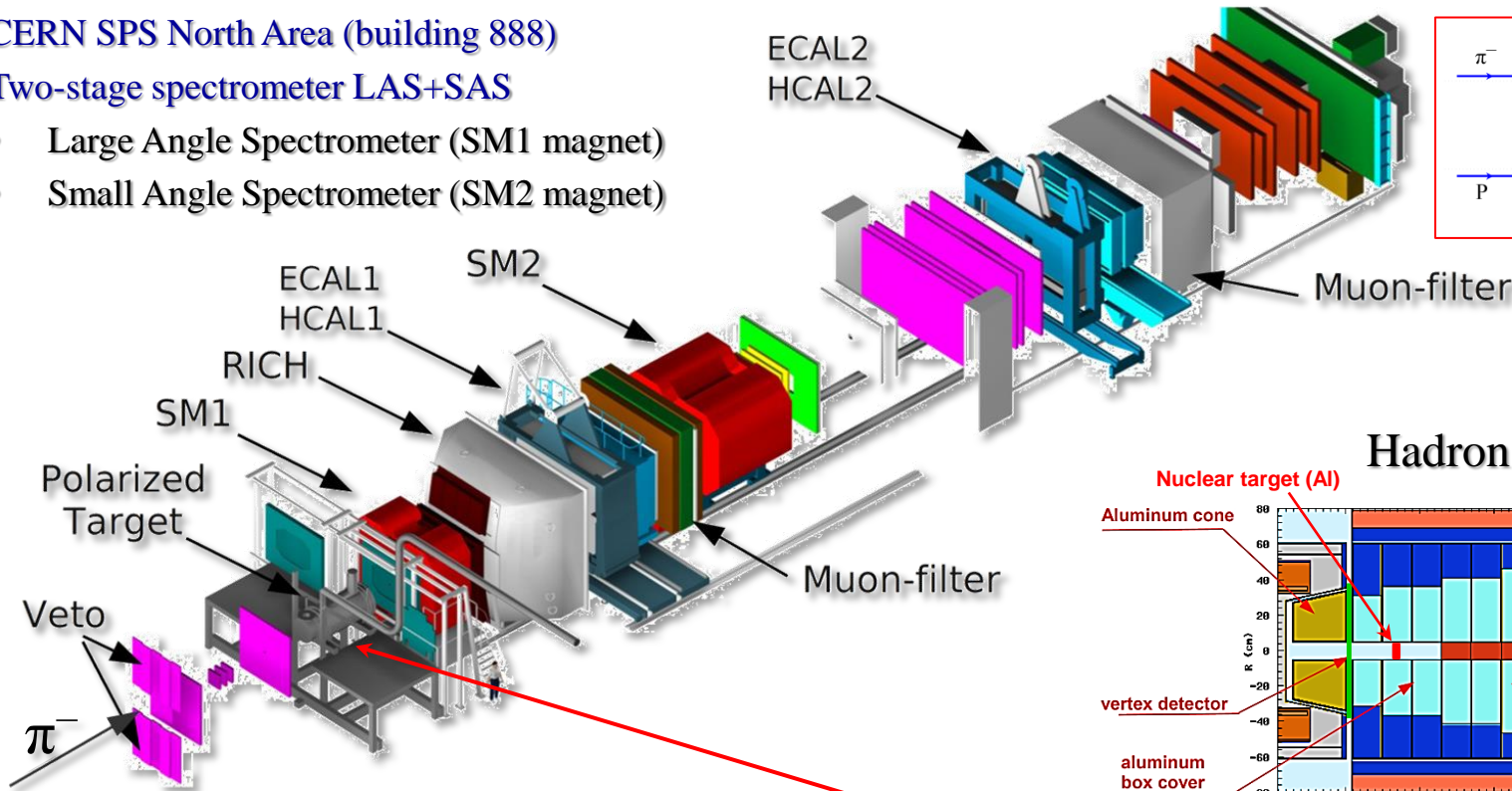
COMPASS experimental setup: Phase II (DY programme)

COmmon MUon Proton Apparatus for Structure and Spectroscopy

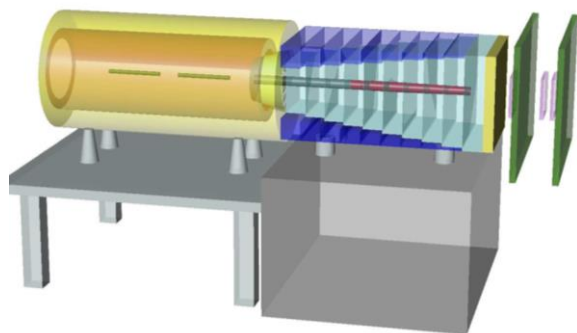
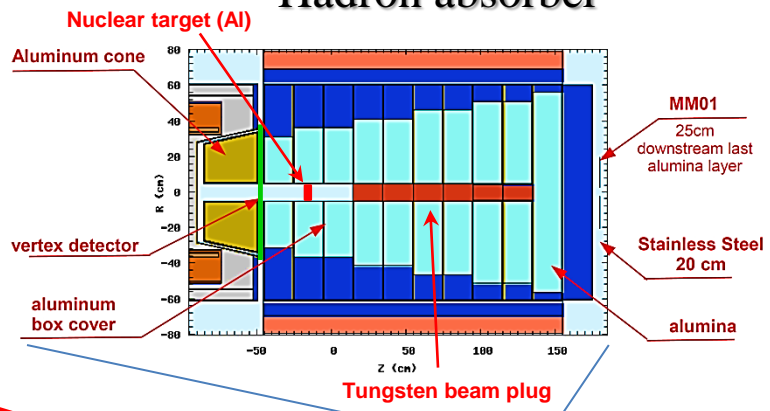
CERN SPS North Area (building 888)

Two-stage spectrometer LAS+SAS

- Large Angle Spectrometer (SM1 magnet)
- Small Angle Spectrometer (SM2 magnet)



Hadron absorber



- Primary beam - 400 GeV p from SPS
 - impinging on Be production target (T6)
- 190 GeV secondary hadron beams
 - h^- beam: 97% π^- , 2% K^- , 1% p
 - h^+ beam: 75% p , 24% π^+ , 1% K^+
- 160 GeV tertiary muon beams
 - μ^\pm longitudinally polarized

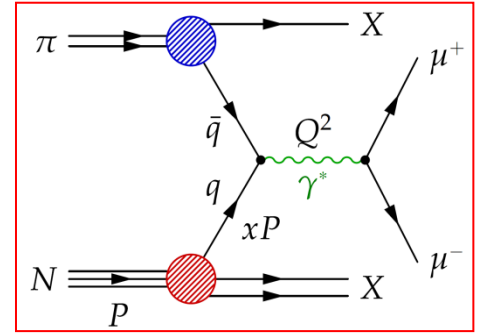
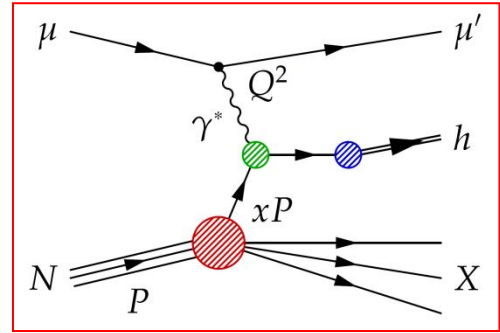
The COMPASS Experiment at the CERN SPS

Broad Physics Program to study Structure and Excitation Spectrum of Hadrons

Increasing resolution scale
(momentum transfer)

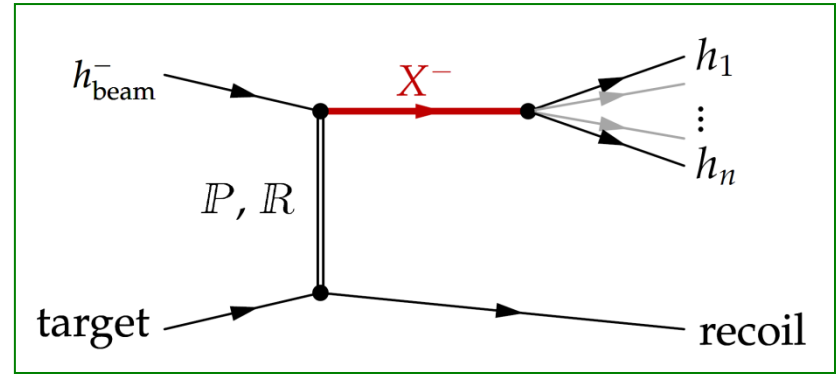
Nucleon structure

- Hard scattering of μ^\pm and π^- off (un)polarized P/D targets
- Study of nucleon spin structure
- Parton distribution functions and fragmentation functions



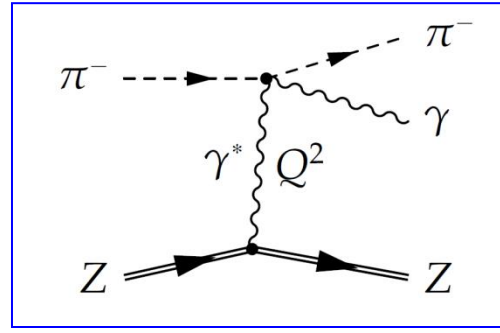
Hadron spectroscopy

- Diffractive $\pi(K)$ dissociation reaction with proton target
- PWA technique employed
- High-precision measurement of light-meson excitation spectrum
- Search for exotic states



Chiral dynamics

- Test chiral perturbation theory in $\pi(K) \gamma$ reactions
- π^\pm and K^\pm polarizabilities
- Chiral anomaly $F_{3\pi}$



The COMPASS Experiment at the CERN SPS

Broad Physics Program to study Structure and Excitation Spectrum of Hadrons

PRL 114, 062002 (2015)

Measurement of the Charged-Pion Polarizability

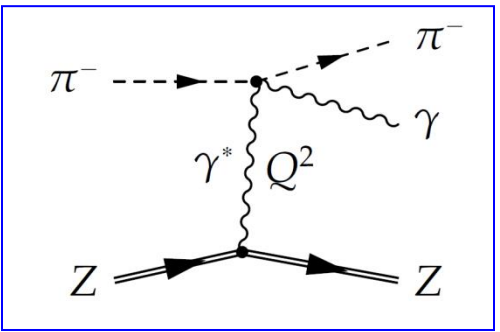
(COMPASS Collaboration)

(Received 2 June 2014; revised manuscript received 24 December 2014; published 10 February 2015)

The COMPASS collaboration at CERN has investigated pion Compton scattering, $\pi^- \gamma \rightarrow \pi^- \gamma$, at center-of-mass energy below 3.5 pion masses. The process is embedded in the reaction $\pi^- \text{Ni} \rightarrow \pi^- \gamma \text{Ni}$, which is initiated by 190 GeV pions impinging on a nickel target. The exchange of quasilocal photons is selected by isolating the sharp Coulomb peak observed at smallest momentum transfers, $Q^2 < 0.0015 \text{ (GeV}/c)^2$. From a sample of 63 000 events, the pion electric polarizability is determined to be $\alpha_\pi = (2.0 \pm 0.6_{\text{stat}} \pm 0.7_{\text{syst}}) \times 10^{-4} \text{ fm}^3$ under the assumption $\alpha_\pi = -\beta_\pi$, which relates the electric and magnetic dipole polarizabilities. It is the most precise measurement of this fundamental low-energy parameter of strong interaction that has been addressed since long by various methods with conflicting outcomes. While this result is in tension with previous dedicated measurements, it is found in agreement with the expectation from chiral perturbation theory. An additional measurement replacing pions by muons, for which the cross-section behavior is unambiguously known, was performed for an independent estimate of the systematic uncertainty.

$$\alpha_\pi = (2.0 \pm 0.6_{\text{stat}} \pm 0.7_{\text{syst}}) \times 10^{-4} \text{ fm}^3$$

Increasing resolution scale
(momentum transfer)

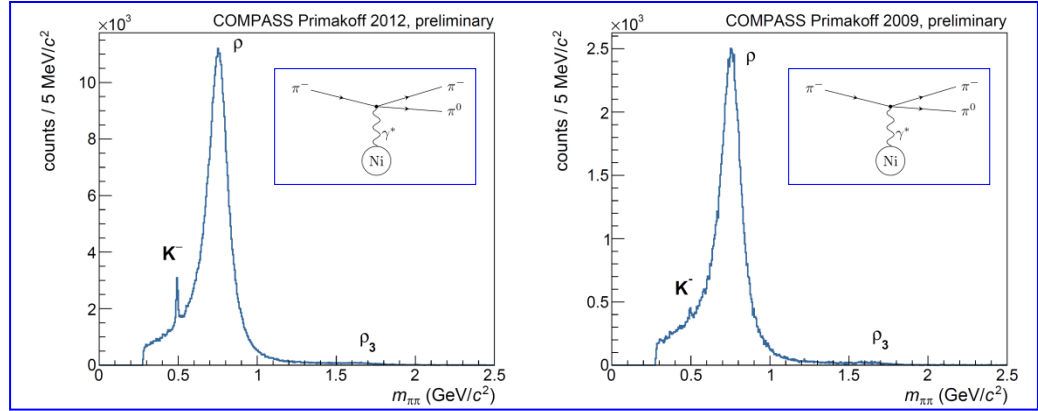


Chiral dynamics

- Test chiral perturbation theory in $\pi(K) \gamma$ reactions
- π^\pm and K^\pm polarizabilities
- Chiral anomaly $F_{3\pi}$

ongoing analysis:

study of chiral anomaly in $\pi^- \gamma \rightarrow \pi^- \pi^0$

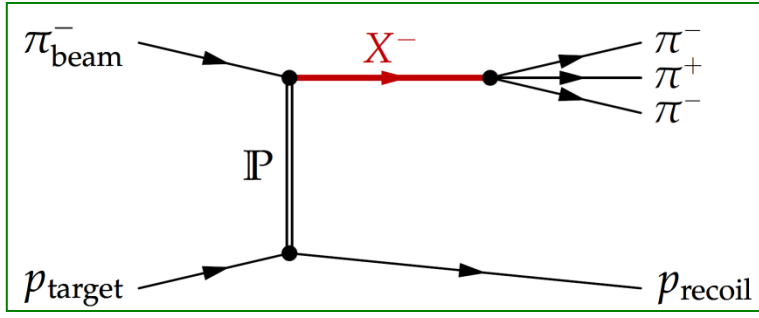




The COMPASS Experiment at the CERN SPS

Broad Physics Program to study Structure and Excitation Spectrum of Hadrons

Increasing resolution scale (momentum transfer)

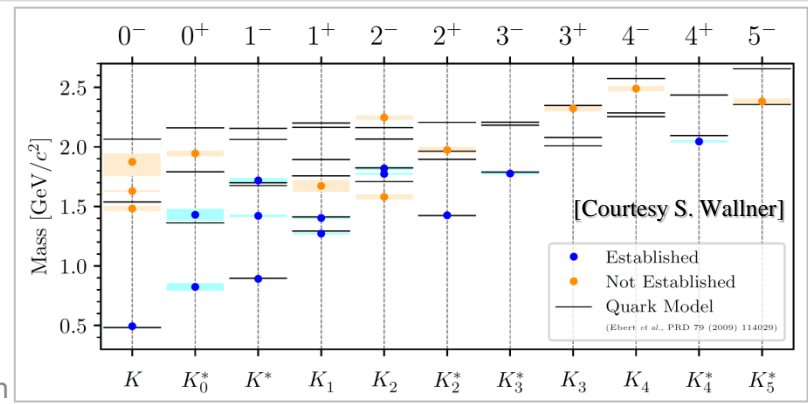
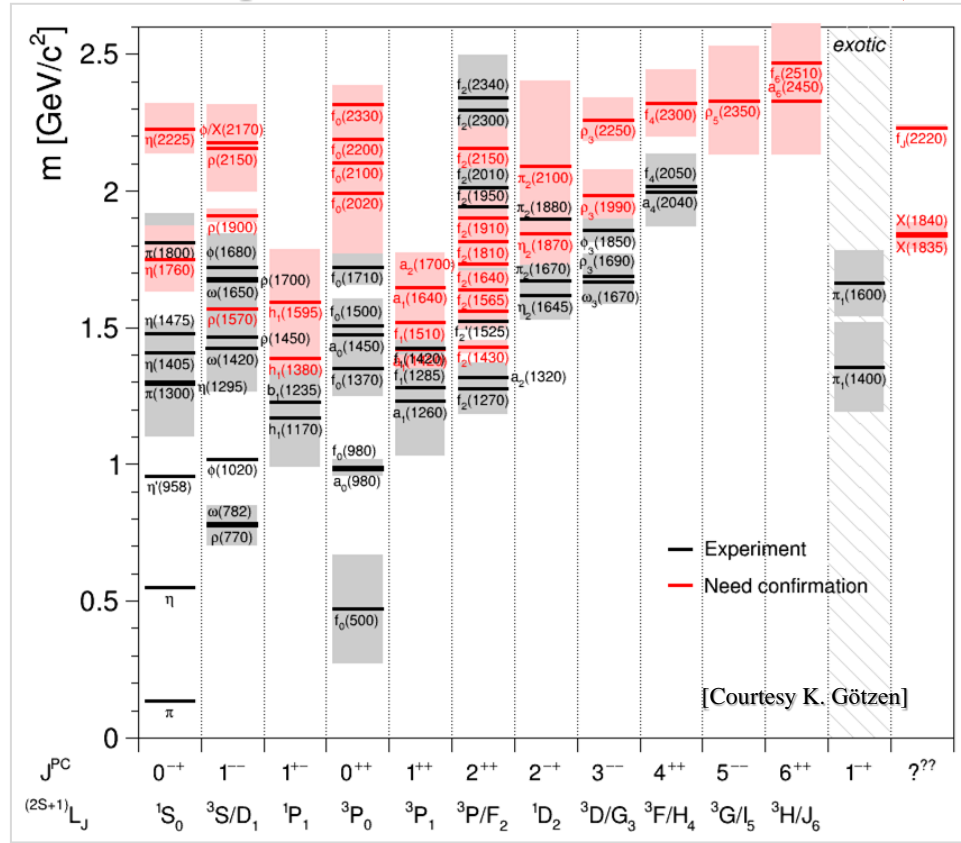


Hadron spectroscopy

- Diffractive $\pi(K)$ dissociation reaction with proton target
- PWA technique employed
- High-precision measurement of light-meson excitation spectrum
- Search for exotic states

Chiral dynamics

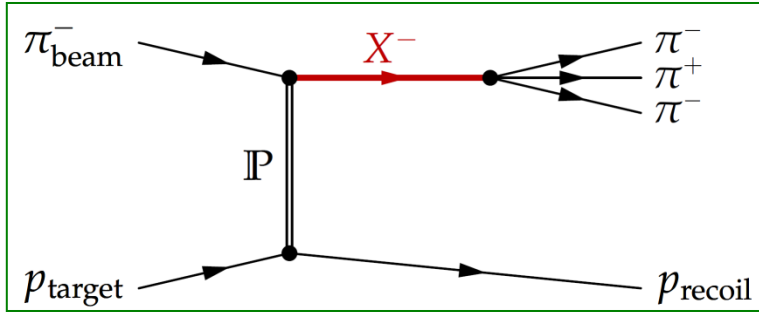
- Test chiral perturbation theory in $\pi(K) \gamma$ reactions
- π^\pm and K^\pm polarizabilities
- Chiral anomaly $F_{3\pi}$



The COMPASS Experiment at the CERN SPS

Broad Physics Program to study Structure and Excitation Spectrum of Hadrons

Increasing resolution scale
(momentum transfer)



Hadron spectroscopy

- Diffractive $\pi(K)$ dissociation reaction with proton target
- PWA technique employed
- High-precision measurement of light-meson excitation spectrum
- Search for exotic states

Chiral dynamics

- Test chiral perturbation theory in $\pi(K) \gamma$ reactions
- π^\pm and K^\pm polarizabilities
- Chiral anomaly $F_{3\pi}$

2021-2022 analyses/activities

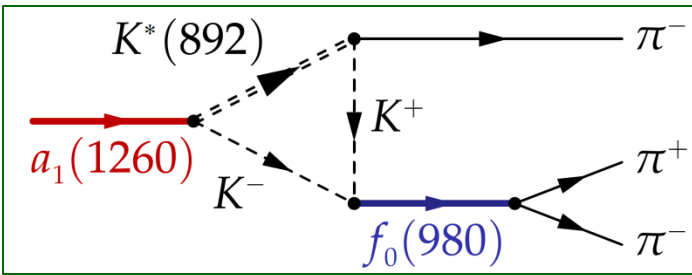
Study of π_1 states $\pi^- p \rightarrow b_1(1235)\pi^- p$ $\pi^- p \rightarrow f_1(1285)\pi^- p$	new study event selection
Study of π_1 states $\pi^- p \rightarrow \pi^- \eta^{(\prime)} p$	ongoing study improved event selection
Triangle singularity as the origin of the $a_1(1420)$ in $\pi^- p \rightarrow \pi^- \pi^- \pi^+ p$	August 2021 PRL 127 (2021) 082501
The exotic meson $\pi_1(1600)$ with $J^{PC} = 1^{-+}$ and its decay into $\rho(770)\pi$	January 2022 PRD 105(2022)1,012005
Excited kaons in: $K^- p \rightarrow K^- \pi^- \pi^+ p$	ongoing study systematic effects
Excited kaons in: $K^- p \rightarrow \pi^- K_S^0 p$ $K^- p \rightarrow \Lambda p p$	new study event selection
Isovector resonances in: $\pi^- p \rightarrow K^- K_S^0 p$	new study event selection



The COMPASS Experiment at the CERN SPS

Broad Physics Program to study Structure and Excitation Spectrum of Hadrons

Increasing resolution scale (momentum transfer)



Hadron spectroscopy

- Diffractive $\pi(K)$ dissociation reaction with proton target
- PWA technique employed
- High-precision measurement of light-meson excitation spectrum
- Search for exotic states

Chiral dynamics

- Test chiral perturbation theory in $\pi(K) \gamma$ reactions
- π^\pm and K^\pm polarizabilities
- Chiral anomaly $F_{3\pi}$

PHYSICAL REVIEW LETTERS **127**, 082501 (2021)

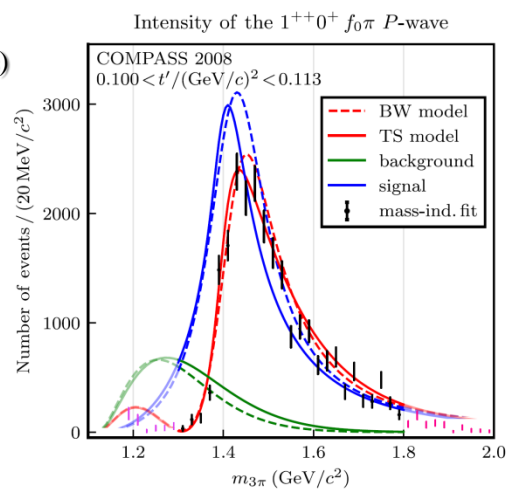
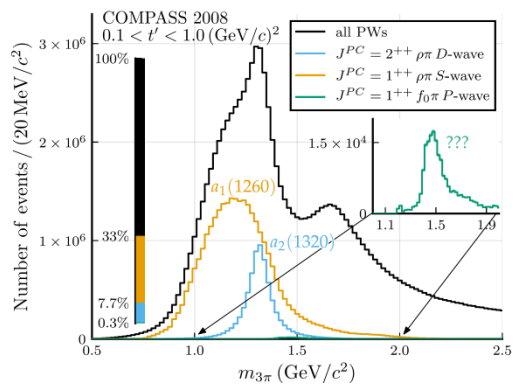
Triangle Singularity as the Origin of the $a_1(1420)$

(Received 3 July 2020; revised 4 May 2021; accepted 26 May 2021; published 18 August 2021)

The COMPASS Collaboration experiment recently discovered a new isovector resonancelike signal with axial-vector quantum numbers, the $a_1(1420)$, decaying to $f_0(980)\pi$. With a mass too close to and a width smaller than the axial-vector ground state $a_1(1260)$, it was immediately interpreted as a new light exotic meson, similar to the X, Y, Z states in the hidden-charm sector. We show that a resonancelike signal fully matching the experimental data is produced by the decay of the $a_1(1260)$ resonance into $K^*(\rightarrow K\pi)\bar{K}$ and subsequent rescattering through a triangle singularity into the coupled $f_0(980)\pi$ channel. The amplitude for this process is calculated using a new approach based on dispersion relations. The triangle-singularity model is fitted to the partial-wave data of the COMPASS experiment. Despite having fewer parameters, this fit shows a slightly better quality than the one using a resonance hypothesis and thus eliminates the need for an additional resonance in order to describe the data. We thereby demonstrate for the first time in the light-meson sector that a resonancelike structure in the experimental data can be described by rescattering through a triangle singularity, providing evidence for a genuine three-body effect.

DOI: 10.1103/PhysRevLett.127.082501

COMPASS, PRD 95 (2017) 032004
Surprising Signal with $J^{PC} = 1^{++}$ (1.4 GeV/c)

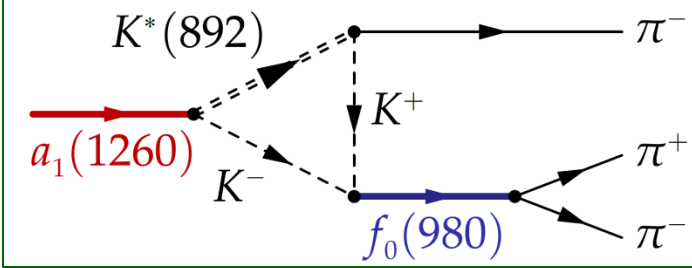


For this and other topics see CERN-EP-seminar

The COMPASS Experiment at the CERN SPS

Broad Physics Program to study Structure and Excitation Spectrum of Hadrons

Increasing resolution scale (momentum transfer)



Hadron spectroscopy

- Diffractive $\pi(K)$ dissociation reaction with proton target
- PWA technique employed
- High-precision measurement of light-meson excitation spectrum
- Search for exotic states

Chiral dynamics

- Test chiral perturbation theory in $\pi(K) \gamma$ reactions
- π^\pm and K^\pm polarizabilities
- Chiral anomaly $F_{3\pi}$

FLAVOUR PHYSICS | NEWS

COMPASS points to triangle singularity

23 August 2021

CERN COURIER

sciencealert Trending

(MirageC/Moment/Getty Images)

PHYSICS

Physicists Glimpse Signs of 'Triangle Singularity' in Unexpected First

PAUL SUTTER, LIVE SCIENCE
9 SEPTEMBER 2021

Physicists sifting through old particle accelerator data have found evidence of a highly-elusive, never-before-seen process: a so-called triangle singularity.

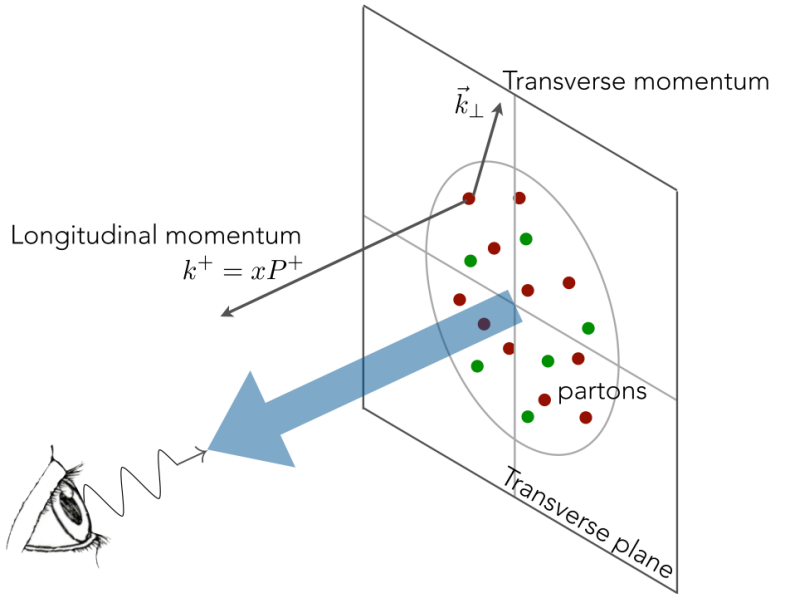
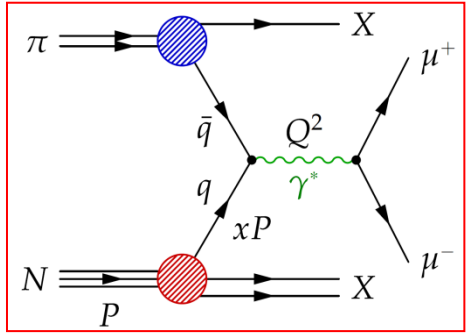
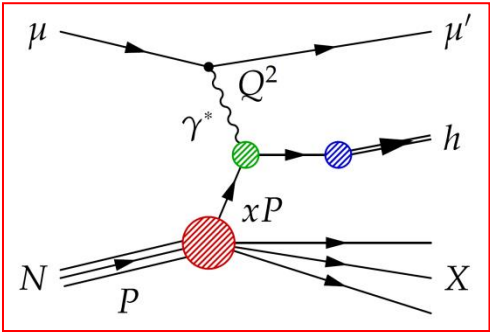
First envisioned by Russian physicist Lev Landau in the 1950s, a triangle singularity refers to a rare subatomic process where particles exchange identities before flying away from each other.

The COMPASS Experiment at the CERN SPS

Broad Physics Program to study Structure and Excitation Spectrum of Hadrons

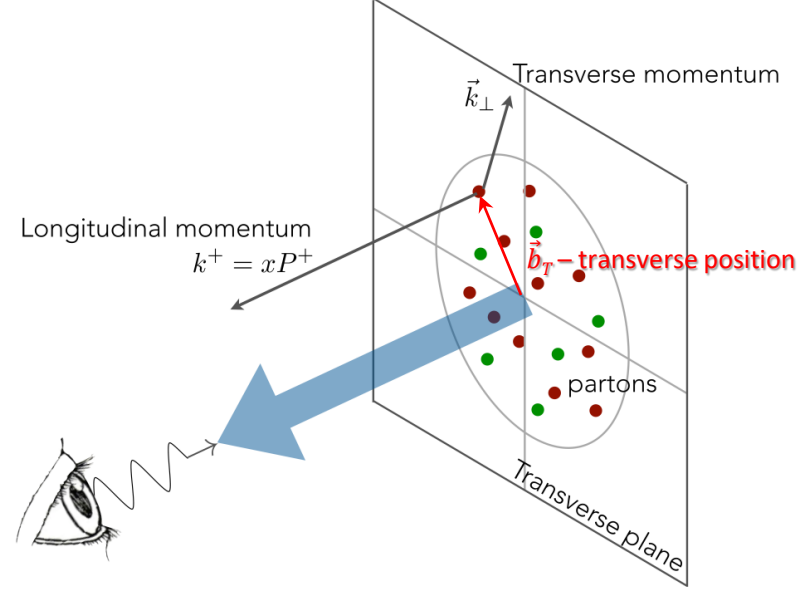
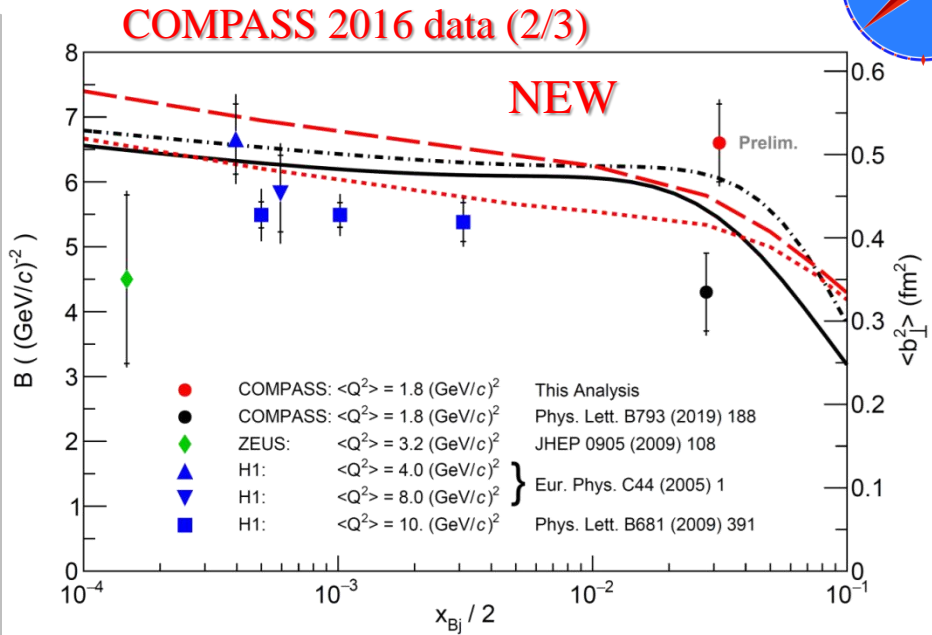
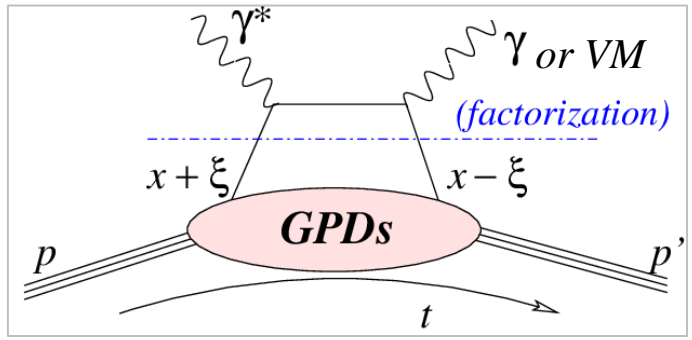
Increasing resolution scale
(momentum transfer)

- Nucleon structure**
 - Hard scattering of μ^\pm and π^- off (un)polarized P/D targets
 - Study of nucleon spin structure
 - Parton distribution functions and fragmentation functions
- Hadron spectroscopy**
 - Diffractive $\pi(K)$ dissociation reaction with proton target
 - PWA technique employed
 - High-precision measurement of light-meson excitation spectrum
 - Search for exotic states
- Chiral dynamics**
 - Test chiral perturbation theory in $\pi(K) \gamma$ reactions
 - π^\pm and K^\pm polarizabilities
 - Chiral anomaly $F_{3\pi}$



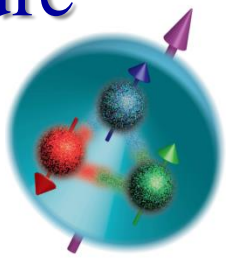
Nucleon transverse structure

- Transverse position \vec{b}_T of partons
 - Correlation between \vec{b}_T and x
 - Complementary to TMD PDFs
- 8 generalized parton distribution functions (GPDs)
 - Contain information about parton orbital angular momentum
 - Mostly unknown
- Measured in exclusive processes:
 - Deeply virtual Compton scattering (DVCS): $\mu + N \rightarrow \mu + \gamma + N$
 - Hard exclusive meson production (HEMP): $\mu + N \rightarrow \mu + VM + N$ with $VM = \pi^0, \rho(770), \omega(782), \dots$



Nucleon transverse structure

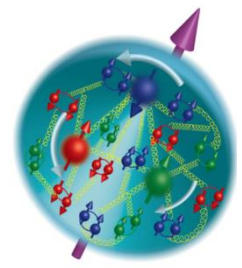
- 1964 Quark model



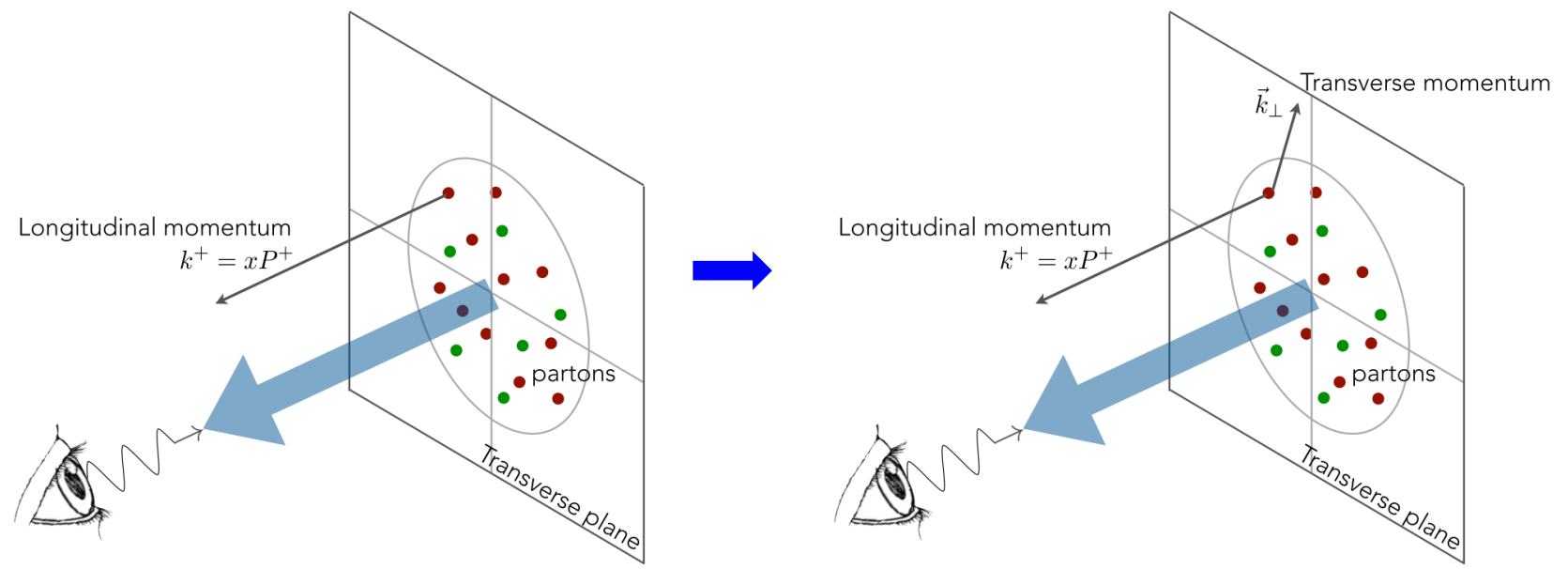
- 1969 Parton model



- 1973 asymptotic freedom and QCD



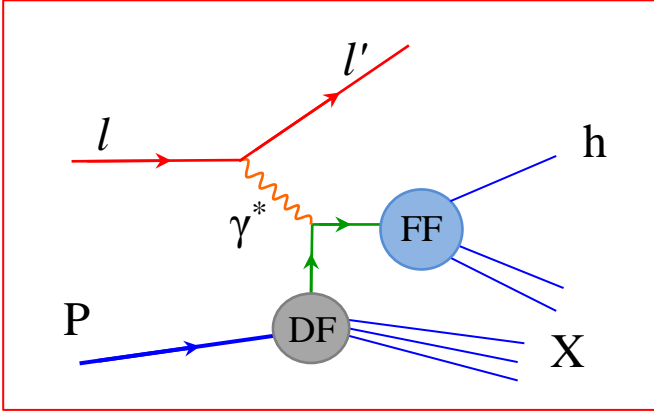
- 1978 intrinsic transverse motion of quarks and azimuthal asymmetries





Cahn effect in SIDIS

$$\frac{d\sigma}{dx dy dz dp_T^2 d\phi_h d\phi_S} = \left[\frac{\alpha}{xyQ^2} \frac{y^2}{2(1-\varepsilon)} \left(1 + \frac{\gamma^2}{2x} \right) \right] (F_{UU,T} + \varepsilon F_{UU,L}) \times \left(1 + \sqrt{2\varepsilon(1+\varepsilon)} A_{UU}^{\cos\phi_h} \cos\phi_h + \dots \right)$$



Cahn effect

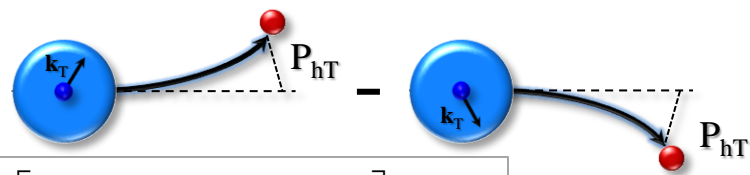
R.N. Cahn, **PLB 78 (1978)**



The point that there are azimuthal dependences, which arise from the transverse momenta of the partons was clearly stated in this papers:

- T.P. Cheng and A. Zee, **Phys. Rev. D6 (1972)** 885;
- F. Ravndal, **Phys. Lett. 43B (1973)** 301.
- R.L. Kingsley, **Phys. Rev. D10 (1974)** 1580;
- A.M. Kotsinyan, **Teor. Mat. Fiz. 24 (1975)** 206;

$$k_T \rightarrow \cos\varphi_q \rightarrow \cos\varphi_h$$

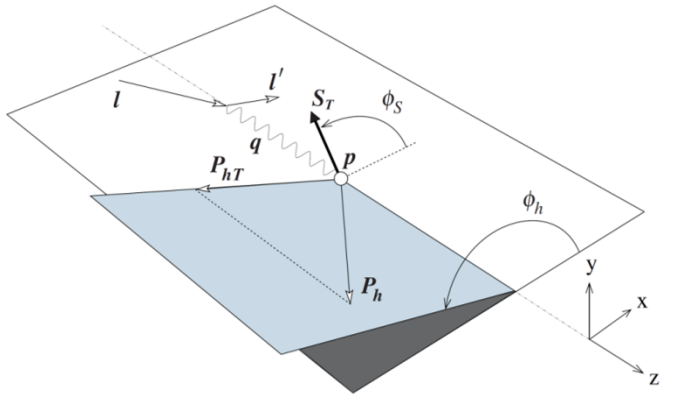


$$\hat{s} \approx xs \left[1 - 2\sqrt{1-y} \frac{k_T}{Q} \cdot \cos\varphi_q \right]$$

$$\hat{u} \approx -xs(1-y) \left[1 - \frac{2k_T}{Q\sqrt{1-y}} \cdot \cos\varphi_q \right]$$


$$\hat{t} = -Q^2 = -xys, \quad \text{where } s = (l + P)^2$$

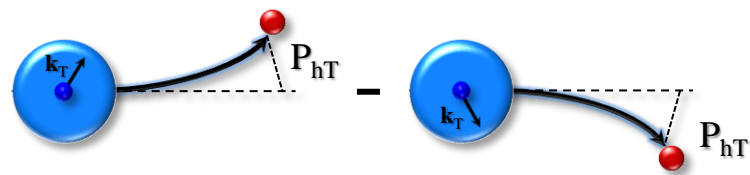
$$d\sigma^{lp \rightarrow l'hX} \propto d\sigma^{lq \rightarrow lq} \propto \frac{\hat{s}^2 + \hat{u}^2}{\hat{t}^2}$$



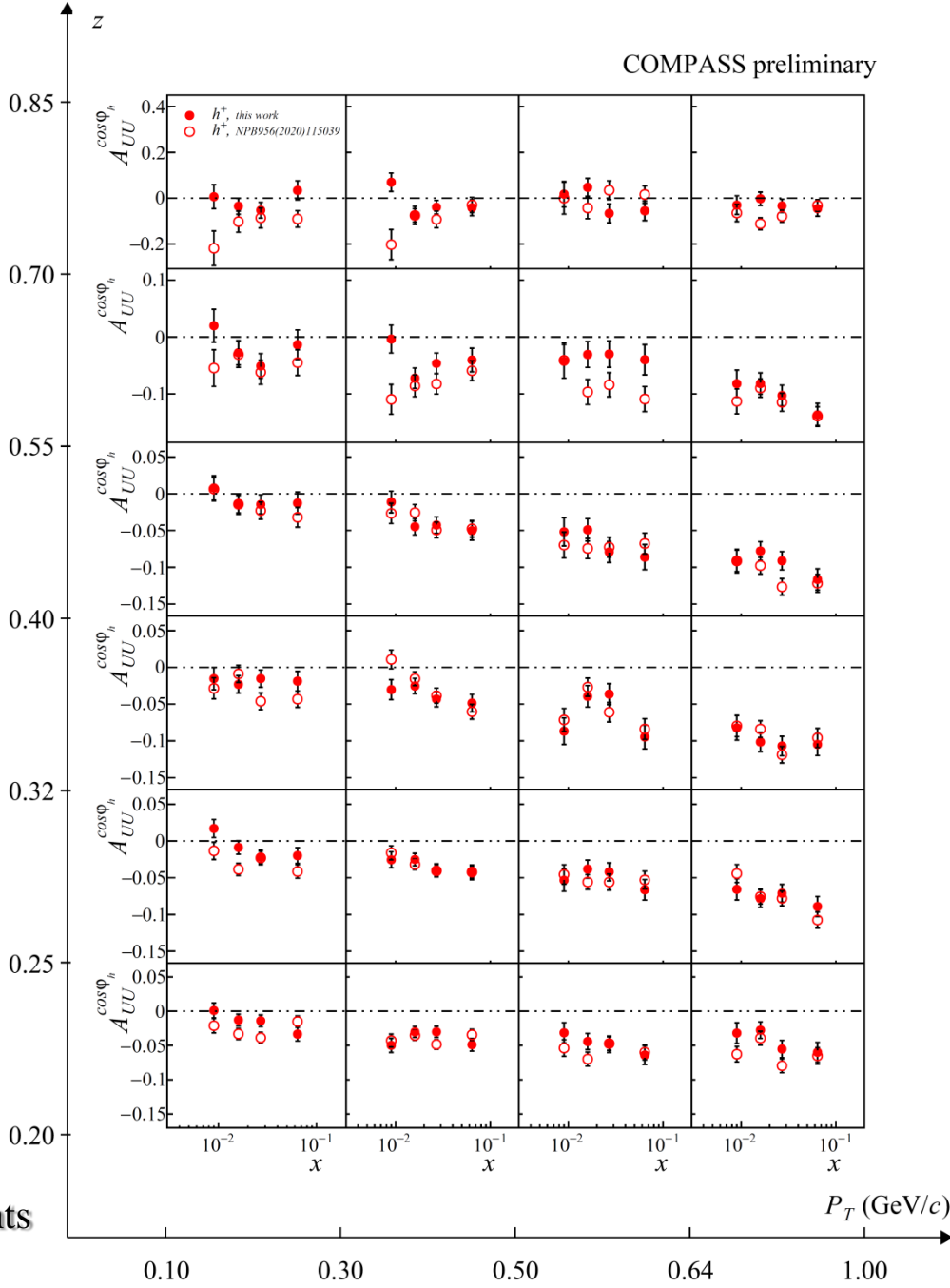
Cahn effect in SIDIS

$$\frac{d\sigma}{dx dy dz dp_T^2 d\phi_h d\phi_S} = \left[\frac{\alpha}{xyQ^2} \frac{y^2}{2(1-\varepsilon)} \left(1 + \frac{\gamma^2}{2x} \right) \right] (F_{UU,T} + \varepsilon F_{UU,L}) \times (1 + \sqrt{2\varepsilon(1+\varepsilon)} A_{UU}^{\cos\phi_h} \cos\phi_h + \dots)$$

Quark	U
Nucleon	$f_1^q(x, k_T^2)$ number density 
U	





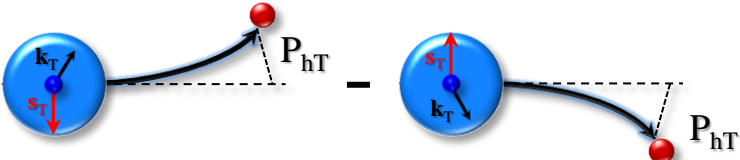
As of 1978 – simplistic kinematic effect:
non-zero k_T induces an azimuthal modulation
 As of 2022 – complex SF (twist-2/3 functions)
 A number of measurements by different experiments



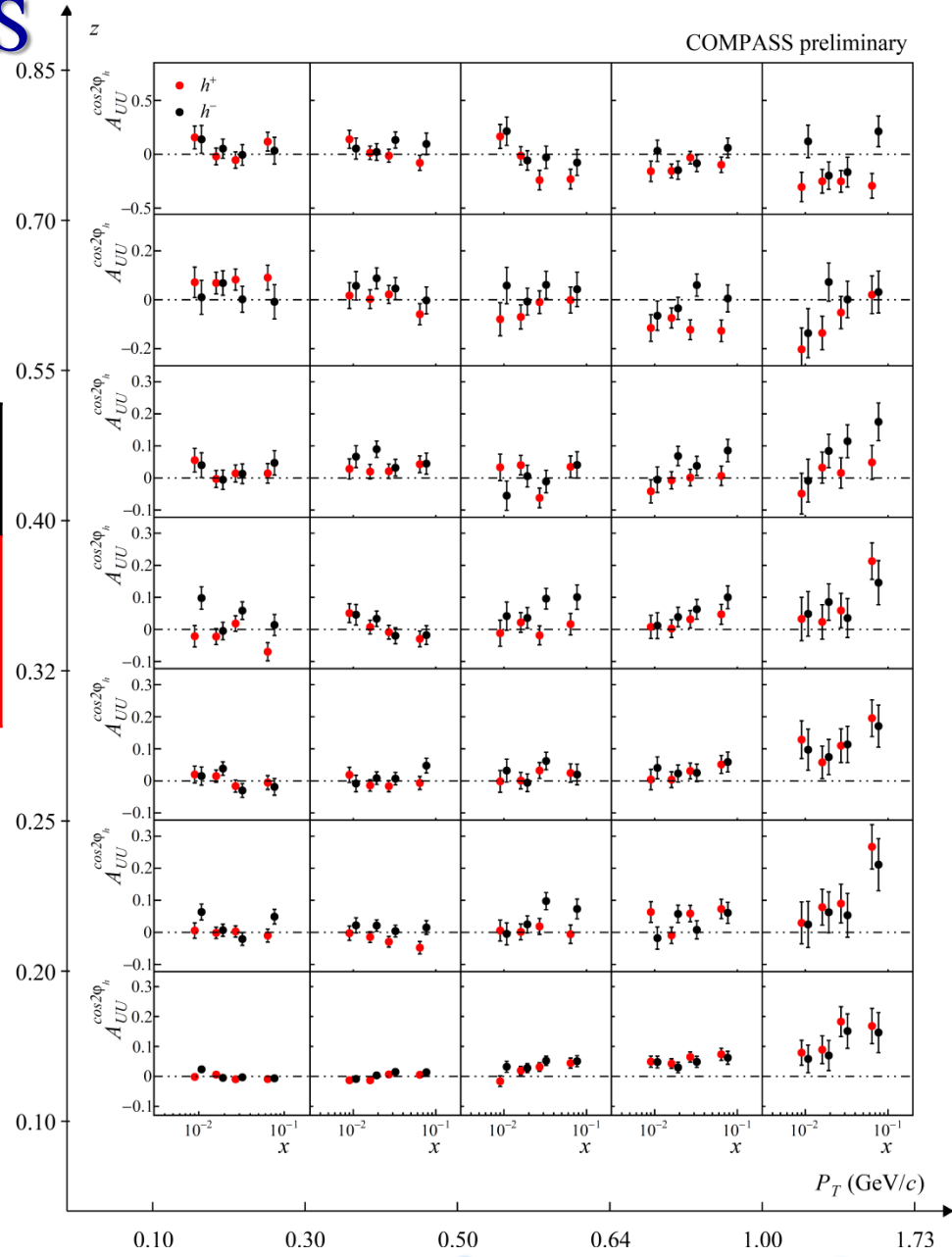
Boer-Mulders effect in SIDIS



$$\frac{d\sigma}{dx dy dz dp_T^2 d\phi_h d\phi_s} = \left[\frac{\alpha}{xyQ^2} \frac{y^2}{2(1-\varepsilon)} \left(1 + \frac{\gamma^2}{2x} \right) \right] (F_{UU,T} + \varepsilon F_{UU,L}) \times (1 + \sqrt{2\varepsilon(1+\varepsilon)} A_{UU}^{\cos\phi_h} \cos\phi_h + \varepsilon A_{UU}^{\cos 2\phi_h} \cos 2\phi_h + \dots)$$

Quark	U		T
Nucleon			
U	$f_1^q(x, k_T^2)$ number density 		$h_1^{\perp q}(x, k_T^2)$ Boer-Mulders 






Arises due to the correlation between quark transverse spin and intrinsic transverse momentum

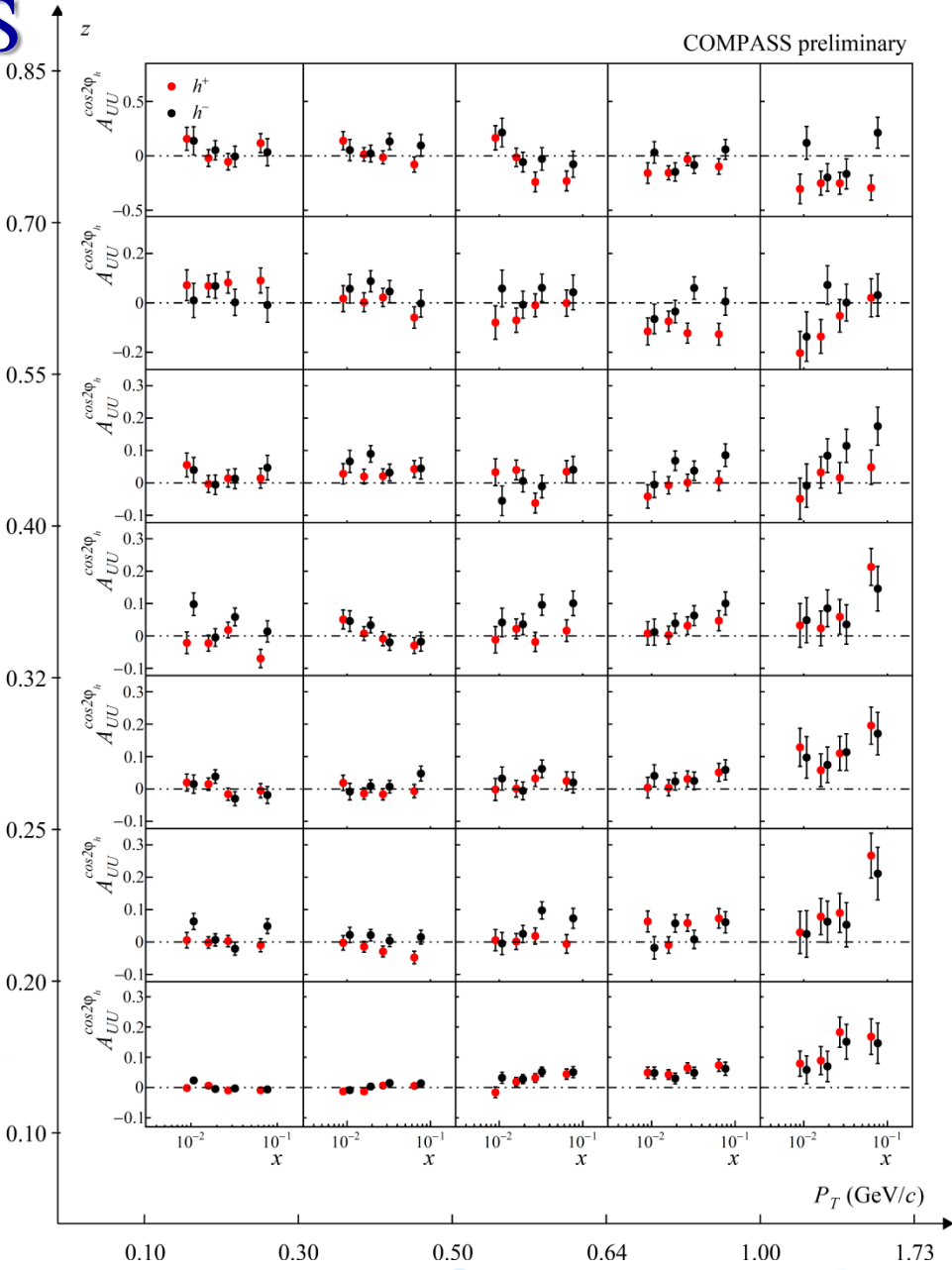
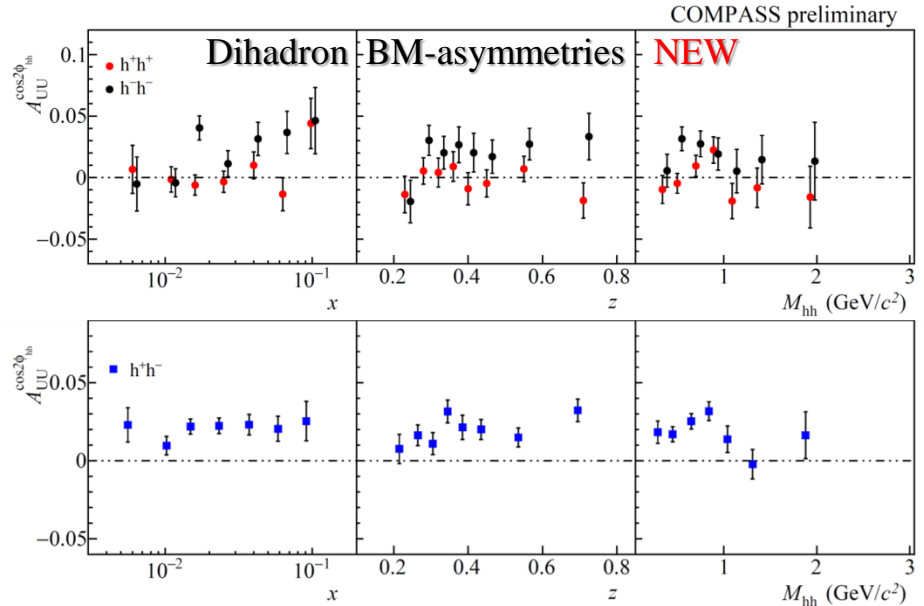


 spin of the quark  k_T

Boer-Mulders effect in SIDIS

$$\frac{d\sigma}{dx dy dz dp_T^2 d\phi_h d\phi_S} = \left[\frac{\alpha}{xyQ^2} \frac{y^2}{2(1-\varepsilon)} \left(1 + \frac{\gamma^2}{2x} \right) \right] (F_{UU,T} + \varepsilon F_{UU,L}) \times (1 + \sqrt{2\varepsilon(1+\varepsilon)} A_{UU}^{\cos\phi_h} \cos\phi_h + \varepsilon A_{UU}^{\cos 2\phi_h} \cos 2\phi_h + \dots)$$

Quark	U		T
Nucleon			
U	$f_1^q(x, k_T^2)$ number density 		$h_1^{\perp q}(x, k_T^2)$ Boer-Mulders  - 

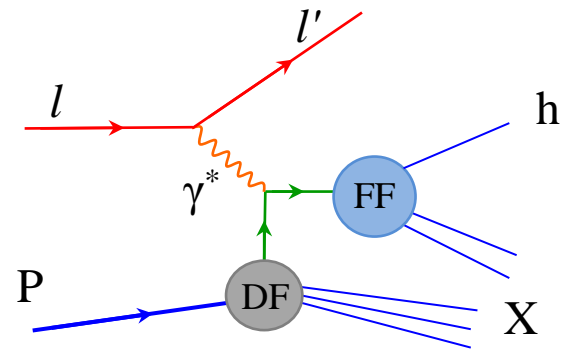




SIDIS x-section and TMDs at twist-2

$$\frac{d\sigma}{dx dy dz dp_T^2 d\phi_h d\phi_s} = \text{All measured by COMPASS}$$

$$\left[\frac{\alpha}{xyQ^2} \frac{y^2}{2(1-\varepsilon)} \left(1 + \frac{\gamma^2}{2x} \right) \right] (F_{UU,T} + \varepsilon F_{UU,L})$$



$$\times \left\{ \begin{array}{l} \left[\begin{array}{l} 1 + \sqrt{2\varepsilon(1+\varepsilon)} A_{UU}^{\cos\phi_h} \cos\phi_h + \varepsilon A_{UU}^{\cos 2\phi_h} \cos 2\phi_h \\ + \lambda \sqrt{2\varepsilon(1-\varepsilon)} A_{LU}^{\sin\phi_h} \sin\phi_h \end{array} \right] \\ + S_L \left[\begin{array}{l} \sqrt{2\varepsilon(1+\varepsilon)} A_{UL}^{\sin\phi_h} \sin\phi_h + \varepsilon A_{UL}^{\sin 2\phi_h} \sin 2\phi_h \\ + S_L \lambda \left[\sqrt{1-\varepsilon^2} A_{LL} + \sqrt{2\varepsilon(1-\varepsilon)} A_{LL}^{\cos\phi_h} \cos\phi_h \right] \end{array} \right] \\ + S_T \left[\begin{array}{l} A_{UT}^{\sin(\phi_h-\phi_s)} \sin(\phi_h-\phi_s) \\ + \varepsilon A_{UT}^{\sin(\phi_h+\phi_s)} \sin(\phi_h+\phi_s) \\ + \varepsilon A_{UT}^{\sin(3\phi_h-\phi_s)} \sin(3\phi_h-\phi_s) \\ + \sqrt{2\varepsilon(1+\varepsilon)} A_{UT}^{\sin\phi_s} \sin\phi_s \\ + \sqrt{2\varepsilon(1+\varepsilon)} A_{UT}^{\sin(2\phi_h-\phi_s)} \sin(2\phi_h-\phi_s) \end{array} \right] \\ + S_T \lambda \left[\begin{array}{l} \sqrt{(1-\varepsilon^2)} A_{LT}^{\cos(\phi_h-\phi_s)} \cos(\phi_h-\phi_s) \\ + \sqrt{2\varepsilon(1-\varepsilon)} A_{LT}^{\cos\phi_s} \cos\phi_s \\ + \sqrt{2\varepsilon(1-\varepsilon)} A_{LT}^{\cos(2\phi_h-\phi_s)} \cos(2\phi_h-\phi_s) \end{array} \right] \end{array} \right\}$$

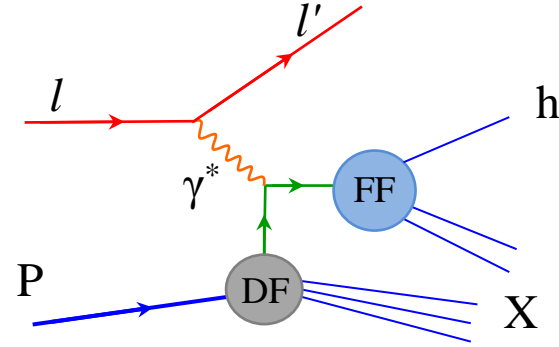
Quark \ Nucleon	U	L	T
U	number density		Boer-Mulders
L		helicity	worm-gear L
T	Sivers	Kotzinian-Mulders worm-gear T	transversity pretzelosity

↑ spin of the nucleon
 ↑ spin of the quark
 ↗ k_T

SIDIS x-section and TMDs at twist-2

$$\frac{d\sigma}{dx dy dz dp_T^2 d\phi_h d\phi_s} = \text{All measured by COMPASS}$$

$$\left[\frac{\alpha}{xyQ^2} \frac{y^2}{2(1-\varepsilon)} \left(1 + \frac{\gamma^2}{2x} \right) \right] (F_{UU,T} + \varepsilon F_{UU,L})$$



$$\times \left\{ \begin{array}{l} \left[\begin{array}{l} 1 + \sqrt{2\varepsilon(1+\varepsilon)} A_{UU}^{\cos\phi_h} \cos\phi_h + \varepsilon A_{UU}^{\cos 2\phi_h} \cos 2\phi_h \\ + \lambda \sqrt{2\varepsilon(1-\varepsilon)} A_{LU}^{\sin\phi_h} \sin\phi_h \end{array} \right] \\ \left[\begin{array}{l} + S_L \left[\sqrt{2\varepsilon(1+\varepsilon)} A_{UL}^{\sin\phi_h} \sin\phi_h + \varepsilon A_{UL}^{\sin 2\phi_h} \sin 2\phi_h \right] \\ + S_L \lambda \left[\sqrt{1-\varepsilon^2} A_{LL} + \sqrt{2\varepsilon(1-\varepsilon)} A_{LL}^{\cos\phi_h} \cos\phi_h \right] \end{array} \right] \\ \left[\begin{array}{l} A_{UT}^{\sin(\phi_h-\phi_s)} \sin(\phi_h-\phi_s) \\ + \varepsilon A_{UT}^{\sin(\phi_h+\phi_s)} \sin(\phi_h+\phi_s) \\ + \varepsilon A_{UT}^{\sin(3\phi_h-\phi_s)} \sin(3\phi_h-\phi_s) \\ + \sqrt{2\varepsilon(1+\varepsilon)} A_{UT}^{\sin\phi_s} \sin\phi_s \\ + \sqrt{2\varepsilon(1+\varepsilon)} A_{UT}^{\sin(2\phi_h-\phi_s)} \sin(2\phi_h-\phi_s) \end{array} \right] \\ \left[\begin{array}{l} \sqrt{(1-\varepsilon^2)} A_{LT}^{\cos(\phi_h-\phi_s)} \cos(\phi_h-\phi_s) \\ + \sqrt{2\varepsilon(1-\varepsilon)} A_{LT}^{\cos\phi_s} \cos\phi_s \\ + \sqrt{2\varepsilon(1-\varepsilon)} A_{LT}^{\cos(2\phi_h-\phi_s)} \cos(2\phi_h-\phi_s) \end{array} \right] \end{array} \right.$$

$$A_{UT}^{\sin(\phi_h-\phi_s)} \propto f_{1T}^{\perp q} \otimes D_{1q}^h$$

$$A_{UT}^{\sin(\phi_h+\phi_s)} \propto h_1^q \otimes H_{1q}^{\perp h}$$

$$A_{UT}^{\sin(3\phi_h-\phi_s)} \propto h_{1T}^{\perp q} \otimes H_{1q}^{\perp h}$$

$$A_{UT}^{\sin(\phi_s)} \overset{WW}{\propto} Q^{-1} \left(h_1^q \otimes H_{1q}^{\perp h} + f_{1T}^{\perp q} \otimes D_{1q}^h + \dots \right)$$

$$A_{UT}^{\sin(2\phi_h-\phi_s)} \overset{WW}{\propto} Q^{-1} \left(h_{1T}^{\perp q} \otimes H_{1q}^{\perp h} + f_{1T}^{\perp q} \otimes D_{1q}^h + \dots \right)$$

$$A_{LT}^{\cos(\phi_h-\phi_s)} \propto g_{1T}^q \otimes D_{1q}^h$$

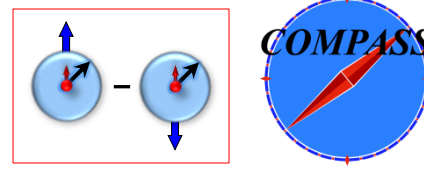
$$A_{LT}^{\cos(\phi_s)} \overset{WW}{\propto} Q^{-1} \left(g_{1T}^q \otimes D_{1q}^h + \dots \right)$$

$$A_{LT}^{\cos(2\phi_h-\phi_s)} \overset{WW}{\propto} Q^{-1} \left(g_{1T}^q \otimes D_{1q}^h + \dots \right)$$

Twist-2

Twist-3

SIDIS TSAs: Collins effect and Transversity



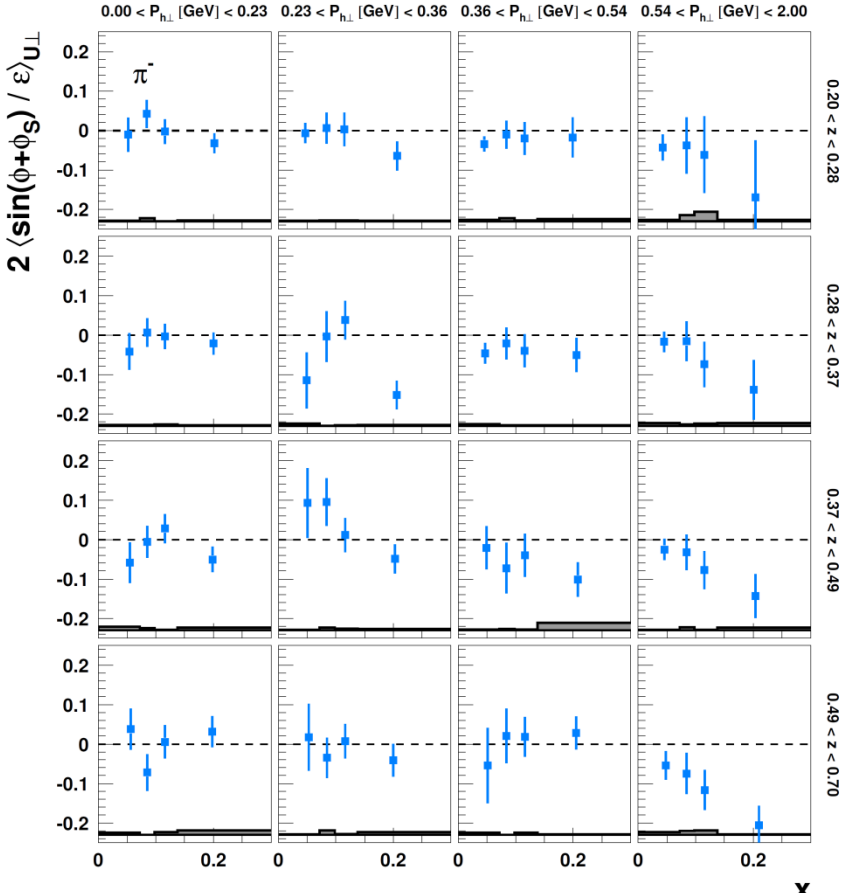
$$\frac{d\sigma}{dx dy dz dp_T^2 d\phi_h d\phi_S} \propto (F_{UU,T} + \varepsilon F_{UU,L}) \left\{ 1 + \dots + S_T \varepsilon A_{UT}^{\sin(\phi_h + \phi_S)} \sin(\phi_h + \phi_S) + \dots \right\}$$

$$F_{UT}^{\sin(\phi_h + \phi_S)} = C \left[-\frac{\hat{h} \cdot p_T}{M_h} h_1^q H_{1q}^{\perp h} \right]$$

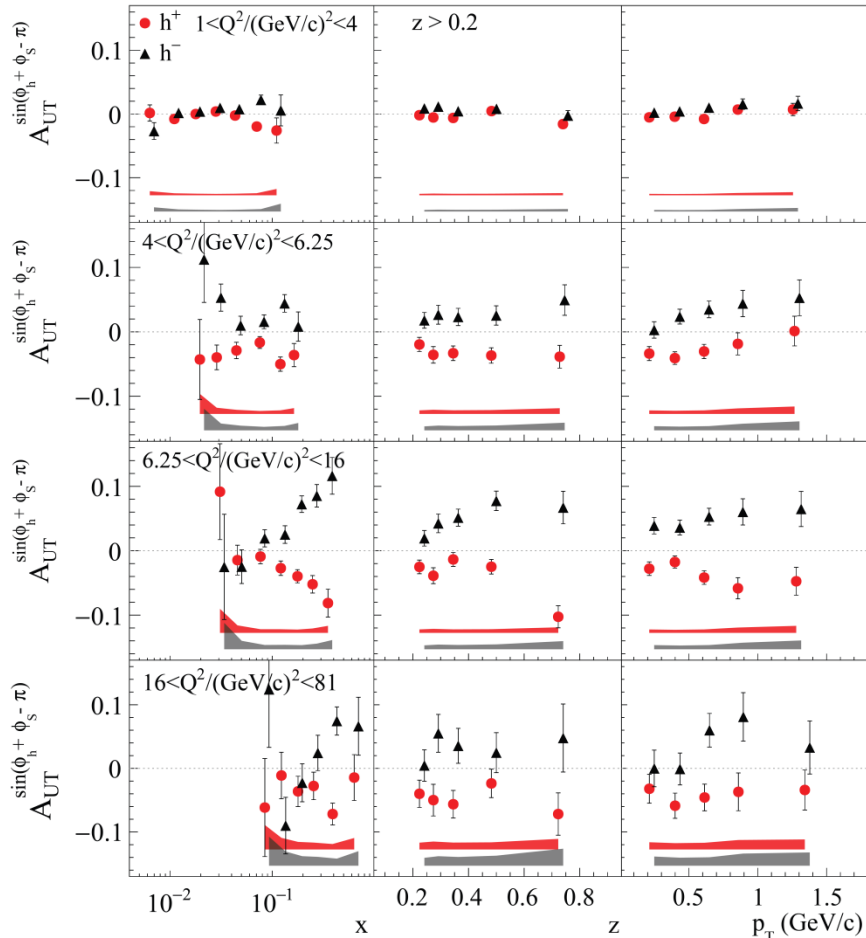


- Measured on P/D in SIDIS and in dihadron SIDIS
- Compatible results COMPASS/HERMES (Q² is different by a factor of ~2-3)
- No impact from Q²-evolution?

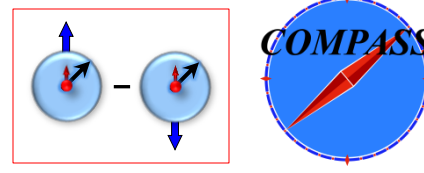
HERMES, JHEP 12 (2020) 010



COMPASS, PBL 770 (2017) 138



SIDIS TSAs: Collins effect and Transversity



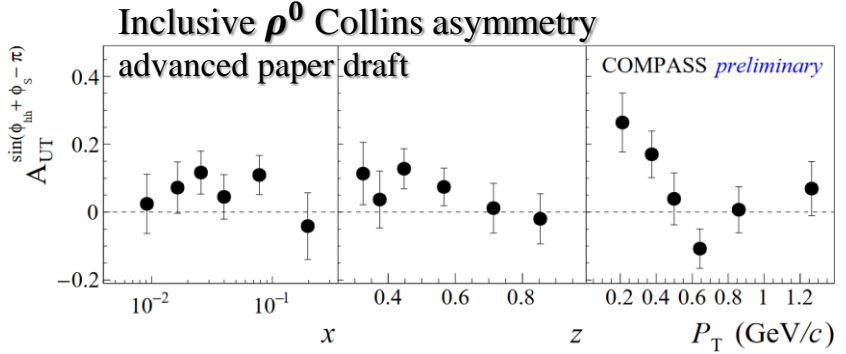
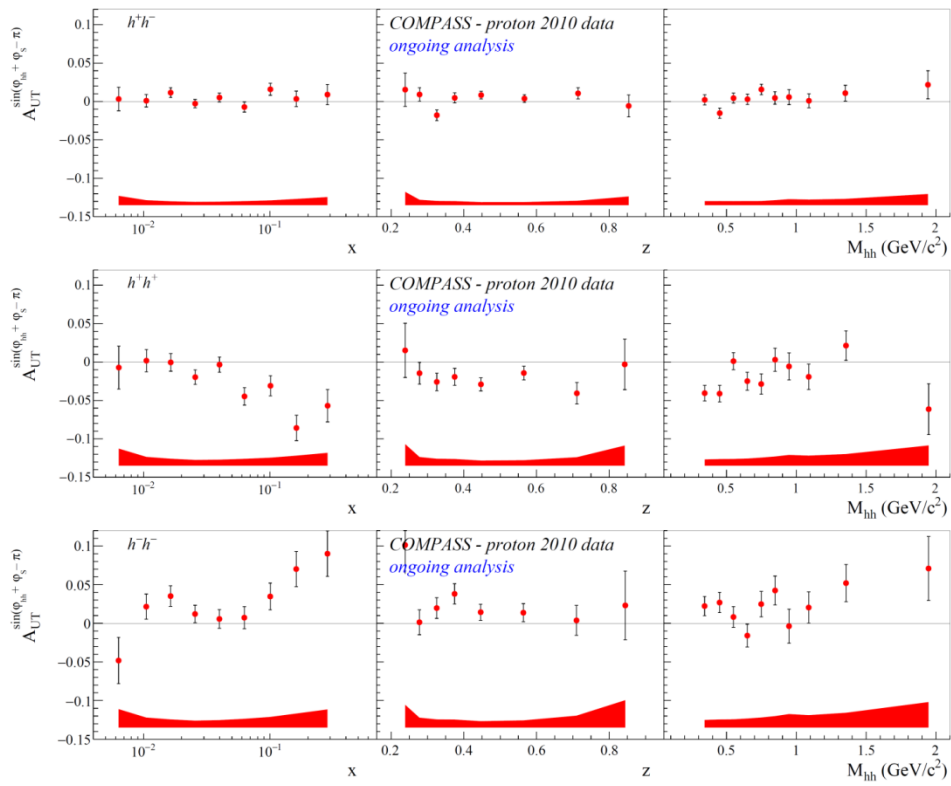
$$\frac{d\sigma}{dx dy dz dp_T^2 d\phi_h d\phi_S} \propto (F_{UU,T} + \varepsilon F_{UU,L}) \left\{ 1 + \dots + S_T \varepsilon A_{UT}^{\sin(\phi_h + \phi_S)} \sin(\phi_h + \phi_S) + \dots \right\}$$

$$F_{UT}^{\sin(\phi_h + \phi_S)} = C \left[-\frac{\hat{h} \cdot p_T}{M_h} h_1^q H_{1q}^{\perp h} \right]$$

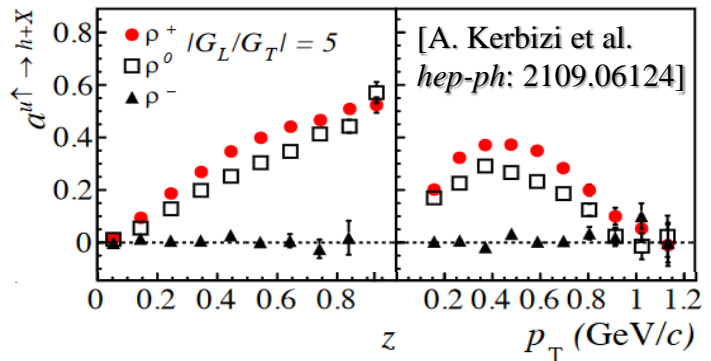


- Measured on P/D in SIDIS and in dihadron SIDIS
- Compatible results COMPASS/HERMES (Q² is different by a factor of ~2-3)
- No impact from Q²-evolution?

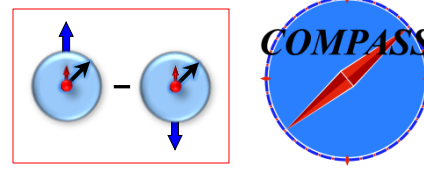
Ongoing analysis: Collins-like dihadron TSAs



- indication for a positive asymmetry
- opposite to pi⁺ and pi⁰ as predicted by the models
- Large effect at small P_T



SIDIS TSAs: Collins effect and Transversity



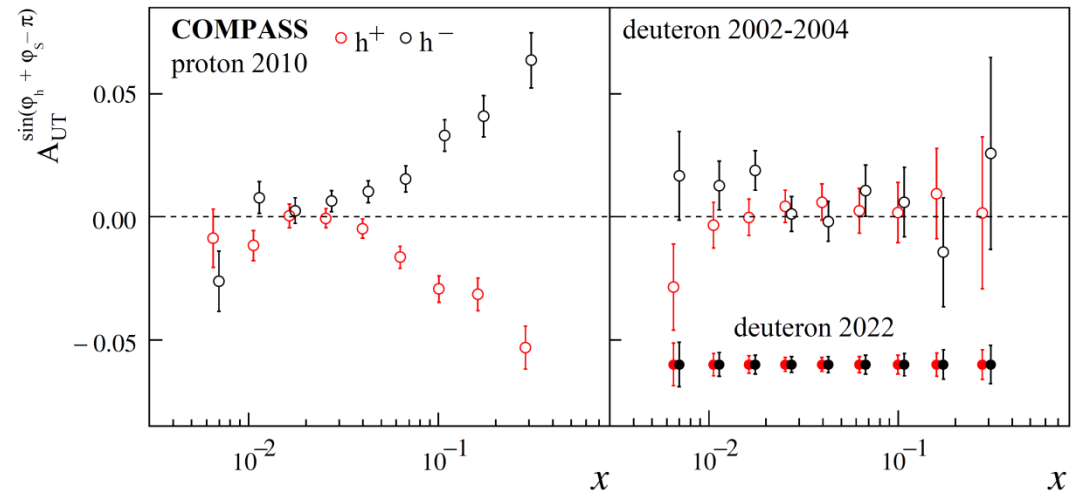
$$\frac{d\sigma}{dx dy dz dp_T^2 d\phi_h d\phi_S} \propto (F_{UU,T} + \varepsilon F_{UU,L}) \left\{ 1 + \dots + S_T \varepsilon A_{UT}^{\sin(\phi_h + \phi_S)} \sin(\phi_h + \phi_S) + \dots \right\}$$

$$F_{UT}^{\sin(\phi_h + \phi_S)} = C \left[-\frac{\hat{h} \cdot p_T}{M_h} h_1^q H_{1q}^{\perp h} \right]$$

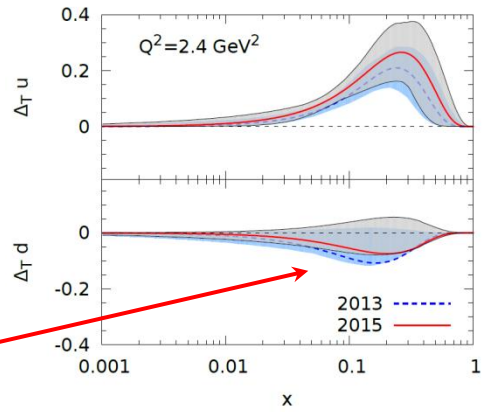
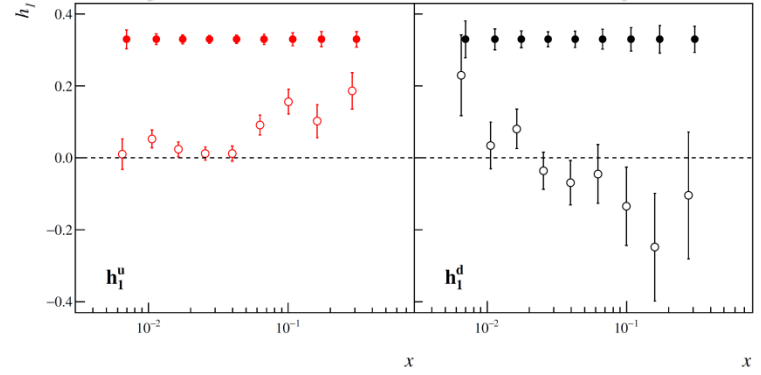


- Measured on P/D in SIDIS and in dihadron SIDIS
- Compatible results COMPASS/HERMES (Q² is different by a factor of ~2-3)
- **No impact from Q²-evolution?**
- Extensive phenomenological studies and various global fits by different groups

[Addendum to the COMPASS-II Proposal]
Projected uncertainties for Collins asymmetry



Projected uncertainties for transversity PDF



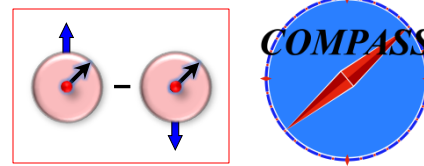
COMPASS-II (2022)

- Deuteron measurement to be repeated
- Will be crucial to constrain the transversity TMD PDF for the d-quark

SIDIS TSAs: Sivers effect

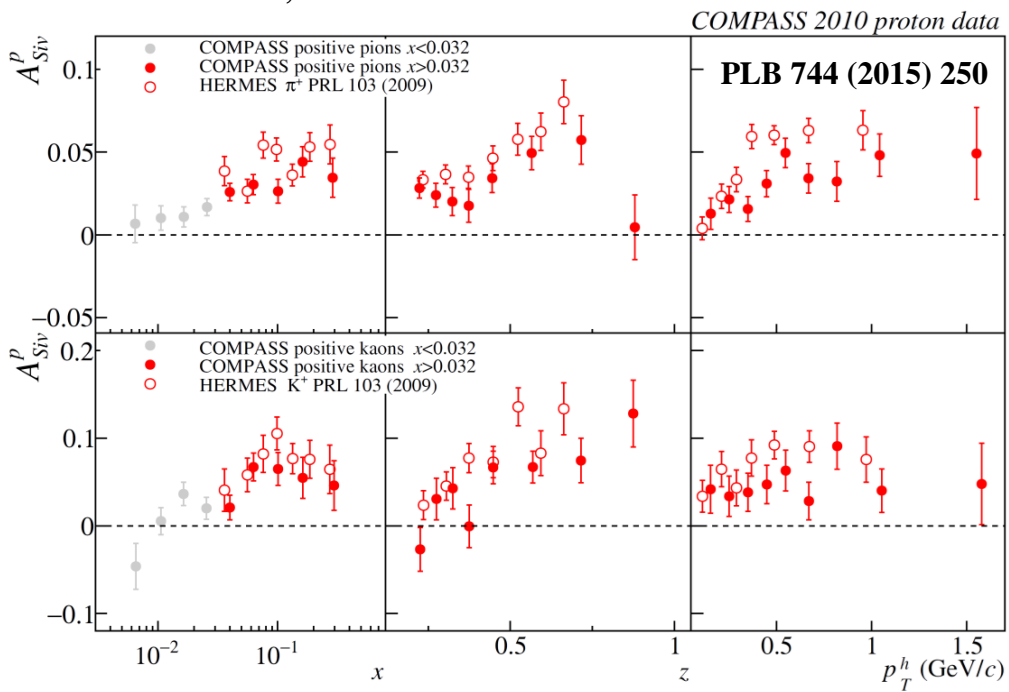
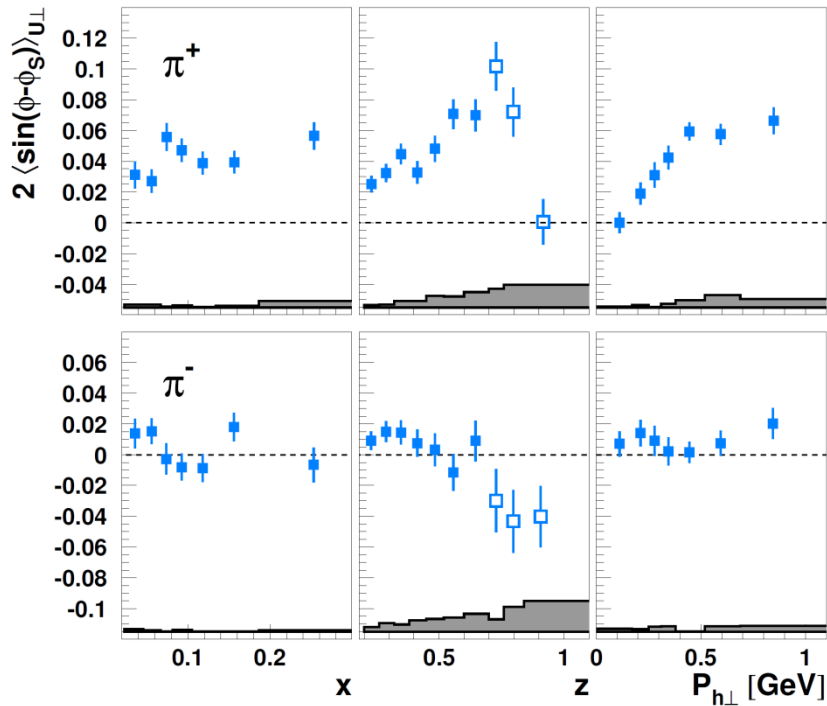
$$\frac{d\sigma}{dx dy dz dp_T^2 d\phi_h d\phi_S} \propto (F_{UU,T} + \varepsilon F_{UU,L}) \left\{ 1 + \dots + S_T A_{UT}^{\sin(\phi_h - \phi_S)} \sin(\phi_h - \phi_S) + \dots \right\}$$

$$F_{UT,T}^{\sin(\phi_h - \phi_S)} = C \left[-\frac{\hat{h} \cdot \mathbf{k}_T}{M} f_{1T}^{\perp q} D_{1q}^h \right], F_{UT,L}^{\sin(\phi_h - \phi_S)} = 0$$



- Measured on proton and deuteron
- Expected to change sign between SIDIS and Drell-Yan

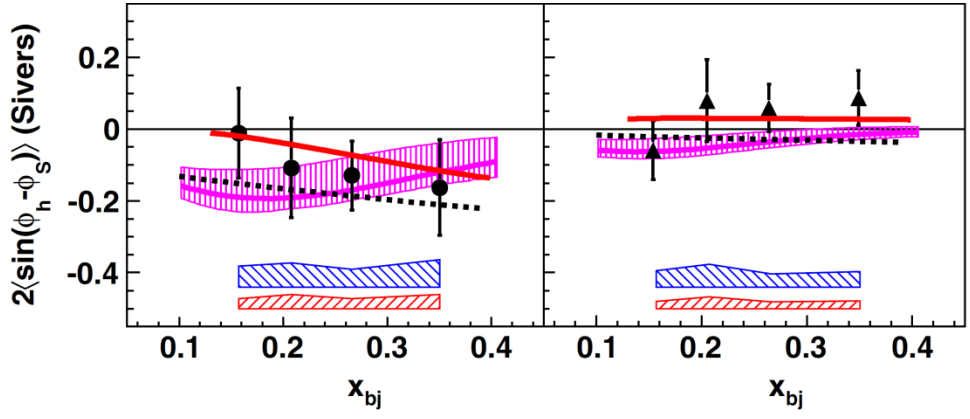
HERMES, JHEP 12 (2020) 010



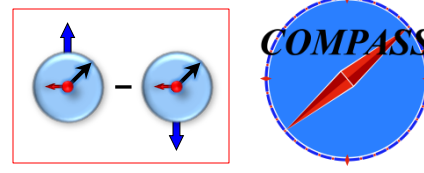
COMPASS 2010 proton data

PLB 744 (2015) 250

JLab Hall A PRL 107, 072003 (2011)



SIDIS TSAs: Kotzinian-Mulders asymmetry

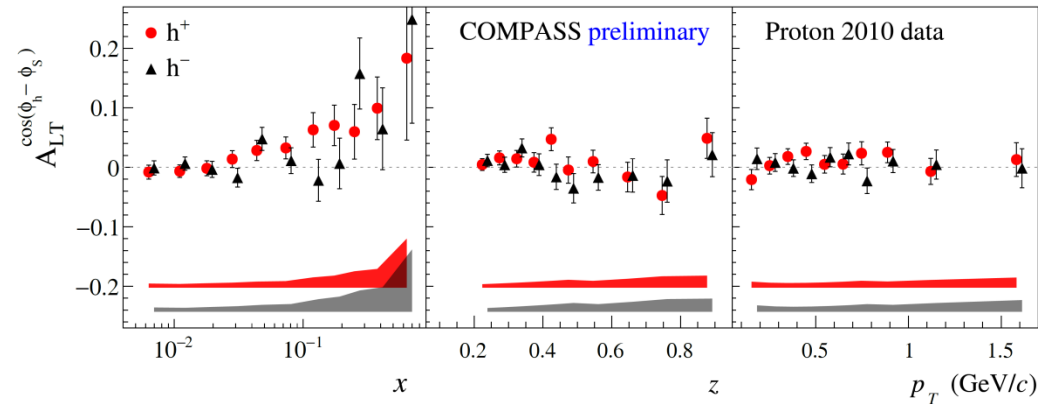


$$\frac{d\sigma}{dx dy dz dp_T^2 d\phi_h d\phi_S} \propto (F_{UU,T} + \varepsilon F_{UU,L}) \left\{ 1 + \dots + \lambda S_T \sqrt{(1-\varepsilon^2)} A_{LT}^{\cos(\phi_h - \phi_S)} \cos(\phi_h - \phi_S) + \dots \right\}$$

$$F_{LT}^{\cos(\phi_h - \phi_S)} = C \left[\frac{\hat{h} \cdot \mathbf{k}_T}{M} g_{1T}^q D_{1q}^h \right]$$



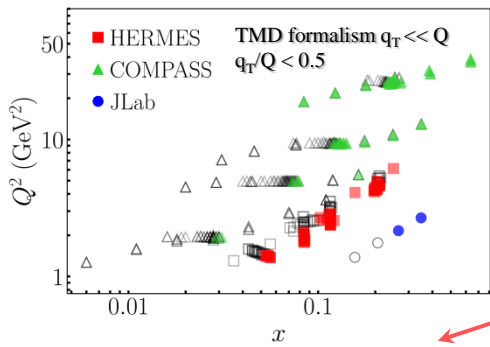
COMPASS, PBL 770 (2017) 138; PoS QCDEV2017 (2018) 042



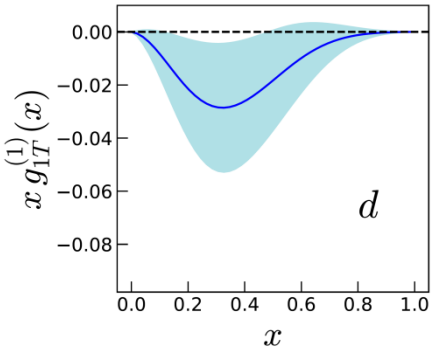
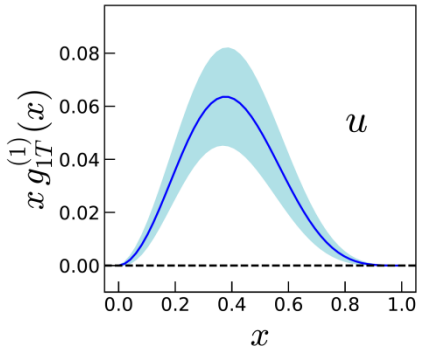
COMPASS/HERMES/CLAS6 results

$$A_{LT}^{\cos(\phi_h - \phi_S)}$$

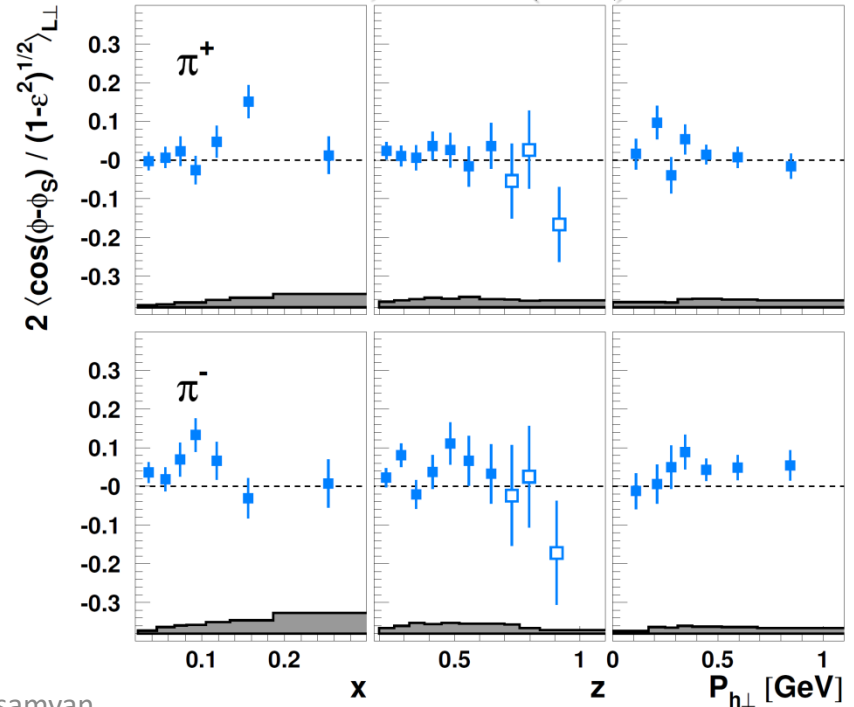
- Only “twist-2” ingredients
- **Sizable non-zero effect for h⁺ !**
- **Similar effect at HERMES**



First global QCD analysis of the g_{1T} TMD PDF using SIDIS data



HERMES, JHEP 12 (2020) 010



COMPASS 2022 run: new unique deuteron data to come



hermes proton [H]
95 data points
Airapetian et al., P.R.L. 103 (09) 152002

Jefferson Lab neutron [³He]
6 data points
Qian et al., P.R.L. 107 (11) 072003

COMPASS 2009 deuteron [²HD]
88 data points
Alekseev et al., P.L. B673 (09) 127

COMPASS 2017 Proton [NH₃]
111 data points
Adolph et al., P.L. B770 (17) 138

Pavia group fits

Bacchetta, Delcarro, Pisano, Radici, in preparation

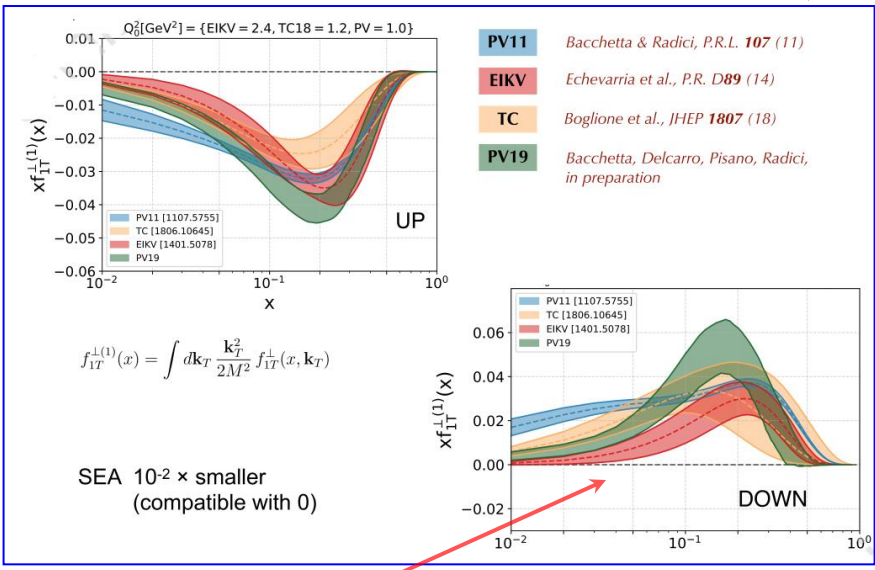
analysis of statistical error with replica method (200)
68% confidence level

Same kinematic cuts applied to unpolarized

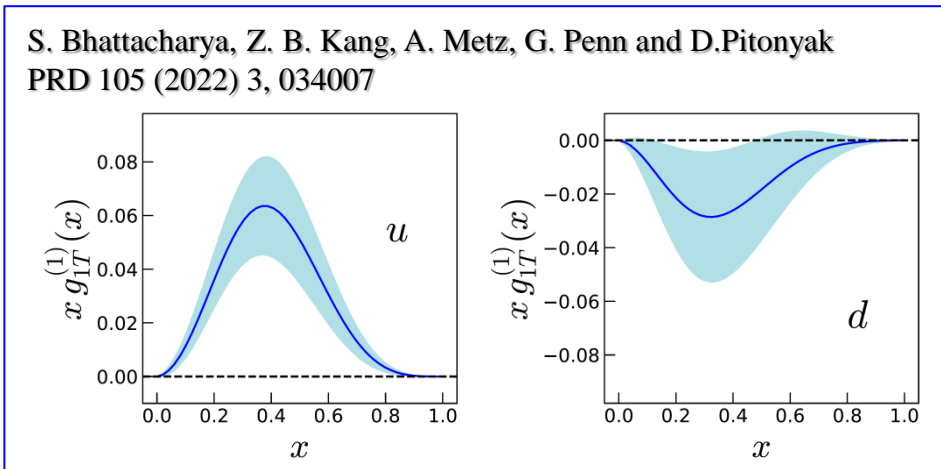
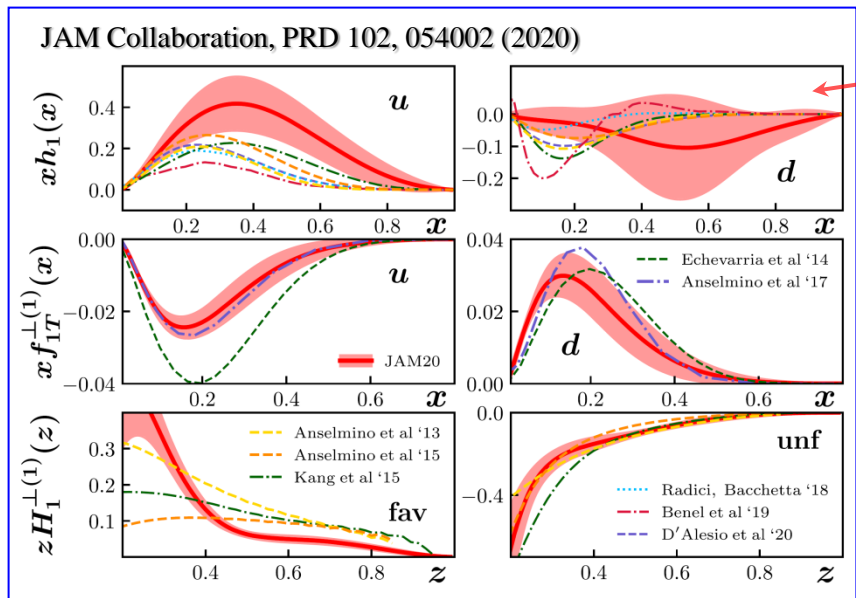
x, z, P_{HT} data projections

$Q^2 \geq 1.4 \text{ GeV}^2$ $0.2 \leq z \leq 0.7$
 $P_{HT} < \min[0.2Q, 0.7Qz] + 0.5 \text{ GeV}$

300 data points → **118 data fitted**
14 free parameters
 $\chi^2/\text{d.o.f.} = 1.06 \pm 0.10$



COMPASS 2022 deuteron run





SIDIS and single-polarized DY x-sections at twist-2 (LO)

SIDIS

$$\frac{d\sigma^{LO}}{dx dy dz dp_T^2 d\phi_h d\phi_S} \propto (F_{UU,T} + \varepsilon F_{UU,L})$$

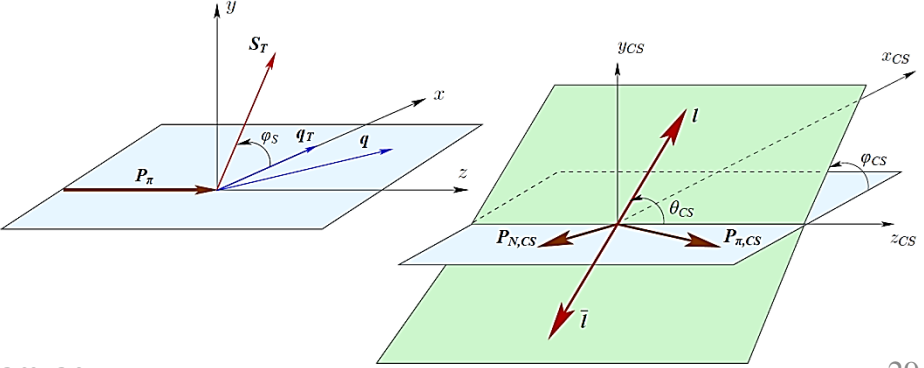
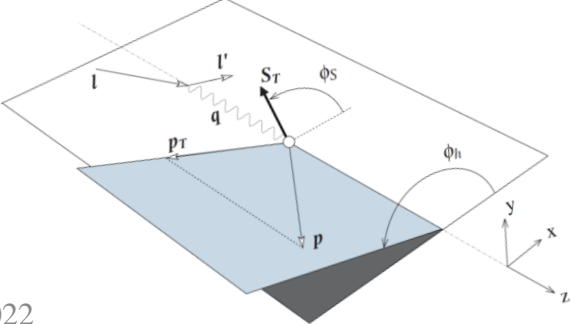
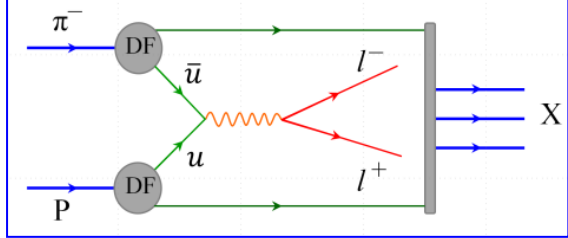
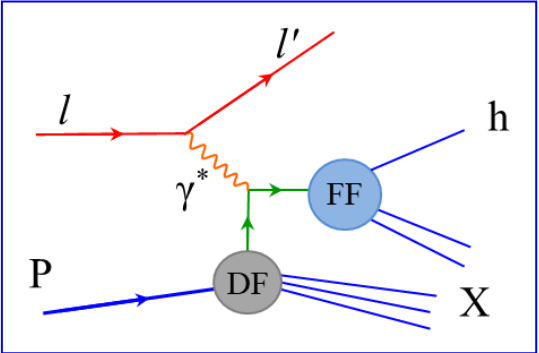
$$\times \left\{ \begin{aligned} &1 + \varepsilon A_{UU}^{\cos 2\phi_h} \cos 2\phi_h \\ &+ S_L \varepsilon A_{UL}^{\sin 2\phi_h} \sin 2\phi_h + S_L \lambda \sqrt{1-\varepsilon^2} A_{LL} \\ &+ S_T \begin{bmatrix} A_{UT}^{\sin(\phi_h-\phi_S)} \sin(\phi_h-\phi_S) \\ + \varepsilon A_{UT}^{\sin(\phi_h+\phi_S)} \sin(\phi_h+\phi_S) \\ + \varepsilon A_{UT}^{\sin(3\phi_h-\phi_S)} \sin(3\phi_h-\phi_S) \end{bmatrix} \\ &+ S_T \lambda \left[\sqrt{(1-\varepsilon^2)} A_{LT}^{\cos(\phi_h-\phi_S)} \cos(\phi_h-\phi_S) \right] \end{aligned} \right\}$$

DY

$$\frac{d\sigma^{LO}}{dq^4 d\Omega} \propto F_U^1 (1 + \cos^2 \theta_{CS})$$

$$\times \left\{ \begin{aligned} &1 + D_{[\sin^2 \theta_{CS}]} A_U^{\cos 2\varphi_{CS}} \cos 2\varphi_{CS} \\ &+ S_L \sin^2 \theta_{CS} A_L^{\sin 2\varphi_{CS}} \sin 2\varphi_{CS} \\ &+ S_T \begin{bmatrix} A_T^{\sin \varphi_S} \sin \varphi_S \\ + D_{[\sin^2 \theta_{CS}]} \left(A_T^{\sin(2\varphi_{CS}-\varphi_S)} \sin(2\varphi_{CS}-\varphi_S) \right. \\ \left. + A_T^{\sin(2\varphi_{CS}+\varphi_S)} \sin(2\varphi_{CS}+\varphi_S) \right) \end{bmatrix} \end{aligned} \right\}$$

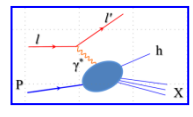
where $D_{[\sin^2 \theta_{CS}]} = \sin^2 \theta_{CS} / (1 + \cos^2 \theta_{CS})$



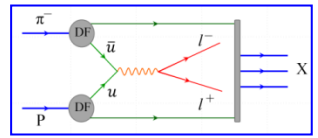


SIDIS and single-polarized DY x-sections at twist-2 (LO)

$$\frac{d\sigma^{LO}}{dx dy dz dp_T^2 d\phi_h d\phi_S} \propto (F_{UU,T} + \varepsilon F_{UU,L})$$



$$\frac{d\sigma^{LO}}{dq^4 d\Omega} \propto F_U^1 (1 + \cos^2 \theta_{CS})$$



$$\left\{ \begin{aligned} & 1 + \varepsilon A_{UU}^{\cos 2\phi_h} \cos 2\phi_h \\ & + S_L \varepsilon A_{UL}^{\sin 2\phi_h} \sin 2\phi_h + S_L \lambda \sqrt{1 - \varepsilon^2} A_{LL} \\ & + S_T \begin{bmatrix} A_{UT}^{\sin(\phi_h - \phi_S)} \sin(\phi_h - \phi_S) \\ + \varepsilon A_{UT}^{\sin(\phi_h + \phi_S)} \sin(\phi_h + \phi_S) \\ + \varepsilon A_{UT}^{\sin(3\phi_h - \phi_S)} \sin(3\phi_h - \phi_S) \end{bmatrix} \\ & + S_T \lambda \left[\sqrt{(1 - \varepsilon^2)} A_{LT}^{\cos(\phi_h - \phi_S)} \cos(\phi_h - \phi_S) \right] \end{aligned} \right\} \times \left\{ \begin{aligned} & 1 + D_{[\sin^2 \theta_{CS}]} A_U^{\cos 2\varphi_{CS}} \cos 2\varphi_{CS} \\ & + S_L \sin^2 \theta_{CS} A_L^{\sin 2\varphi_{CS}} \sin 2\varphi_{CS} \\ & + S_T \begin{bmatrix} A_T^{\sin \varphi_S} \sin \varphi_S \\ + D_{[\sin^2 \theta_{CS}]} \left(A_T^{\sin(2\varphi_{CS} - \varphi_S)} \sin(2\varphi_{CS} - \varphi_S) \right. \\ \left. + A_T^{\sin(2\varphi_{CS} + \varphi_S)} \sin(2\varphi_{CS} + \varphi_S) \right) \end{bmatrix} \end{aligned} \right\}$$

SIDIS-DY bridge

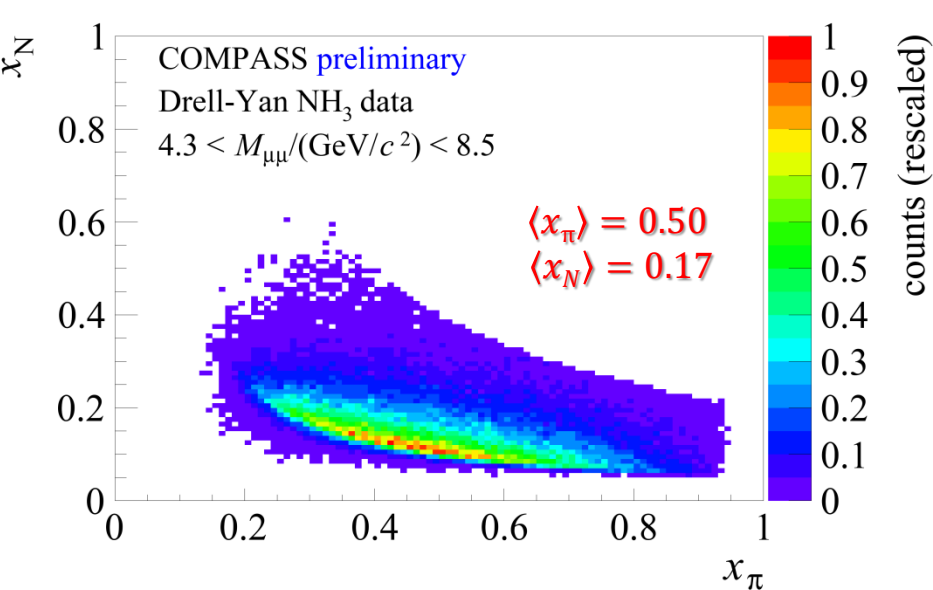
where $D_{[\sin^2 \theta_{CS}]} = \sin^2 \theta_{CS} / (1 + \cos^2 \theta_{CS})$

$A_{UU}^{\cos 2\phi_h} \propto \underline{h_1^{\perp q}} \otimes \underline{H_{1q}^{\perp h}} + \dots$	Boer-Mulders	$A_U^{\cos 2\varphi_{CS}} \propto \underline{h_{1,\pi}^{\perp q}} \otimes \underline{h_{1,p}^{\perp q}}$
$A_{UT}^{\sin(\phi_h - \phi_S)} \propto \underline{f_{1T}^{\perp q}} \otimes \underline{D_{1q}^h}$	Sivers	$A_T^{\sin \varphi_S} \propto \underline{f_{1,\pi}^q} \otimes \underline{f_{1T,p}^{\perp q}}$
$A_{UT}^{\sin(\phi_h + \phi_S)} \propto \underline{h_1^q} \otimes \underline{H_{1q}^{\perp h}}$	Transversity	$A_T^{\sin(2\varphi_{CS} - \varphi_S)} \propto \underline{h_{1,\pi}^{\perp q}} \otimes \underline{h_{1,p}^q}$
$A_{UT}^{\sin(3\phi_h - \phi_S)} \propto \underline{h_{1T}^{\perp q}} \otimes \underline{H_{1q}^{\perp h}}$	Pretzelosity	$A_T^{\sin(2\varphi_{CS} + \varphi_S)} \propto \underline{h_{1,\pi}^{\perp q}} \otimes \underline{h_{1T,p}^{\perp q}}$

Complementary information from two different channels :

- SIDIS-DY bridging of nucleon TMD PDFs; Universality studies;
- **Sign-change of T-odd Sivers and Boer-Mulders TMD PDFs;**
- Multiple access to Collins FF $H_{1q}^{\perp h}$ and pion Boer-Mulders PDF $h_{1,\pi}^{\perp q}$

Single-polarized DY measurements at COMPASS



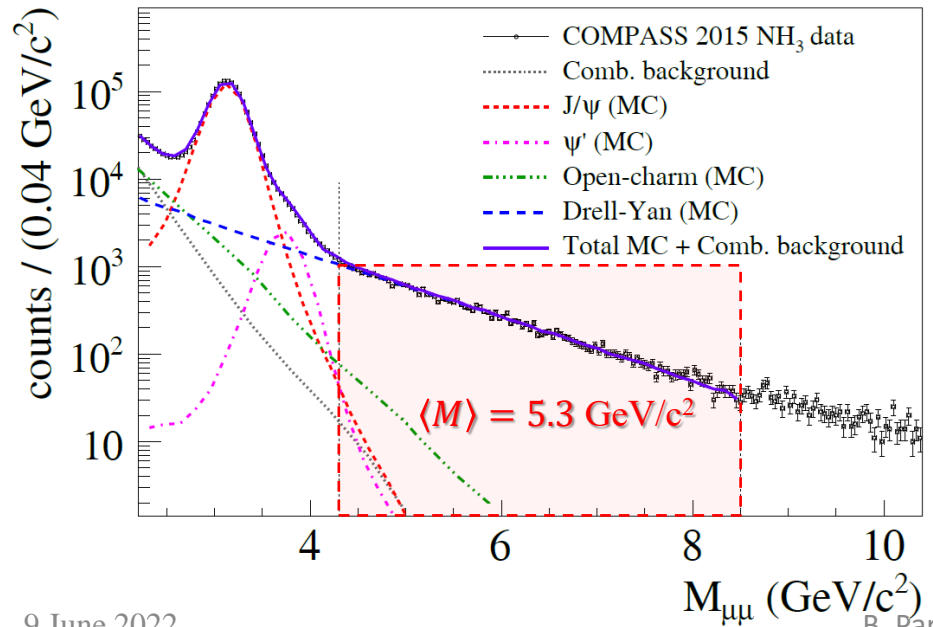
$$\frac{d\sigma^{LO}}{dq^4 d\Omega} \propto F_U^1 (1 + \cos^2 \theta_{CS})$$

$$\times \left\{ 1 + \underbrace{D_{[\sin^2 \theta_{CS}]} A_U^{\cos 2\varphi_{CS}} \cos 2\varphi_{CS}}_{\text{green box}} + S_L \sin^2 \theta_{CS} A_L^{\sin 2\varphi_{CS}} \sin 2\varphi_{CS} \right.$$

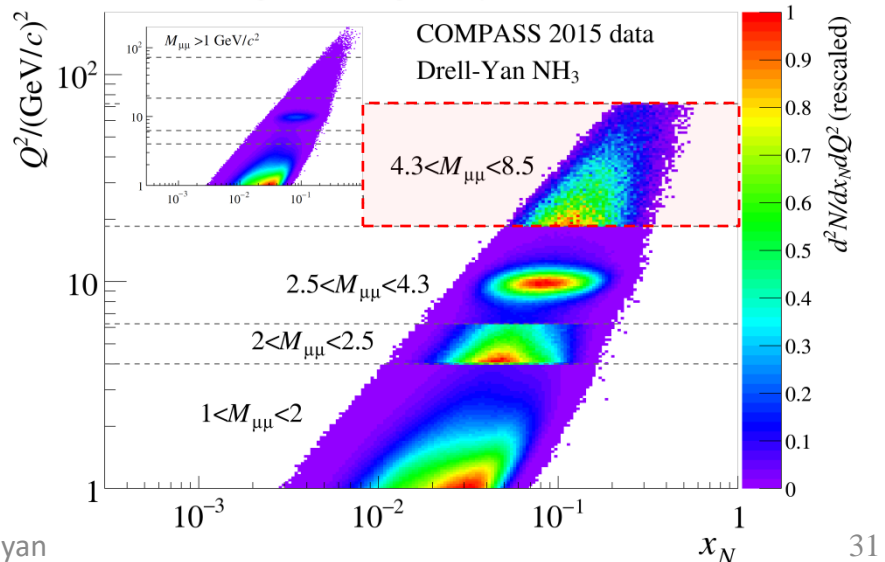
$$\left. + S_T \left[A_T^{\sin \varphi_S} \sin \varphi_S + D_{[\sin^2 \theta_{CS}]} \left(A_T^{\sin(2\varphi_{CS} - \varphi_S)} \sin(2\varphi_{CS} - \varphi_S) + A_T^{\sin(2\varphi_{CS} + \varphi_S)} \sin(2\varphi_{CS} + \varphi_S) \right) \right] \right\}$$

$$D_{[\sin^2 \theta_{CS}]} = \sin^2 \theta_{CS} / (1 + \cos^2 \theta_{CS})$$

HM events are in the valence quark range

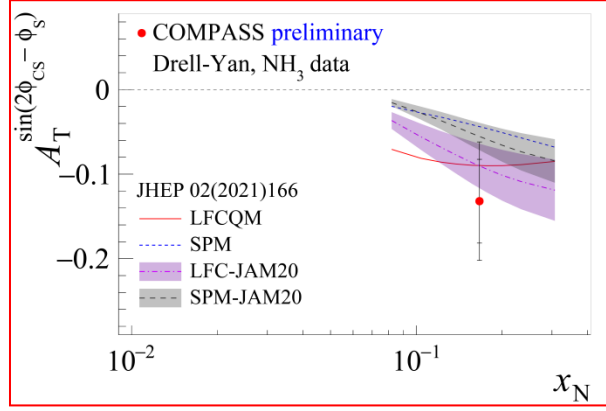
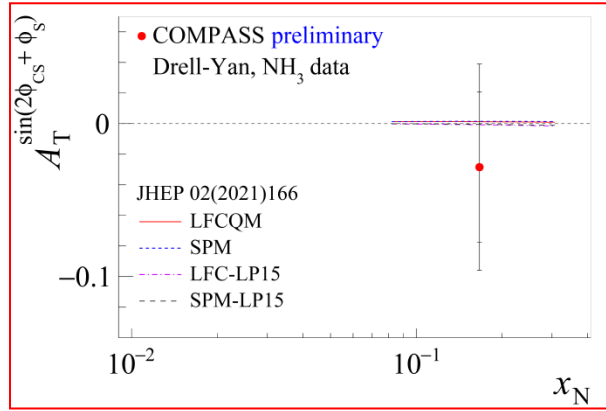
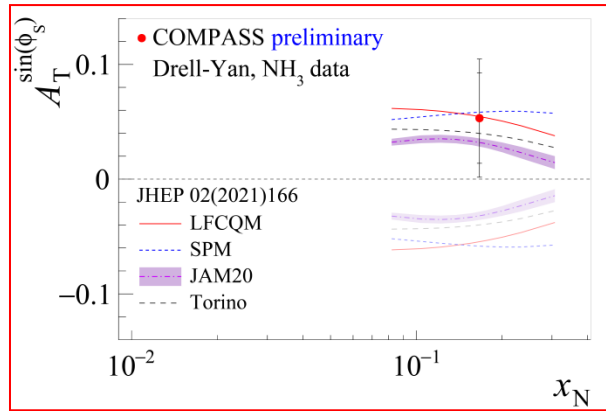
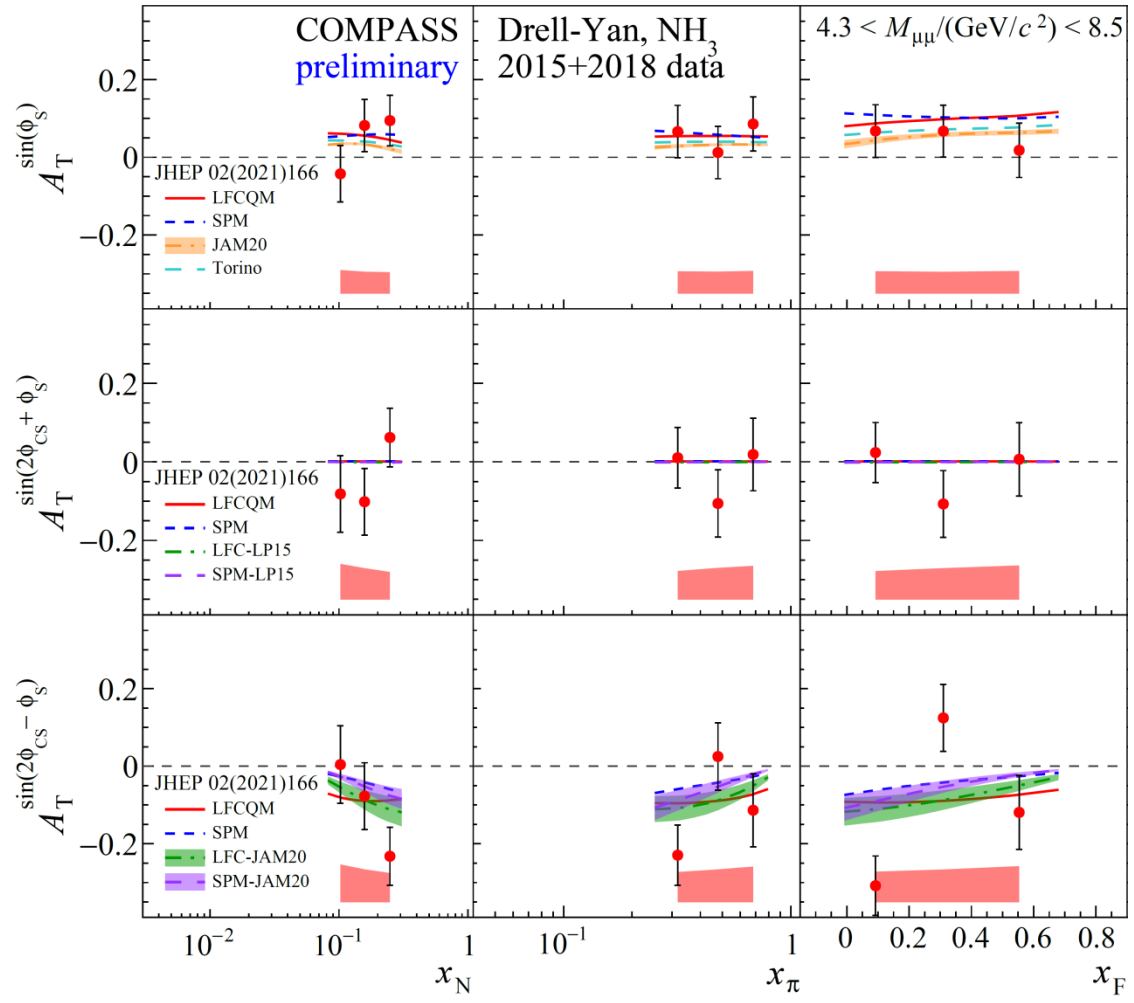


4.3 < M / (GeV/c²) < 8.5 “High mass” range
 Beyond charmonium region, background < 3%
 Valence region → largest asymmetries



DY TSAs at COMPASS (high-mass range)

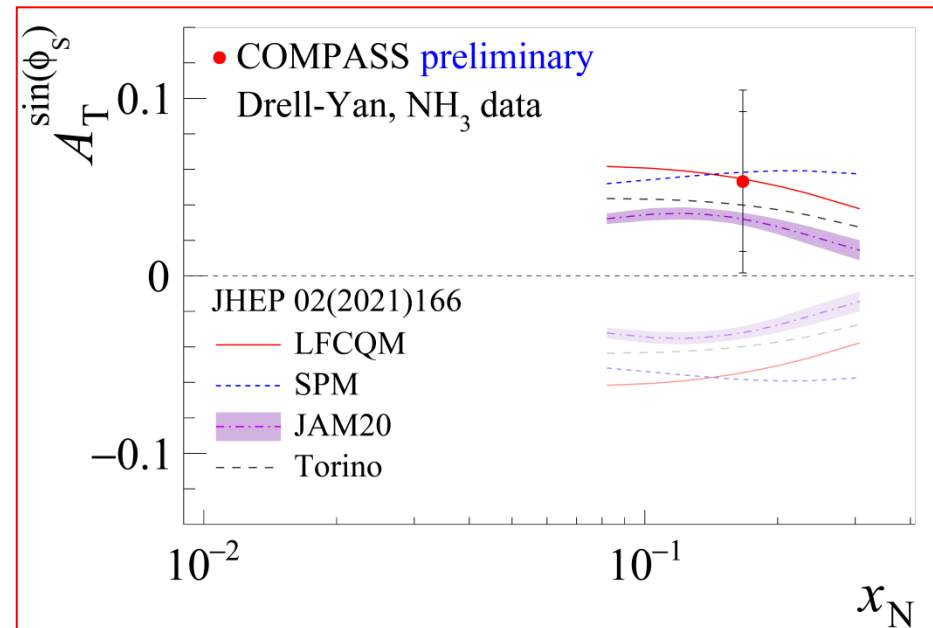
Theory curves based on S. Bastami et al. JHEP 02, (2021),166



- General agreement with available theory predictions

DY TSAs at COMPASS (high-mass range)

- During phase I COMPASS has measured all possible SIDIS TSAs.
 - Non-zero Sivers and Collins SIDIS-TSAs in the Drell-Yan “high-mass range”: PLB 770 (2017) 138
- In 2017 COMPASS has published the results for the **first polarized DY measurements**: PRL 119, 112002 (2017)
- The second year of polarized DY data-taking was performed in 2018
- Re-production and re-analysis of both 2015 2018 data is over
- Final results have been presented at DIS-2022 and other conferences: **the paper is in preparation**
- **COMPASS data favors the sign-change of Sivers TMD PDF**





- COMPASS spectrometer status (2021-2022)

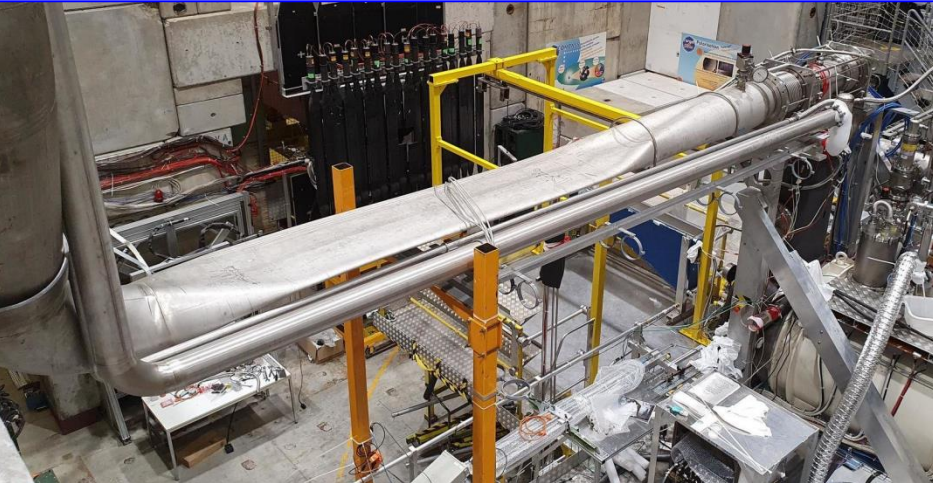
COMPASS PT 2021 run

Original plan

- 34 days {
 - 28/04: Target material loading
 - 15/05: Start of NMR calibration
 - 15/05: Switch to dilution mode
 - 01/06: Dynamic nuclear polarization tuning
 - 42 days for polarization studies
 - 12/07: Ready for data taking
- } 58 days

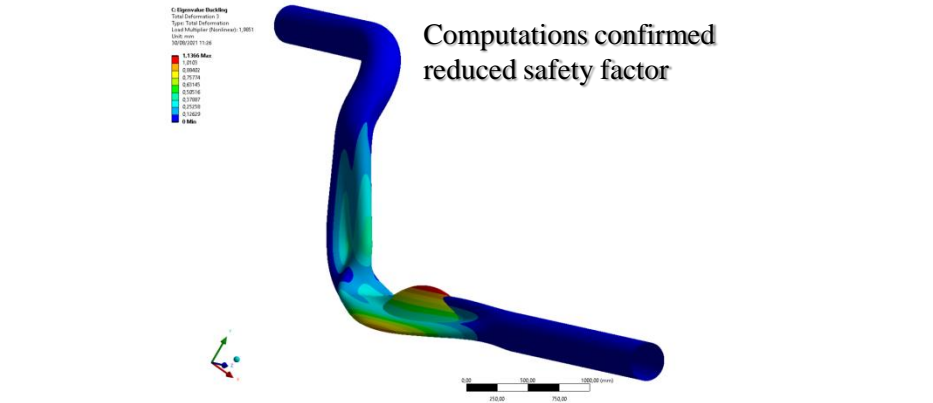
Reality

- 28/04: Target material loading
- 13/05: Ice on beam window, TH vacuum leak
- 27/05: Target unloading, indium sealing defect noticed
- 01/06: Starting CryoLab and in-situ leak-tests (20 d.)
- 30/06: Target material loading (delay - 45 d)
- 03/07: ^3He pumping line buckled (not COMPASS resp.)
- 05/07: Target material unloaded, pipe dismantled
- 10/07: First low intensity beam*



Buckling of the COMPASS ^3He pumping pipe
 The reason: lower thickness of the pipe (exchanged in April 2019) and missing (not installed) stiffening components.

From the results obtained computationally it can be concluded that the main pumping line of the dilution cryostat collapsed due to a buckling caused essentially by a low safety factor, 2, of the structure due to the low thickness of the pipe geometry, 2mm, and the absence of enough supports or stiffeners. In order to increase the safety factor to 8, the minimum recommended in such structures, it has been proposed to **increase the thickness of the pipe to 3mm and to install supports or stiffeners at a maximum distance of 1 meter** from each other. The safety factor should be increased up to 11.6.





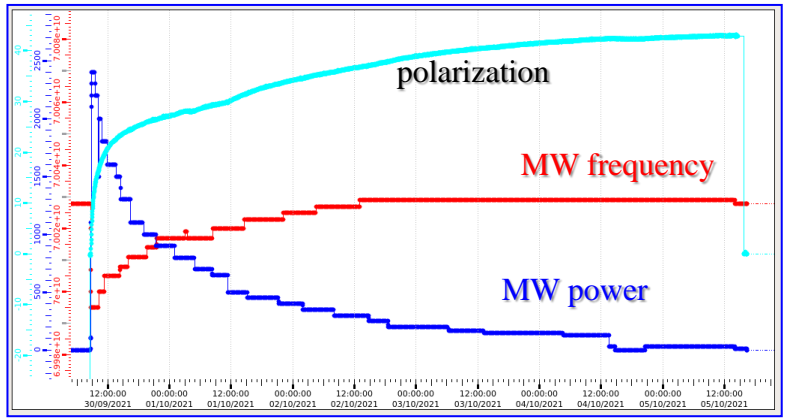
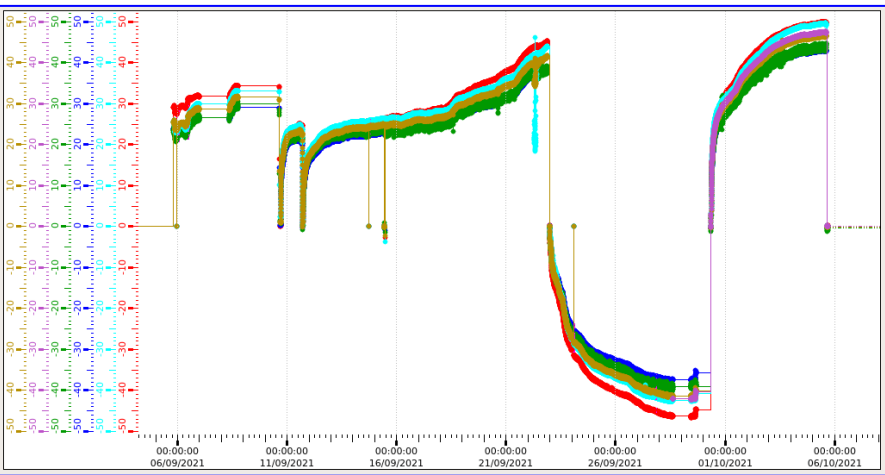
COMPASS PT 2021 run

Original plan

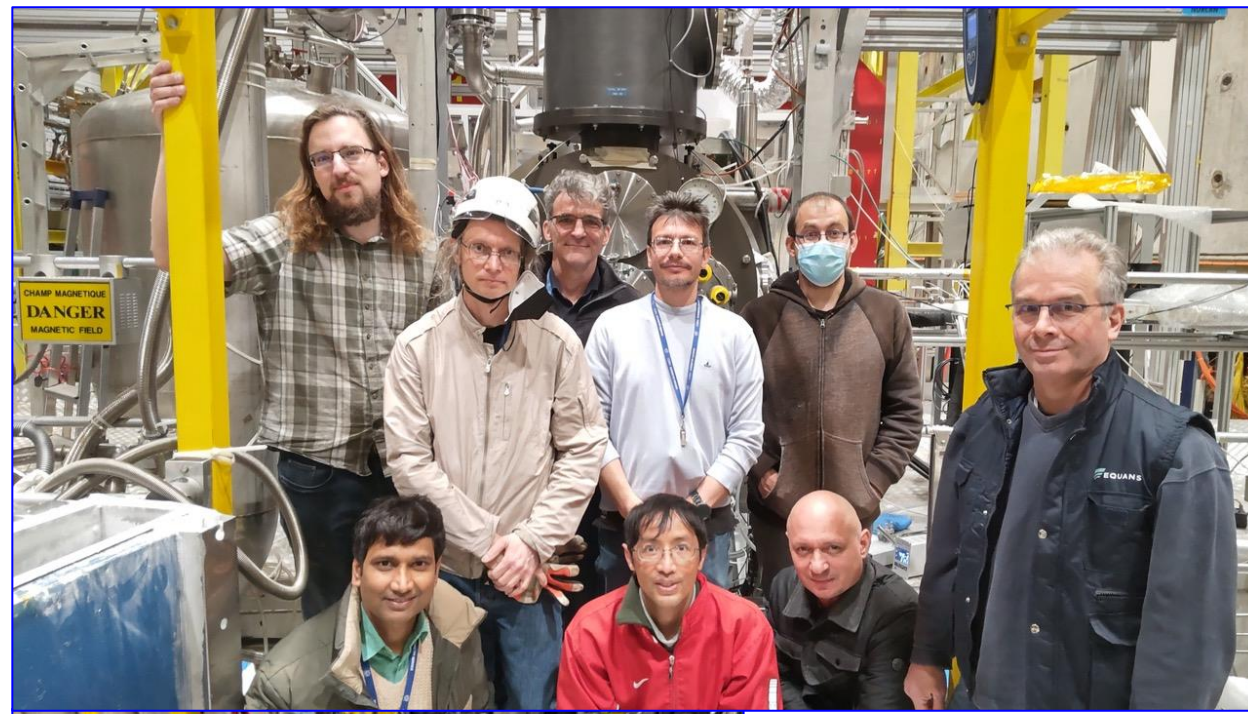
- 28/04:** Target material loading
 - 15/05:** Start of NMR calibration
 - 15/05:** Switch to dilution mode
 - 01/06:** Dynamic nuclear polarization tuning
 - 12/07:** Ready for data taking
- 34 days
- 58 days
- 42 days for polarization studies**

Reality

- 28/04:** Target material loading
 - 13/05:** Ice on beam window, TH vacuum leak
 - 27/05:** Target unloading, indium sealing defect noticed
 - 01/06:** Starting CryoLab and in-situ leak-tests (20 d.)
 - 30/06:** Target material loading (**delay - 45 d**)
 - 03/07:** ^3He pumping line buckled (**not COMPASS resp.**)
 - 05/07:** Target material unloaded, pipe dismantled
 - 10/07: First low intensity beam*
 - 20/07:** New pipe installed (at 280 K), cooling started
 - problems encountered (humidity due to the incident)*
 - 10/08:** Target material loading, start of cooling
 - 16/08: First high intensity beam*
 - 31/08:** Dipole He filling problem solved (EP-DT)
 - 01/09:** 1st dynamic nuclear polarization (**delay - 92 d**)
 - 06/09:** Start of physics data-taking
 - 16/09: Desired intensity and stable beam*
 - 09/09:** 1st DNP based on 2006 settings unsuccessful
 - 10/09:** **Forced start of DNP tuning studies**
 - (central cell, Gunn diode)
 - 23/09:** Desired positive polarization values reached
 - (switching to negative polarization test)
 - 29/09:** Desired negative polarization values reached
 - 30/09:** Build-up optimization test started
 - (MW frequency/power, field homogeneity)
 - 06/10:** End of the run, successful build-up test
- 30 days
- 20 days



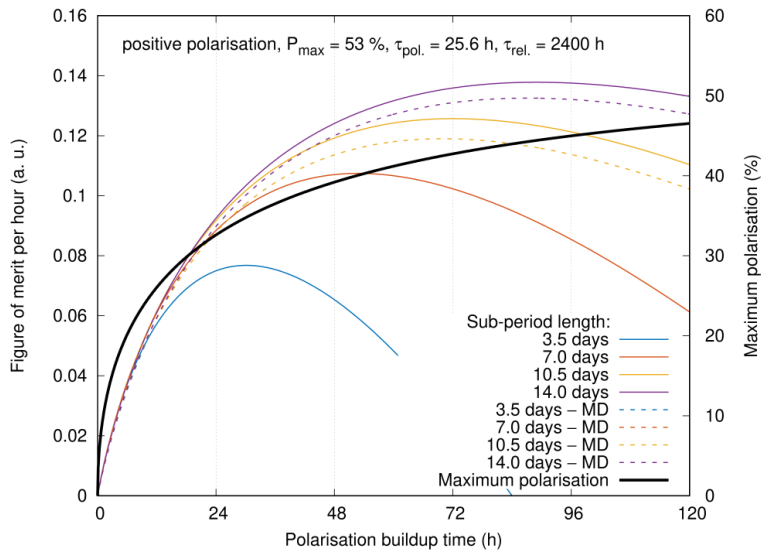
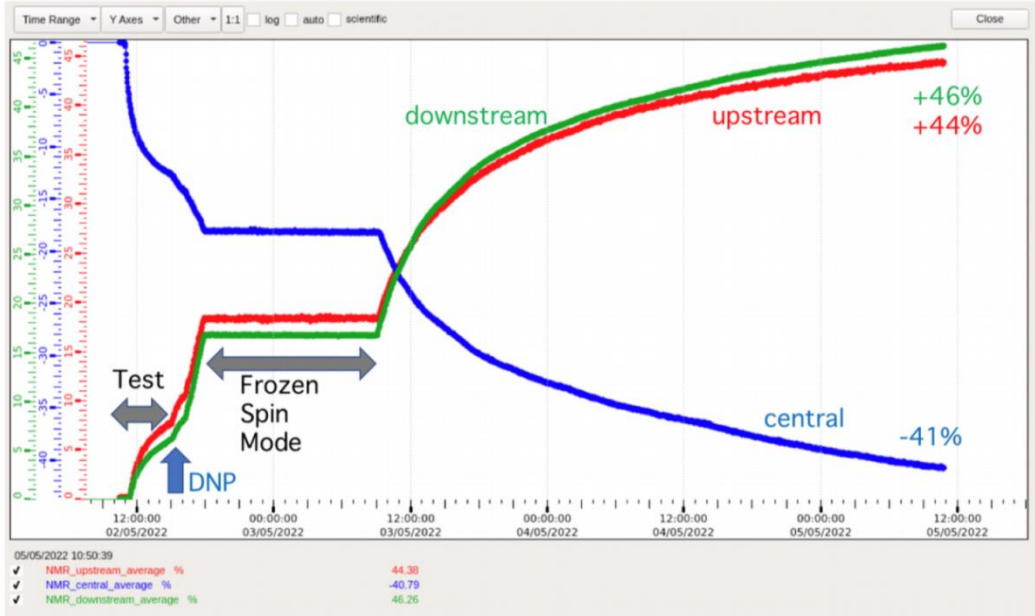
Polarized target - 2022



- 6LiD material successfully loaded (22/03)
 - Indium joint – OK, NMR coil fixed
- All 3 Gunn diodes installed
- TE calibration done (1K, 1.2 K, 1.5K)
- Successful DNP exercises
- Excellent performance of the system



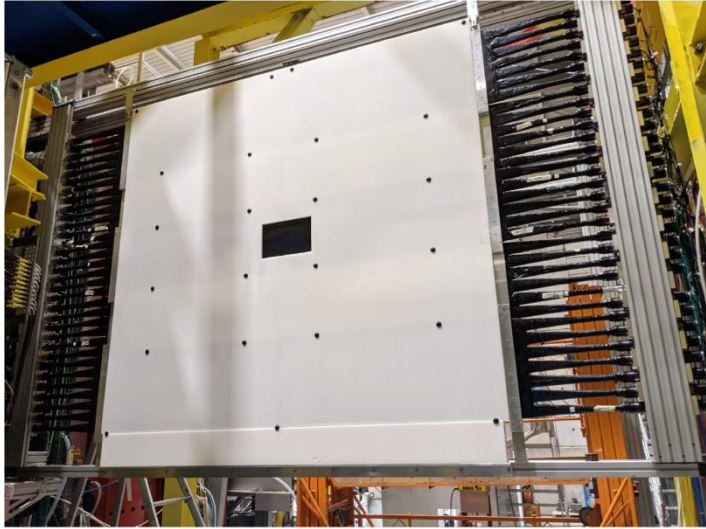
Polarized target



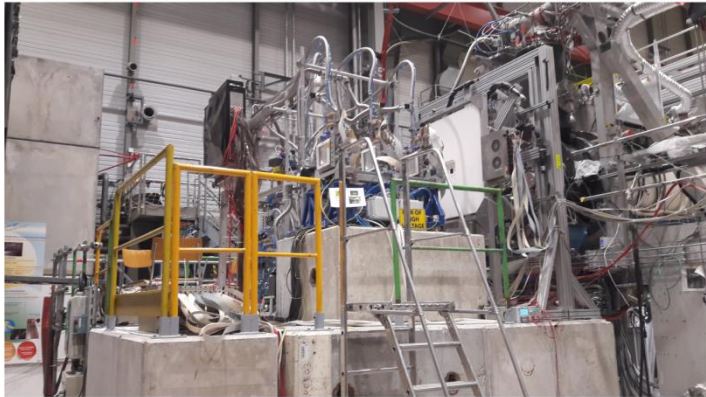
- Excellent performance of new system (Gunn-diodes)
 - Gunn diodes (+ PT equipment) totaling 500 kCHF – 2022 run
- Remote control available
 - Remote shift, reduce the load on the local manpower
- Target polarization values ($\langle P_T \rangle \sim 45\%$) reachable in 2-3 days
- **The data-taking started on Tuesday 07/06**

Spectrometer status by the end of 2021 run

COMPASS Run-coordinator summary report (SPS users meeting)



First LAST hodoscope H1.



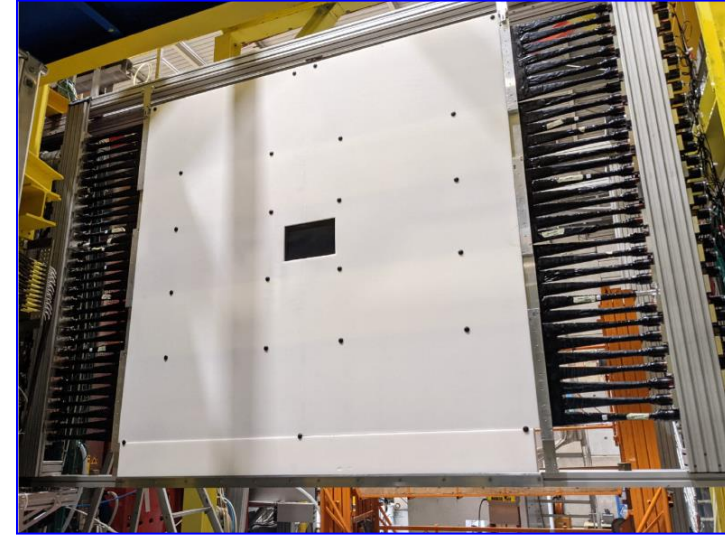
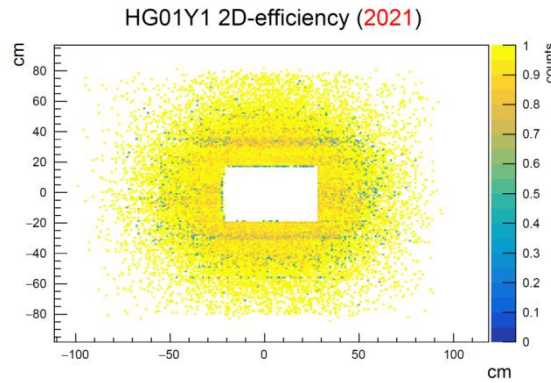
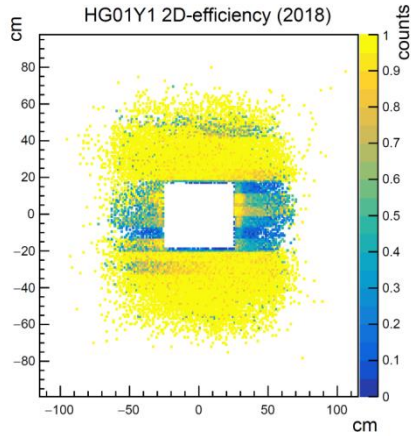
Beam telescope platform.

Spectrometer commissioning was progressing despite the target problems.

- 10. 7. 1st beam delivered.
- 23. 7. Most of the spectrometer ready for commissioning with beam.
- 30. 7. Part of triggers timed in, too low I_{T6} for hodoscope HV scan.
- 6. 8. All trigger OK, spectrometer ready except beam telescope and ECAL1 (not essential for physics).
- 13. 8. Beam telescope platform building (possible after the target was loaded).
- 20. 8. Beam telescope operational (in one week!)
- 27. 8. Chicane in transverse configuration (waiting for target magnet).
- 7. 9. Final trigger tuning, ready for physics (possible after the target dipole was on).

Large effort, fully successful!

Trigger hodoscopes: 2021-2022 repairs

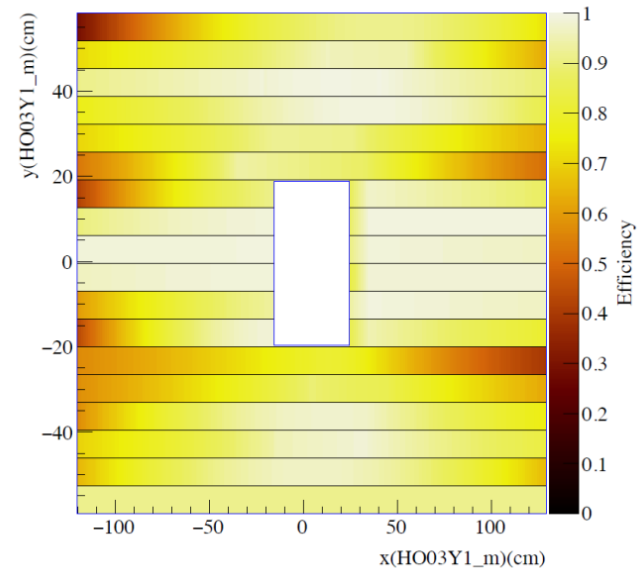


LAST trigger (H01)

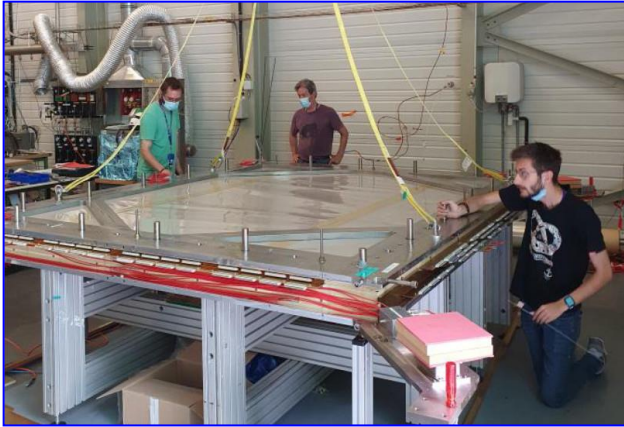
- Inefficient central slabs in 2015-2018
 - New central slabs: scintillators, air light guides, discriminators
 - All slabs checked and repaired if needed
 - The impact to be verified soon with the data

Outer trigger (HO3-HO4)

- Inefficient slabs in 2015-2018
 - New PMTs ordered (beginning of the year)
 - Delivery delay
 - Part of the PMTs installed during commissioning
 - Remaining PMTs will be installed during the run
 - The impact to be seen with the data



Highlight on activities during YETS



DC04 (Saclay)

- Broken wire blocking the operation of Y-plane
- **Repaired within just two weeks**
- Noise on some of the planes (grounding issue)
- Further investigated during Year-End Technical Stop (YETS)

DC05 (Illinois)

- Similar broken wire problem blocking one of the views
- Repaired during YETS
- **Repaired within just two weeks**

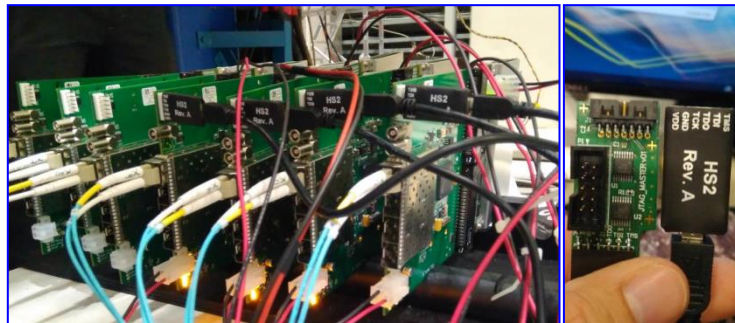
MWPCs (Torino)

- In general, fully operational
- Some noise problems:
 - aging of Al-Mylar windows (bad electrical connection)
 - PB05 station refurbished during YETS
- New iFTDC-based FE (Compatible with streaming readout)
- Installed/tested on plane during 2021 run
- One station (PA05) fully equipped for 2022 run – under tests
- Spared ‘old’ FE cards used for the other stations in 2022

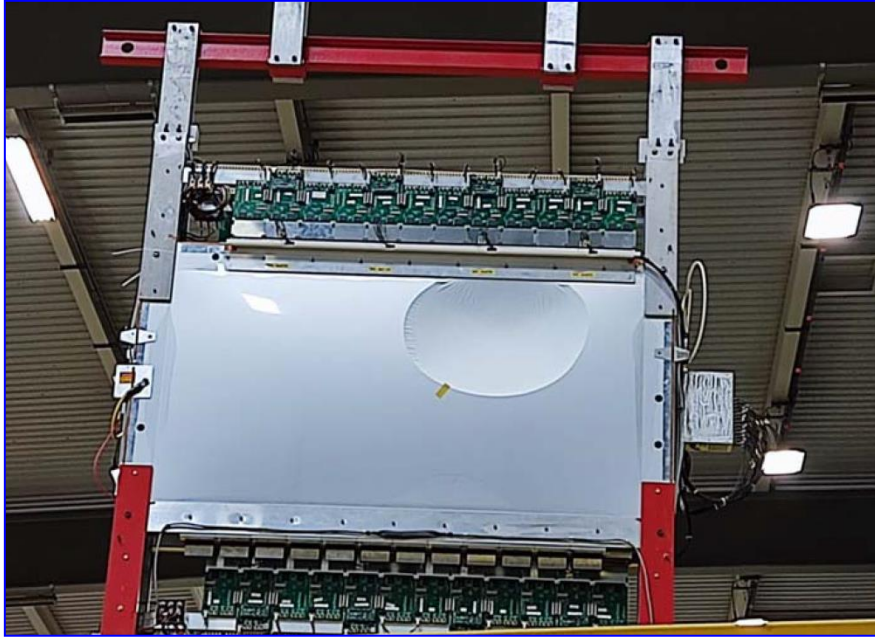


RICH-wall (Torino)

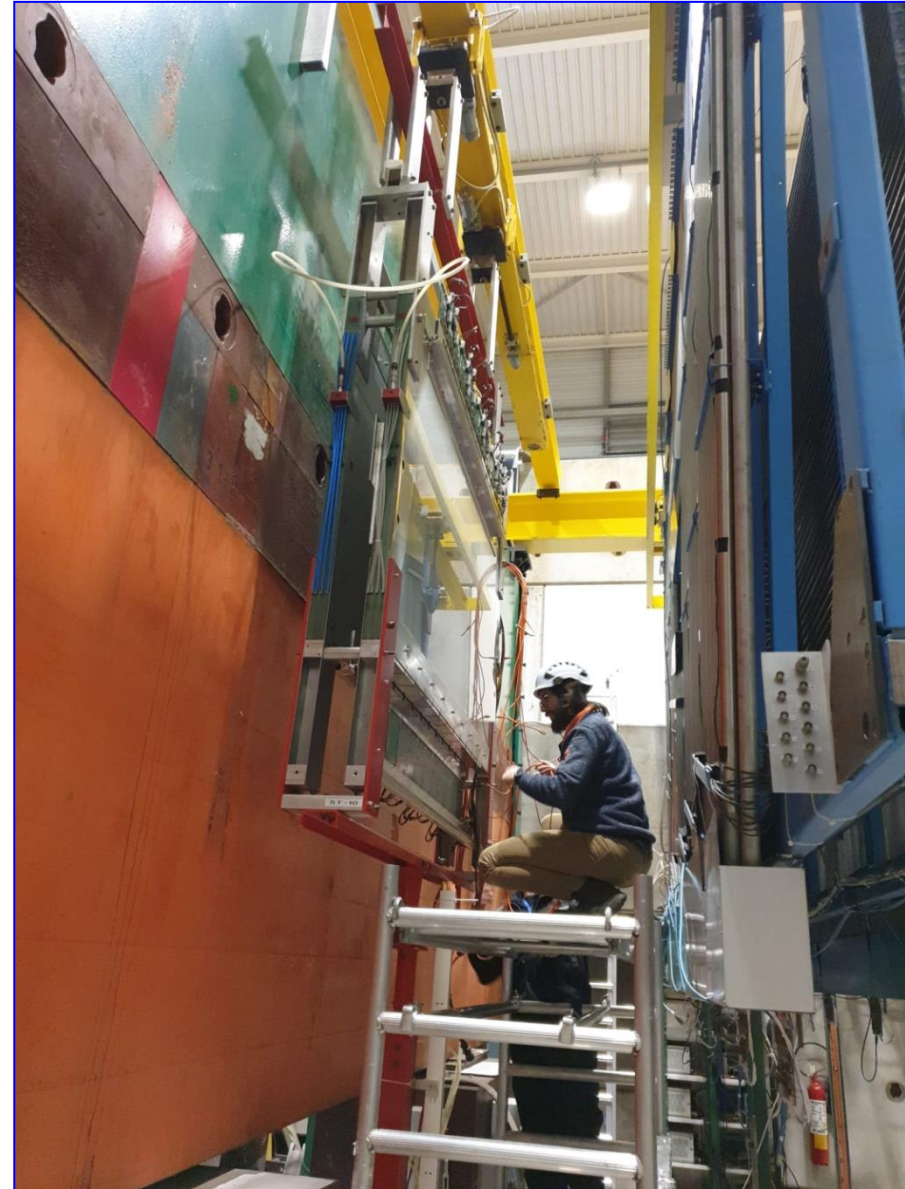
- Fully refurbished, installed and commissioned in June-2021
- Various frontend problems fixed: operated during 2021 run
- Further adjustments during YETS and commissioning-2022



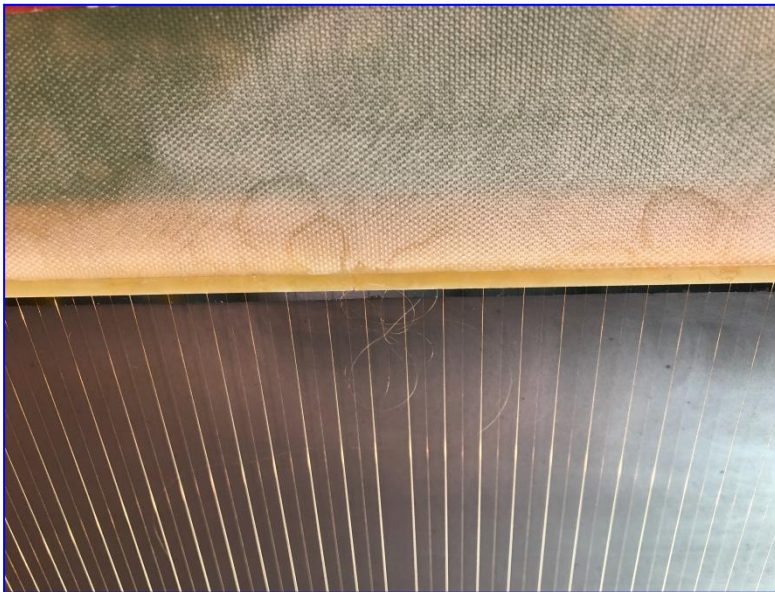
Reparation of MWPC (PB-05 station)



- Detached aluminum layer of aluminized Mylar foil (external window)
 - Caused HV problems
- Chamber repaired during YETS
- In place since February
- All planes fully operational



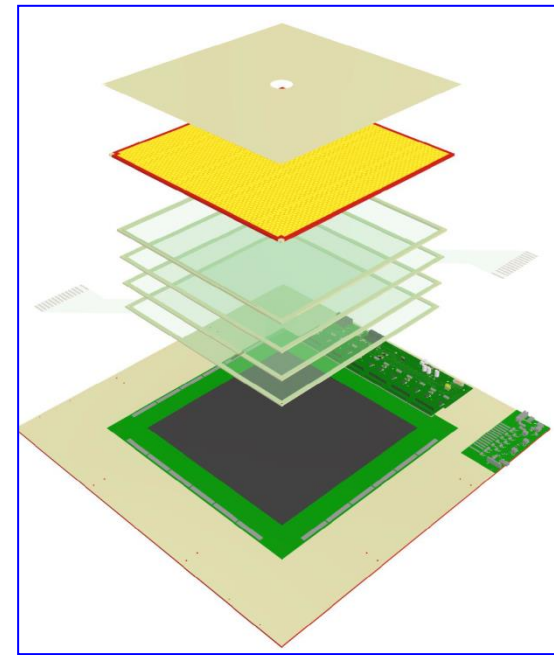
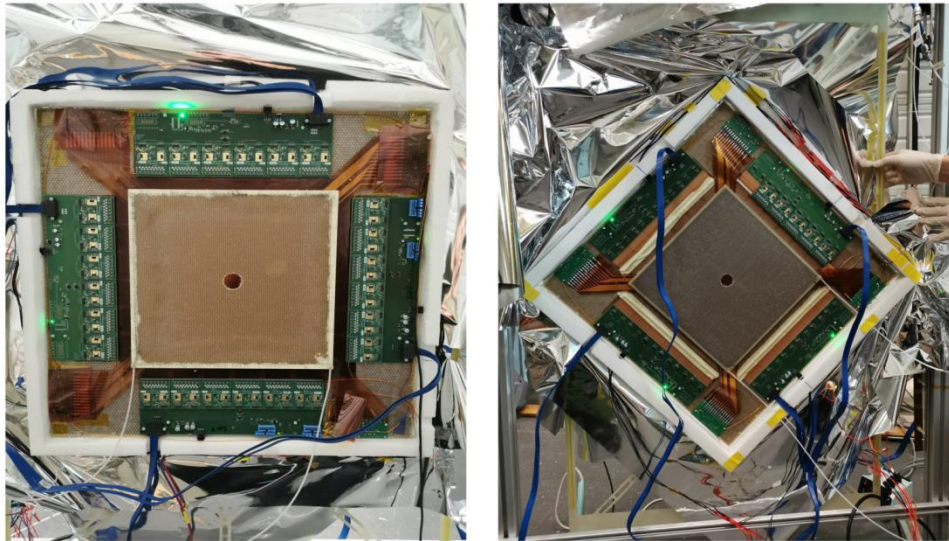
DC05 station repair



DC5 repair during YETS

- Thanks to released COVID-restrictions DC05 team could arrive from Illinois
- Fast operation 14/02-26/02
- Broken wire extracted
- Noise studies during the commissioning
- All planes fully operational

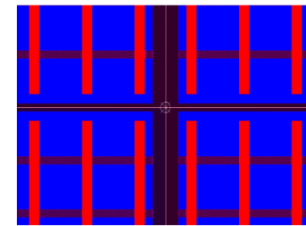
New GEM stations



Two new stations for 2022 run

- 1st station is installed in the spectrometer (GEM-11)
 - Currently under tests
- 2nd station is being prepared for installation
 - Will take place during one of the next technical breaks
- Compatible with streaming readout concept (AMBER)

- Size of active area: $30.7 \times 30.7 \text{ cm}^2$
- Strips divided in center to reduce occupancy
- Triple GEM, foils sectorized on top (13 sectors)
- No spacer grids
- Gas in/out on drift plate, internal distribution



- voltage divider: 3 + 1 cards
- 6×4 front-end cards, 4 supply cards (bus cards)



COMPASS status and plans for 2022 run

2021 Run

- Series of problems during 2021 run (mostly not under COMPASS responsibility)
 - Severe problems with ^3He pumping line
- As expected, the adjustment of the build-up procedure required significant amount of time (26 days instead of programmed 42)
- Gunn-diode performed excellently
 - Two more Gunn-diodes purchased for 2022 run (one Gunn-diode per cell)
- Successful operation of detectors
- Several repairs during YETS

2022 Run

- Constructive interactions with NA64 μ , AMBER and MUonE
 - Collaborative effort to optimize beam-time usage
 - Brainstorming on COMPASS side
 - **To a large extent all solutions proposed by COMPASS have been accepted!**

Data taking started on Wednesday 07/06 – nearly on schedule – great team effort!

- The average polarization is about ~45% (reachable within 2-3 days)
 - 50% in the proposal calculations, faster polarization in 2010, larger target cell radius
- Affecting projected uncertainties (~20% larger)

In order to achieve physics goals of the approved COMPASS transverse deuteron measurements programme, COMPASS needs full run in 2022.



- Backup slides



COMPASS collaboration

Common Muon and Proton Apparatus for Structure and Spectroscopy



25 institutions from 13 countries
– nearly 200 physicists

- CERN SPS north area
- Fixed target experiment
- Approved in 1997 (**25 years**)
- Taking data since 2002 (**20 years**)

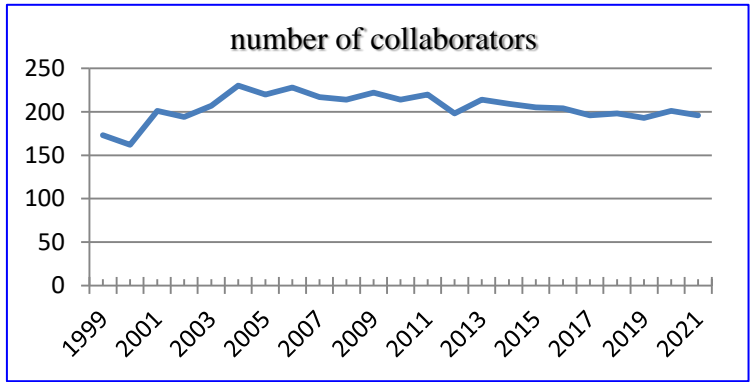
Wide physics program

COMPASS-I

- Data taking 2002-2011
- Muon and hadron beams
- Nucleon spin structure
- Spectroscopy

COMPASS-II

- Data taking 2012-2022
- Primakoff
- DVCS (GPD+SIDIS)
- Polarized Drell-Yan
- **Transverse deuteron SIDIS 2022**



COMPASS web page: <http://wwwcompass.cern.ch>



COMPASS data taking campaigns

Beam	Target	year	Physics programme
μ^+	Polarized deuteron (${}^6\text{LiD}$)	2002 2003 2004	80% Longitudinal 20% Transverse SIDIS
		2006	Longitudinal SIDIS
	Polarized proton (NH_3)	2007	50% Longitudinal 50% Transverse SIDIS
π K p	LH_2 , Ni, Pb, W	2008 2009	Spectroscopy
μ^+	Polarized proton (NH_3)	2010	Transverse SIDIS
		2011	Longitudinal SIDIS
π K p	Ni	2012	Primakoff
μ^\pm	LH_2	2012	Pilot DVCS & HEMP & unpolarized SIDIS
π^-	Polarized proton (NH_3)	2014	Pilot Drell-Yan
		2015 2018	Transverse Drell-Yan
μ^\pm	LH_2	2016 2017	DVCS & HEMP & unpolarized SIDIS
μ^+	Polarized deuteron (${}^6\text{LiD}$)	2021 2022	Transverse SIDIS



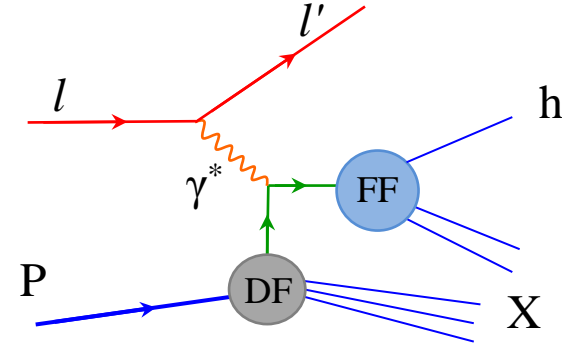
SIDIS x-section and TMDs at twist-2

All measured by COMPASS

$$\frac{d\sigma}{dx dy dz dp_T^2 d\phi_h d\phi_s} =$$

$$\left[\frac{\alpha}{xyQ^2} \frac{y^2}{2(1-\varepsilon)} \left(1 + \frac{\gamma^2}{2x} \right) \right] (F_{UU,T} + \varepsilon F_{UU,L})$$

$$\times \left\{ \begin{array}{l} \left[\begin{array}{l} 1 + \sqrt{2\varepsilon(1+\varepsilon)} A_{UU}^{\cos\phi_h} \cos\phi_h + \varepsilon A_{UU}^{\cos 2\phi_h} \cos 2\phi_h \\ + \lambda \sqrt{2\varepsilon(1-\varepsilon)} A_{LU}^{\sin\phi_h} \sin\phi_h \end{array} \right] \\ + S_L \left[\begin{array}{l} \sqrt{2\varepsilon(1+\varepsilon)} A_{UL}^{\sin\phi_h} \sin\phi_h + \varepsilon A_{UL}^{\sin 2\phi_h} \sin 2\phi_h \\ + S_L \lambda \left[\sqrt{1-\varepsilon^2} A_{LL} + \sqrt{2\varepsilon(1-\varepsilon)} A_{LL}^{\cos\phi_h} \cos\phi_h \right] \end{array} \right] \\ + S_T \left[\begin{array}{l} A_{UT}^{\sin(\phi_h-\phi_s)} \sin(\phi_h-\phi_s) \\ + \varepsilon A_{UT}^{\sin(\phi_h+\phi_s)} \sin(\phi_h+\phi_s) \\ + \varepsilon A_{UT}^{\sin(3\phi_h-\phi_s)} \sin(3\phi_h-\phi_s) \\ + \sqrt{2\varepsilon(1+\varepsilon)} A_{UT}^{\sin\phi_s} \sin\phi_s \\ + \sqrt{2\varepsilon(1+\varepsilon)} A_{UT}^{\sin(2\phi_h-\phi_s)} \sin(2\phi_h-\phi_s) \end{array} \right] \\ + S_T \lambda \left[\begin{array}{l} \sqrt{(1-\varepsilon^2)} A_{LT}^{\cos(\phi_h-\phi_s)} \cos(\phi_h-\phi_s) \\ + \sqrt{2\varepsilon(1-\varepsilon)} A_{LT}^{\cos\phi_s} \cos\phi_s \\ + \sqrt{2\varepsilon(1-\varepsilon)} A_{LT}^{\cos(2\phi_h-\phi_s)} \cos(2\phi_h-\phi_s) \end{array} \right] \end{array} \right\}$$



Quark \ Nucleon	U	L	T
U	$f_1^q(x, \mathbf{k}_T^2)$ number density		$h_1^{\perp q}(x, \mathbf{k}_T^2)$ Boer-Mulders
L		$g_1^q(x, \mathbf{k}_T^2)$ helicity	$h_{1L}^{\perp q}(x, \mathbf{k}_T^2)$ worm-gear L
T	$f_{1T}^{\perp q}(x, \mathbf{k}_T^2)$ Sivers	$g_{1T}^q(x, \mathbf{k}_T^2)$ Kotzinian-Mulders worm-gear T	$h_1^q(x, \mathbf{k}_T^2)$ transversity $h_{1T}^{\perp q}(x, \mathbf{k}_T^2)$ pretzelosity

+ two FFs: $D_{1q}^h(z, P_{\perp}^2)$ and $H_{1q}^{\perp h}(z, P_{\perp}^2)$

SIDIS TSAs: Collins effect and Transversity

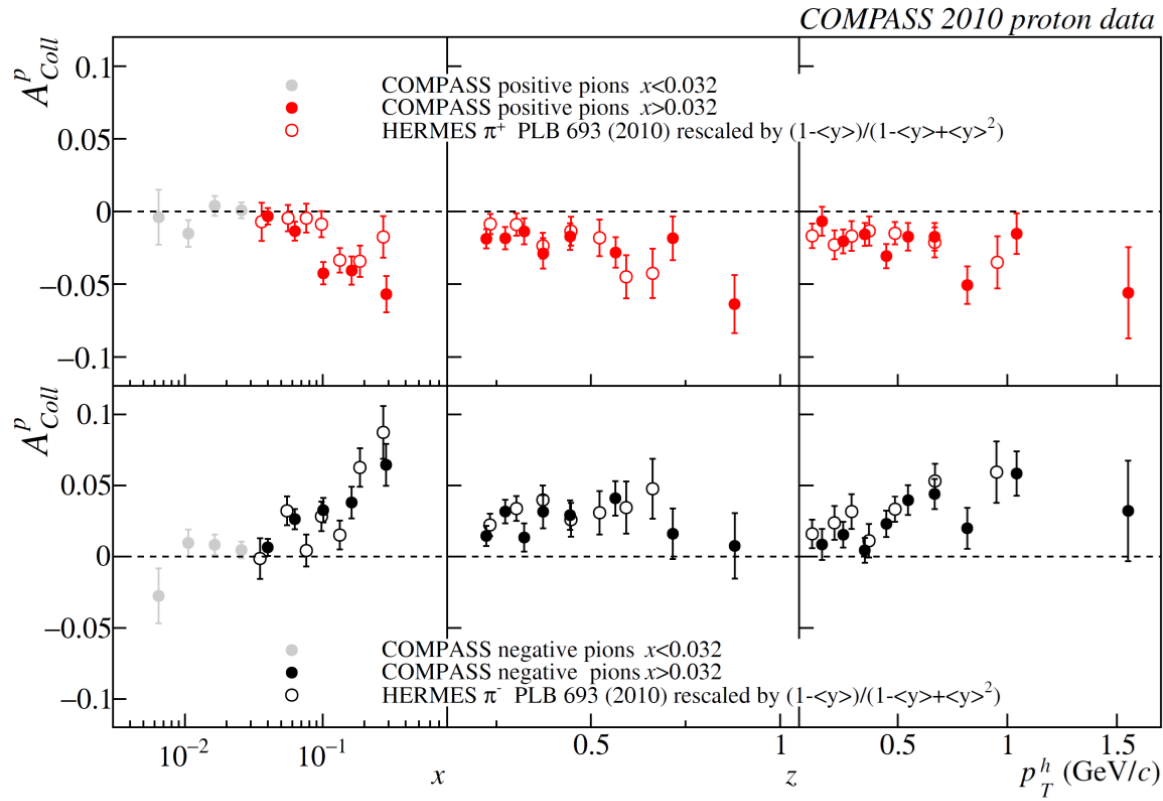
$$\frac{d\sigma}{dx dy dz dp_T^2 d\phi_h d\phi_S} \propto (F_{UU,T} + \varepsilon F_{UU,L}) \left\{ 1 + \dots + S_T \varepsilon A_{UT}^{\sin(\phi_h + \phi_S)} \sin(\phi_h + \phi_S) + \dots \right\}$$

$$F_{UT}^{\sin(\phi_h + \phi_S)} = C \left[-\frac{\hat{h} \cdot p_T}{M_h} h_1^q H_{1q}^{\perp h} \right]$$

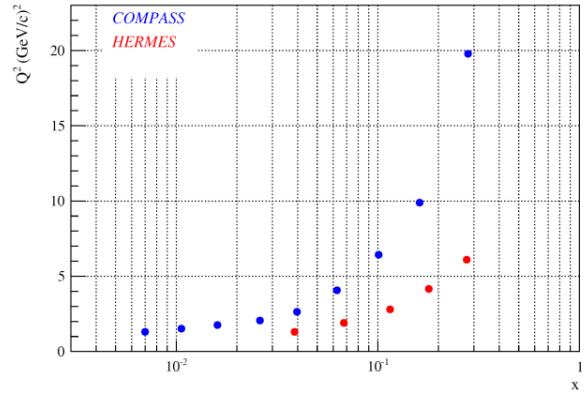
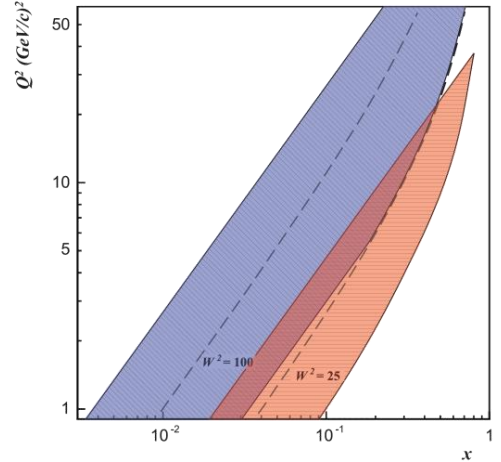


- Measured on P/D in SIDIS and in dihadron SIDIS
- Compatible results COMPASS/HERMES (Q² is different by a factor of ~2-3)
- No impact from Q²-evolution?

COMPASS PLB 744 (2015) 250



COMPASS 2010 proton data





COMPASS legacy: selected highlights

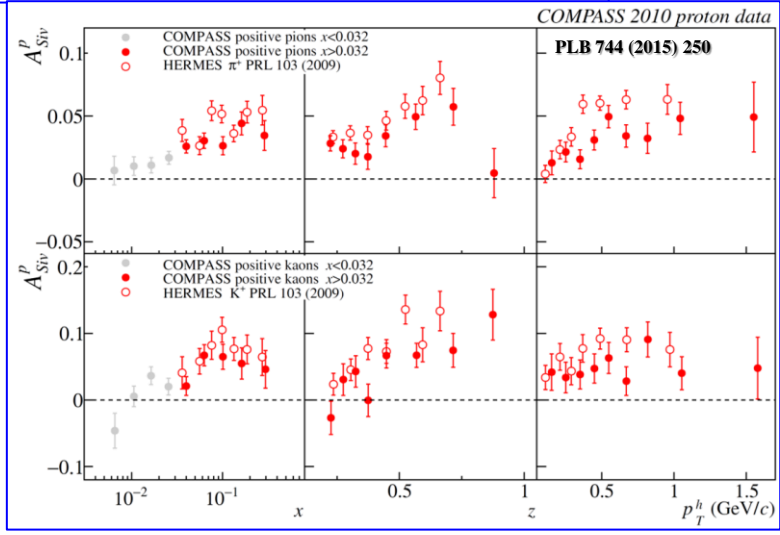
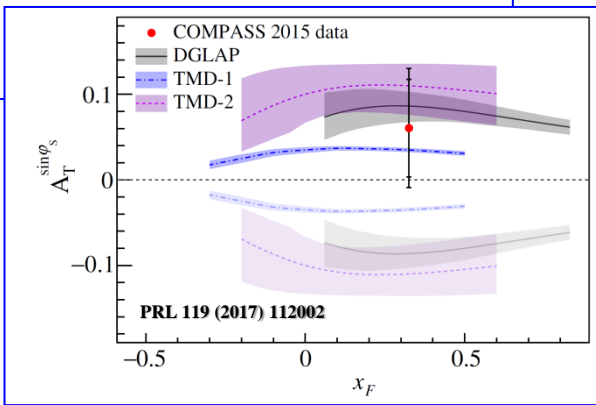
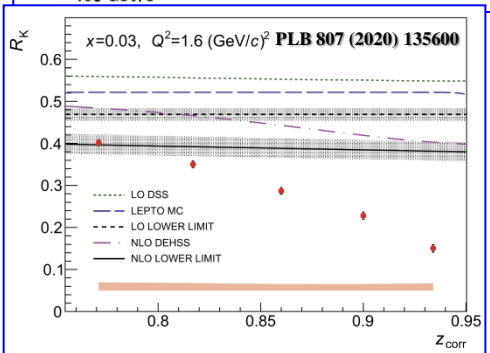
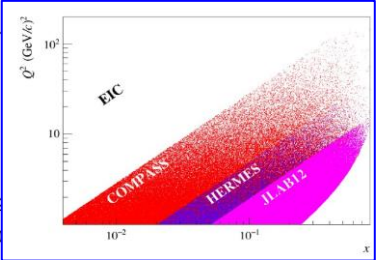
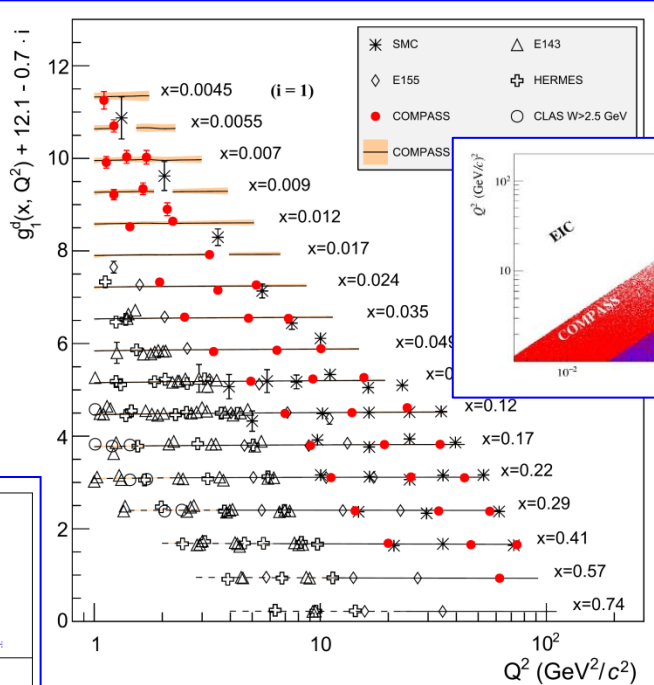
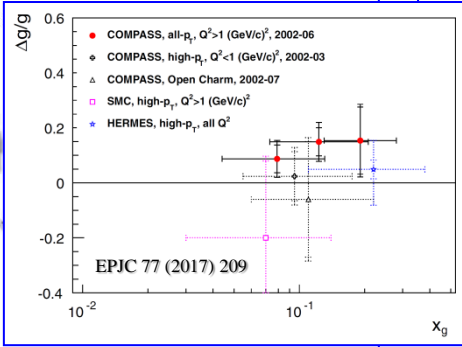
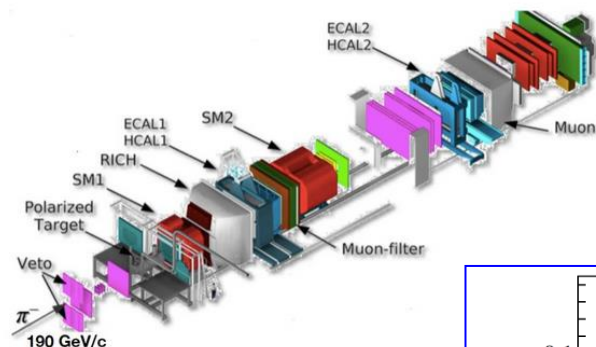
COMPASS results guiding future exploration of hadron structure in CERN's North Area.

Oleg Denisov (INFN), Wolf-Dieter Nowak (DESY), Fulvio Tassarotto (INFN) on behalf of the COMPASS collaboration 16th Sep 2019

EP Newsletter of the EP department

The COMPASS (COmmon Muon and Proton Apparatus for Structure and Spectroscopy) Collaboration at CERN is the most recent one in pursuing the more than 40-years old objective to experimentally elucidate the nucleon's internal structure, in particular its spin dependence. It uses the M2 beam line of the SPS, which provides the only high-energy spin-polarized muon beam in the world. The deep-inelastic scattering (DIS) process serves as a tool for studying in-depth the structure of the nucleon in terms of quarks and gluons and to investigate other phenomena like e.g. nucleon electromagnetic form factors and the strangeness content of the nucleon. Using alternatively high-energy pions or kaons delivered by the M2 beam line, a new era was opened to study exclusively produced multi-meson states, which already led to several new results in meson spectroscopy. In particular, 3-pion and $K\pi\pi$ states were studied through partial-wave analyses with unprecedented high-statistics, allowing one to identify and thoroughly analyze the properties of small signals and to search for new states.

In the last four years, the COMPASS Collaboration used their versatile two-stage combination with different beam and target configurations.



The COMPASS Experiment at the CERN SPS

Broad Physics Program to study Structure and Excitation Spectrum of Hadrons

PRL 114, 062002 (2015)

Measurement of the Charged-Pion Polarizability

Increasing resolution scale
(momentum transfer)

CERN experiment brings precision to a cornerstone of particle physics

Date: February 11, 2015
Source: CERN



CERN Physicists Measure Polarizability of Pion

Feb 16, 2015 by News Staff / Source

« Previous | Next »

Published in
Physics

Tagged as
CERN
COMPASS
LHC
Pion
Strong interaction

Scientists from CERN's COMPASS collaboration have made the most precise measurement ever of the polarizability of pion – the fundamental low-energy parameter of strong interaction.

Follow
f t

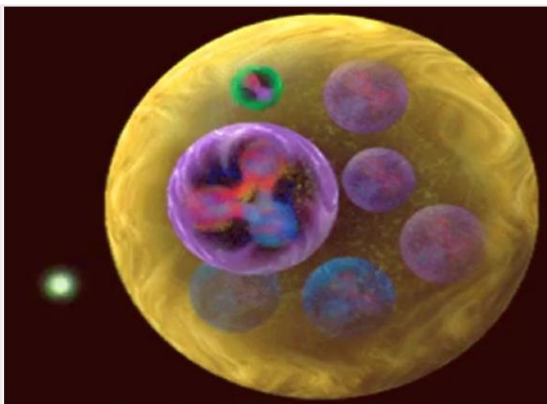
You Might Like



Astrophysicists Detect 35 New Gravitational-Wave Events



New Research Sheds More Light on Electromagnetic Structure of Neutron



An electron (green) hits a proton in a nucleus, creating a pion (green-skinned particle) and transforming the proton into a neutron. Image credit: Joanna Griffin / Jefferson Lab.

NEWS

COMPASS measures the pion polarizability

23 February 2015



CERN experiment brings precision to a cornerstone of particle physics

11 FEBRUARY, 2015



The COMPASS experiment in the North Area on the Prévessin site at CERN studies hadron structure both with pion beams and with muon beams – a powerful combination. Image credit: CERN-EX-1105182-01.

Chiral dynamics

- Test chiral perturbation theory in $\pi(K) \gamma$ reactions
- π^\pm and K^\pm polarizabilities
- Chiral anomaly $F_{3\pi}$

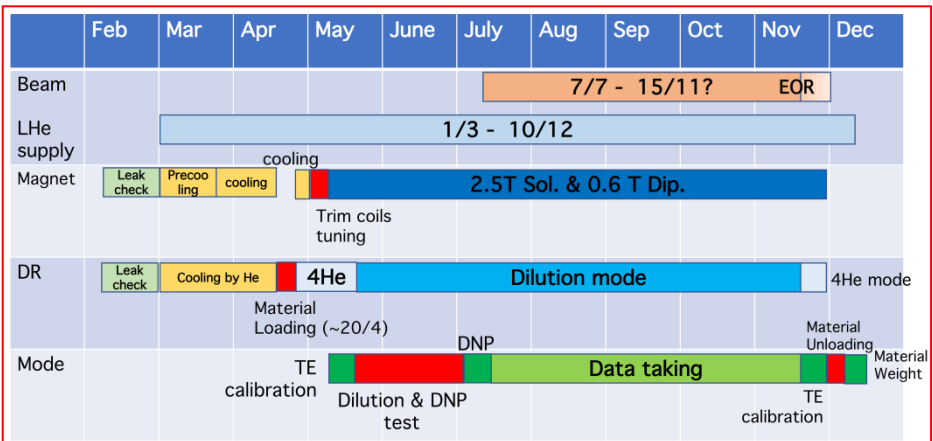


COMPASS PT 2021 run

Original plan

- 28/04:** Target material loading
 - 15/05:** Start of NMR calibration
 - 15/05:** Switch to dilution mode
 - 01/06:** Dynamic nuclear polarization tuning
 - 42 days for polarization studies** ←
 - 12/07:** Ready for data taking
- 34 days }
58 days }

Original schedule as of 25/04



COMPASS deuteron (⁶LiD) target status by the begging of 2021 run

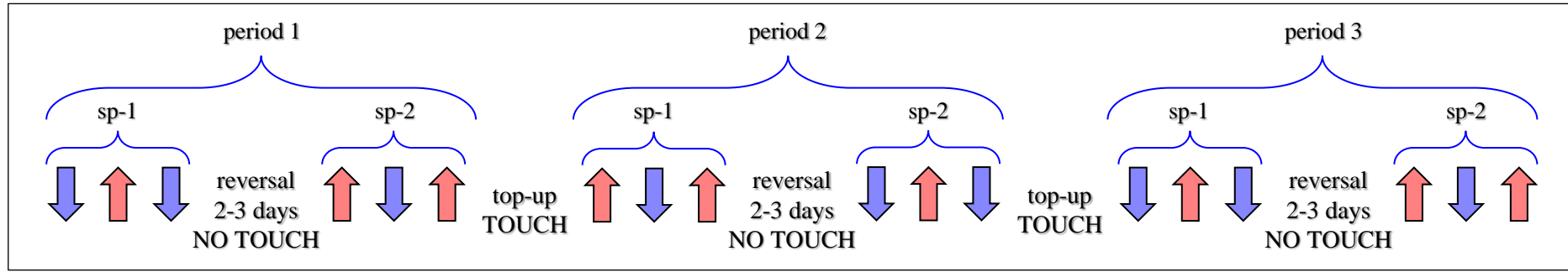
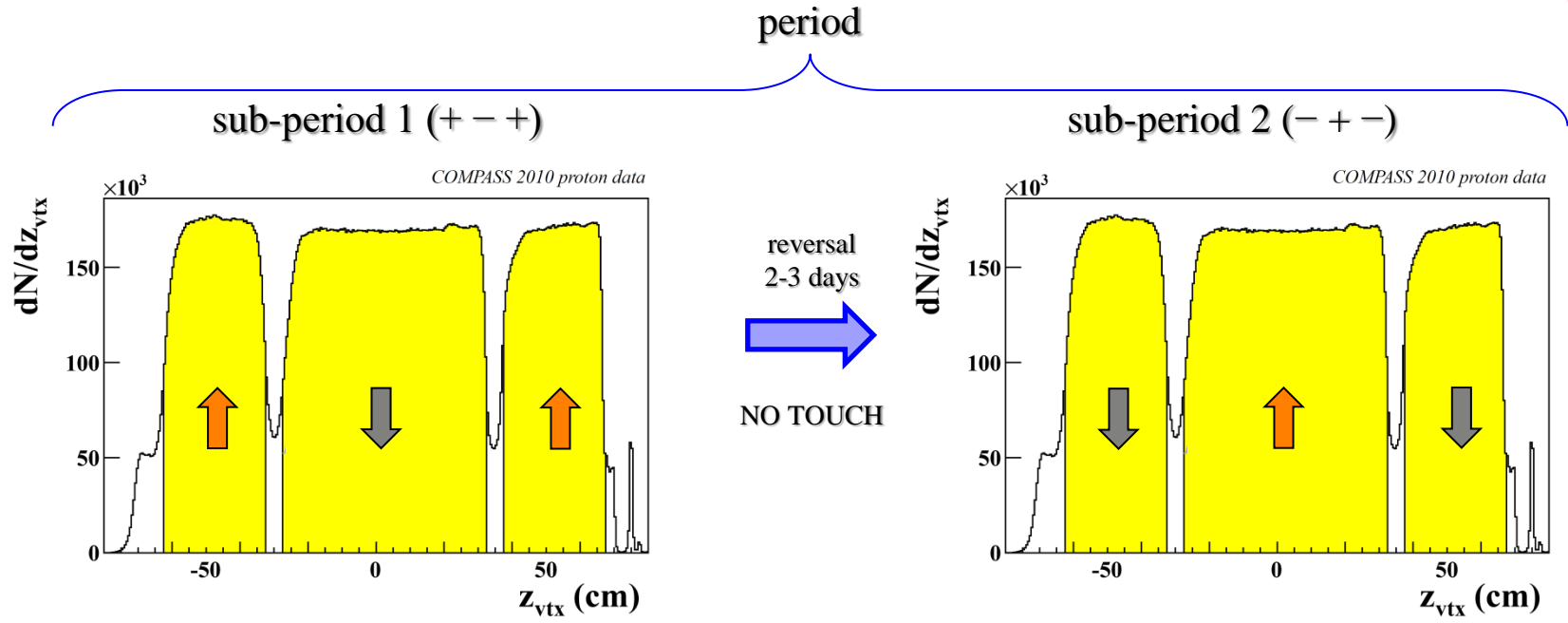
- Last DNP in 2006 (longitudinal run)
- Material tested in the lab in 2019; no evident aging effects observed
- Gunn-diode to be tested for the first time in combination with EIO tubes
- In the proposal: projected value for average polarization ~50% (~2 days of build-up)
- PT magnet refurbished in 2014
- ³He evacuation line exchanged in 2019
- Main MW expert passed away in March 2020
- Main dilution-refrigerator expert absent (COVID restrictions)



- 105 days requested in 2021 (1/2 of the allocation + 30 d for commissioning).
- 85 days of beam allocated (including commissioning) July 12 – October 6



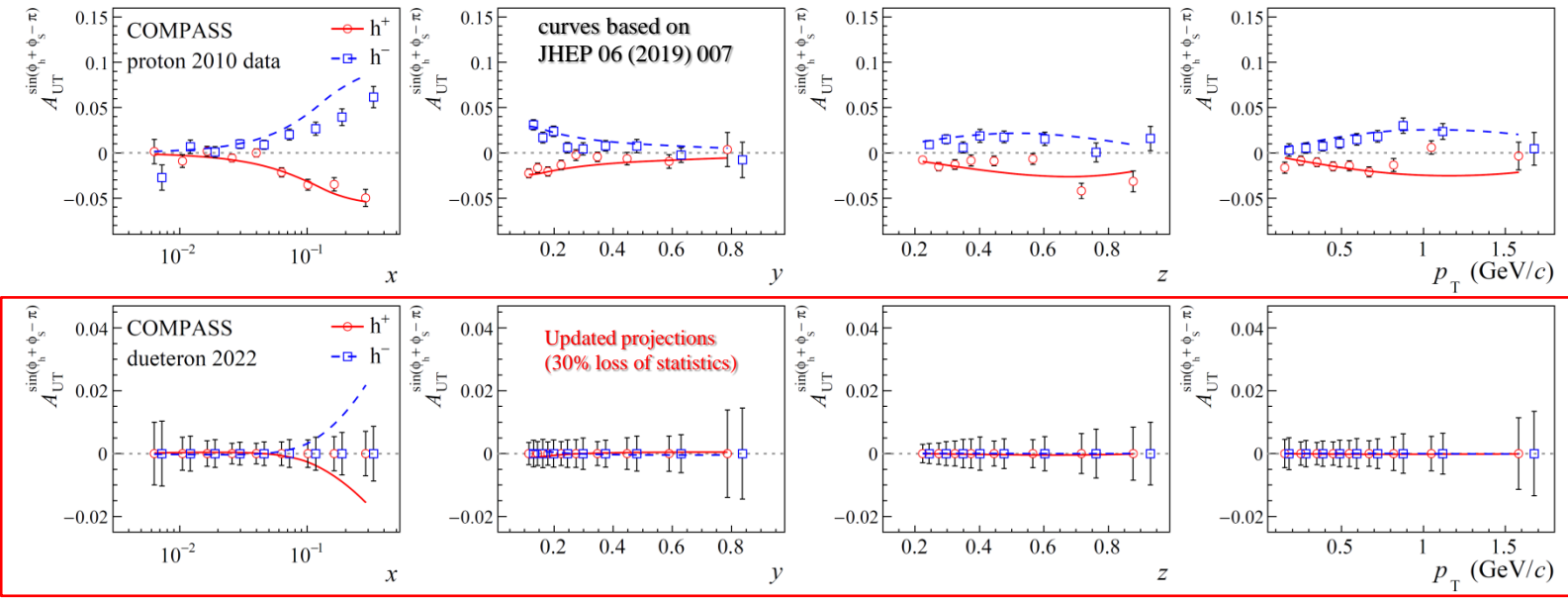
COMPASS transverse data-taking philosophy



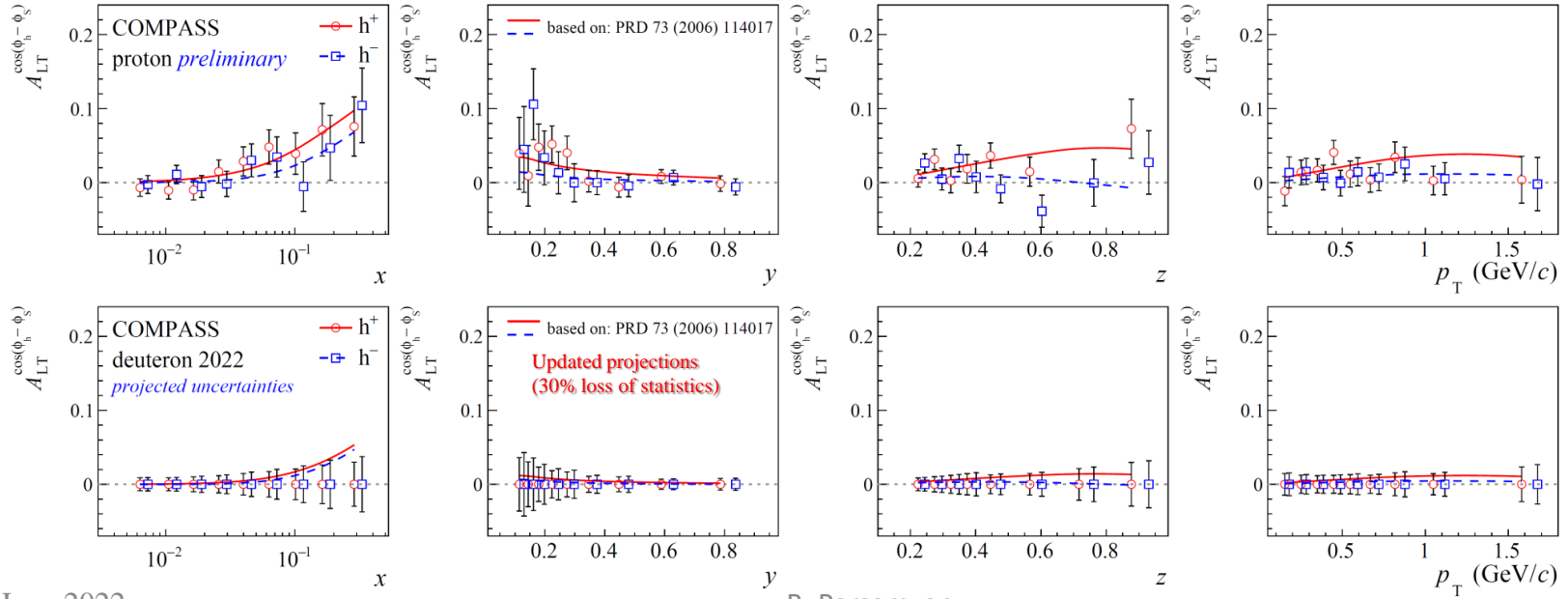
So-called “Reasonable assumption”: before and after the field reversal the ratio of acceptances of the neighboring cells should stay constant



Projected uncertainties



We are at the limit of tolerable loss of statistical precision... **COMPASS has no further room for loss**





Published papers: 2022

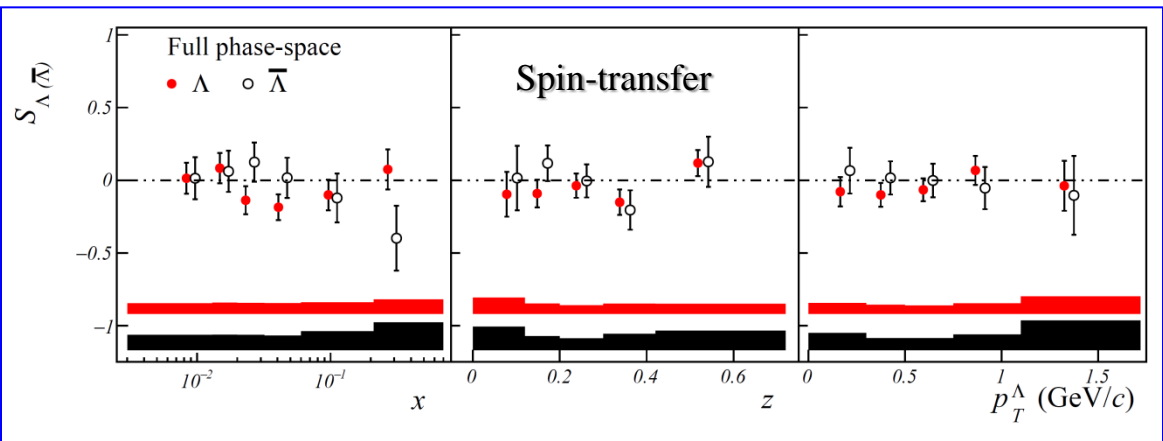
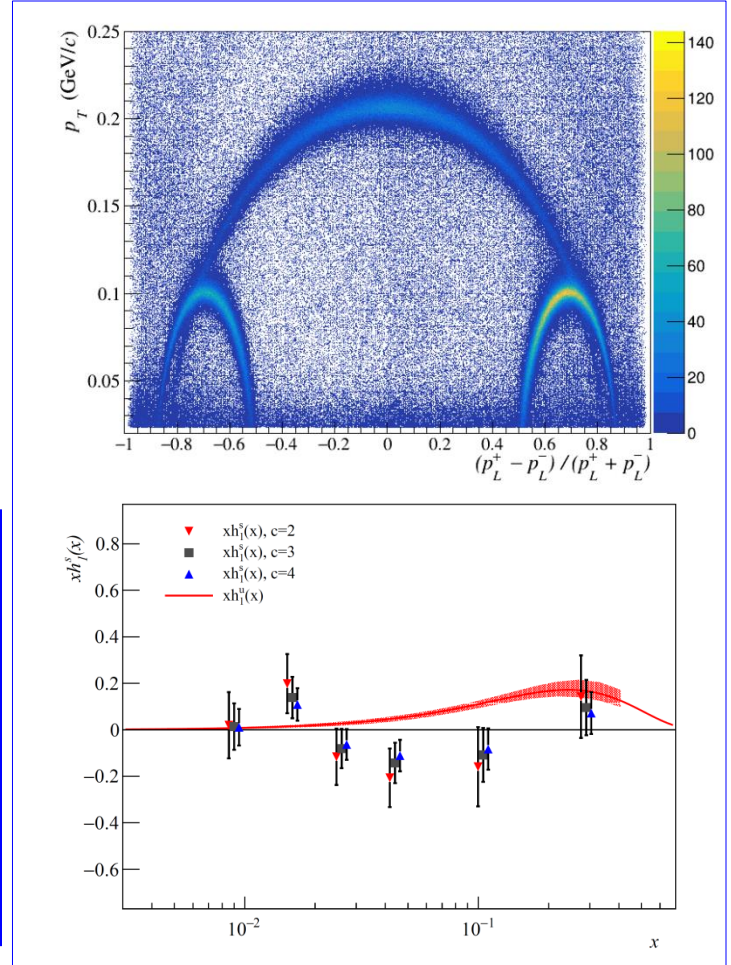
Transversity and Λ polarisation in polarised SIDIS at COMPASS

The COMPASS Collaboration

Published on January 10th
PLB 824 (2022) 136834

Abstract

Based on the observation of target-transverse-spin asymmetries in single-hadron and hadron-pair production in Semi-Inclusive measurements of Deep Inelastic Scattering (SIDIS), the existence of the chiral-odd transversity quark distribution function $h_1^q(x)$ is nowadays well established. Several possible channels to access transversity have been discussed. One major candidate is the measurement of the polarisation of Λ hyperons produced in SIDIS off transversely polarised nucleons, where the transverse polarisation of the struck quark can be transferred to the final-state hyperon. In this article, we present the COMPASS results on the transversity-induced polarisation of Λ and $\bar{\Lambda}$ hyperons produced in SIDIS off transversely polarised protons. Within the experimental uncertainties, no significant deviations from zero could be observed in these data. The results are discussed taking into account the known transversity functions and some models.



The exotic meson $\pi_1(1600)$ with $J^{PC} = 1^{-+}$ and its decay into $\rho(770)\pi$

The COMPASS Collaboration

Abstract

We study the spin-exotic $J^{PC} = 1^{-+}$ amplitude in single-diffractive dissociation of 190 GeV/c pions into $\pi^-\pi^-\pi^+$ using a hydrogen target and confirm the $\pi_1(1600) \rightarrow \rho(770)\pi$ amplitude, which interferes with a non-resonant 1^{-+} amplitude. We demonstrate that conflicting conclusions from previous studies on these amplitudes can be attributed to different analysis models and different treatment of the dependence of the amplitudes on the squared four-momentum transfer and we thus reconcile their experimental findings. We study the non-resonant contributions to the $\pi^-\pi^-\pi^+$ final state using pseudo-data generated on the basis of a Deck model. Subjecting pseudo-data and real data to the same partial-wave analysis, we find good agreement concerning the spectral shape and its dependence on the squared four-momentum transfer for the $J^{PC} = 1^{-+}$ amplitude and also for amplitudes with other J^{PC} quantum numbers. We investigate for the first time the amplitude of the $\pi^-\pi^+$ subsystem with $J^{PC} = 1^{--}$ in the 3π amplitude with $J^{PC} = 1^{-+}$ employing the novel freed-isobar analysis scheme. We reveal this $\pi^-\pi^+$ amplitude to be dominated by the $\rho(770)$ for both the $\pi_1(1600)$ and the non-resonant contribution. We determine the $\rho(770)$ resonance parameters within the three-pion final state. These findings largely confirm the underlying assumptions for the isobar model used in all previous partial-wave analyses addressing the $J^{PC} = 1^{-+}$ amplitude.

Published on January 12th
PRD 105(2022)1,012005

